LAWRENCE
LIVERMORE
NATIONAL
LABORATORY

UCRL-TR-221568

Test Suite for Nuclear Data I: Deterministic Calculations for Critical Assemblies and Replacement Coefficients

J. Pruet, D. A. Brown, M.-A. Descalle

May 23, 2006

This work was performed under the auspices of the U.S. Department of Energy by University of California, Lawrence Livermore National Laboratory under Contract W-7405-Eng-48.

Test Suite for Nuclear Data I: Deterministic Calculations for Critical Assemblies and Replacement Coefficients

J. Pruet, D. A. Brown & M.-A. Descalle

ABSTRACT

We describe tools developed by the Computational Nuclear Physics group for testing the quality of internally developed nuclear data and the fidelity of translations from ENDF formatted data to ENDL formatted data used by Livermore. These tests include S_n calculations for the effective k value characterizing critical assemblies and for replacement coefficients of different materials embedded in the Godiva and Jezebel critical assemblies. For those assemblies and replacement materials for which reliable experimental information is available, these calculations provide an integral check on the quality of data. Because members of the ENDF and reactor communities use calculations for these same assemblies in their validation process, a comparison between their results with ENDF formatted data and our results with data translated into the ENDL format provides a strong check on the accuracy of translations. As a first application of the test suite we present a study comparing ENDL 99 and ENDF/B-V. We also consider the quality of the ENDF/B-V translation previously done by the Computational Nuclear Physics group. No significant errors are found.

1. Introduction

The Computational Nuclear Physics group is in the process of developing formal methods for testing, verifying and validating (V&V) nuclear data. At a minimum, these should result in a process which ensures that the data delivered to customers is usable and does not crash simulation codes. Additionally, tests of nuclear data should be complete enough to assure that translations between different formats preserve the original content of data. This is essential for planned efforts to compare between different laboratories' simulations. It is hard to decipher the impact of differences in the treatment of underlying physics if one isn't sure that the same nuclear data is used in two sets of simulations. Lastly, the V&V process should help detect errors in data or poor quality data.

This report documents a set of tests that rely on measurements performed on critical assemblies. Because some of these assemblies have been very well characterized in laboratory experiments, they can be used to provide stringent checks on nuclear data. In fact,

experimental uncertainties in multiplication rates for critical (or nearly critical) assemblies are often comparable to or smaller than uncertainties associated with calculations for these rates. In many cases uncertainties associated with measurements of cross sections in laboratory scattering experiments imply a range of multiplication rates wildly inconsistent with measurements for critical assemblies. For example, there is roughly a 2% uncertainty in the ^{239}Pu(n,f) cross section evaluated from consideration of neutron scattering experiments. A uniform 2% change in the Pu fission cross section leads to a variation in $k_{\rm eff}$ for the Jezebel assembly of about $\delta k_{\rm eff} \approx 0.01$. Since this is about five times larger than the experimental uncertainty in $k_{\rm eff}$ for Jezebel, this assembly provides a check that is in some ways better than that provided by laboratory scattering measurements. Of course, one can't just use critical assemblies to constrain the fission cross section at the sub percent level because there are also uncertainties in other cross sections, in the energy dependence of the fission cross section, in the spectrum of prompt fission neutrons, and so on.

At the same time, critical assemblies have their limitations. Because of the relative paucity of high energy neutrons emitted following fission, critical assemblies are relatively insensitive to reactions occurring at energies larger than roughly 7 or 10 MeV. Also, neutron multiplication is set by some combination of all the reactions occurring in an assembly. These systems typically don't give information about particular reactions occurring at particular energies. For this reason a data set that correctly reproduces critical assembly characteristics may not be right, it may just have a number of errors that tend to compensate each other.

Our test suite is comprised of the 15 critical assemblies listed in Table 1 and of calculations for replacement coefficients characterizing 41 materials embedded in the Jezebel and Godiva assemblies. Most of the tests are principally sensitive to fission spectrum neutrons and to neutrons with energies in the few hundred keV range. There are also two assemblies in the test suite with enough hydrogen to efficiently thermalize neutrons. However, since our calculations do not include bound state effects (arising from the formation of molecules) or self-shielding, they cannot be viewed as reliable for systems that efficiently moderate neutrons.

The assemblies listed in table 1 contain a relatively limited range of materials and so do not stringently constrain data for a great many isotopes. The current test suite relies mostly on calculations of replacement coefficients for checking data for non-fissile materials. Again, though, these calculations are mostly sensitive to intermediate energy neutrons and not to thermal or high energy neutrons.

Judgments about the quality of data are made by comparing calculations of critical assemblies against measured characteristics of these assemblies. Judgments about the quality of data translations are made by comparing our calculations using data translated from

ENDF into ENDL against calculations using ENDF data that has been translated and processed with NJOY. In this effort we are aided by the work of Stephanie Frankle of Los Alamos. She has developed a set of critical assemblies for validating nuclear data (Frankle 1999) and provided calculations for these assemblies using ENDF data (Frankle 1999b). For the replacement coefficient tests, Spriggs & Busch (2002) have presented calculations using MENDF-5 and MENDF-6. Those authors have also presented a critical re-evaluation of original experimental data.

2. Description of the Test Suite

The test suite is comprised of a set of static neutronics problems. These are calculated with AMTRAN, a Livermore S_n code. This code does not read raw cross section data, but instead works with so called `ndf` files. These are processed representations of the data appropriate for transport calculations.

One shortcoming of the present calculations is that they ignore effects related to the impact of molecular bindings and crystalline lattice structures on neutron interactions. The simplest of these so called $S_{\alpha\beta}$ corrections accounts for the reduced thermal velocities of atoms bound in molecules (e.g. the mean velocity of hydrogen bound in water is $1/\sqrt{18}$ as large as the mean thermal velocity of free hydrogen at the same temperature). There are other subtler effects relating to neutron diffraction and molecular vibrations as well. As we discuss later, our neglect of the $S_{\alpha\beta}$ corrections introduces some error in our calculations, particularly for the water-reflected and solution assemblies.

2.1. Critical Assemblies

A critical assembly is a collection of material in which a non-zero neutron population persists without growing or dying away. Properties of critical or nearly critical assemblies are conventionally expressed in terms of $k_{\rm eff}$, the effective k value defined through

$$\frac{dN}{dt} = \frac{k_{\rm eff} - 1}{\tau} N. \tag{1}$$

Here N is the number of neutrons present in the assembly at time t and τ is roughly viewed as the time between the birth of one generation and the subsequent generation of neutrons in the assembly.

Table 1 lists the assemblies currently included in the test suite. All are spherical and comprised principally of either uranium or plutonium. Several have reflectors surrounding

the fissile material. Two have enough hydrogen to efficiently moderate neutrons.

All of the assemblies in our test suite have been characterized in laboratory experiments. The last column of Table 2 shows evaluated estimates of $k_{\rm eff}$, along with uncertainties in $k_{\rm eff}$, for these systems. These estimates come from CSEWG (1991) and NEA Nuclear Science Committee (1998). There is some argument that the uncertainty in $k_{\rm eff}$ for Jezebel is smaller than has been evaluated. For our applications the uncertainties can be regarded as pretty small already. A smaller uncertainty wouldn't have much influence on our discussion.

It should be noted that the AMTRAN calculations for critical assemblies only include the contribution of prompt post-fission neutrons to $k_{\rm eff}$. Laboratory experiments are also affected by the delayed neutrons emitted following weak decay of fission fragments. The contribution of these delayed neutrons to $k_{\rm eff}$ for an assembly is typically denoted by β and is called "1 dollar". For Godiva $\beta \approx 0.00688$. For Jezebel $\beta \approx 0.00202$. We refer the reader to Spriggs & Busch (2002) for a critical account of the quality of experiments measuring critical assemblies.

2.2. Replacement Coefficients

By themselves bare or reflected critical assemblies are only sensitive to a rather limited range of isotopes. It would be nice to have tests for any isotope in a database. Calculations of replacement coefficients and associated experiments (sometimes called worth measurements) represent such a test.

Roughly, a replacement coefficient for isotopes j represents the change in $k_{\rm eff}$ caused by filling a small hole in a critical assembly with a sample of material j. The idea is that by keeping the hole and sample sizes small the neutron population in the assembly will only be slightly perturbed. In this way replacement coefficients represent a passive measurement of the reactivity of a material. A replacement coefficient can be calculated in the following way. First, calculate $k_{\rm eff}$ for a nearly critical assembly that has a hole cut into it. Call the calculated value k_0. Second, fill the hole with n_m moles of material j and re-calculate $k_{\rm eff}$ (call this k_1). The replacement coefficient is then defined as

$$r = \frac{100}{\beta} \frac{(k_1 - k_0)}{n_m}, \tag{2}$$

and has units of cents per mole. The expression for the replacement coefficient takes this form because perturbation theory predicts that $(k_1 - k_0)$ should be proportional to n_m (Hansen & Maier 1953, 1960).

The replacement coefficient defined above depends on the size of the hole introduced into

the assembly and on the amount of material put into the hole. To remove this dependence, a zero-volume replacement coefficient is sometimes defined. Formally this is viewed as the value of r as the size of the hole tends to zero. In practice it is hard to accurately calculate differences in $k_{\rm eff}$ for very small perturbations, so some approximate limiting procedure is used. We adopt the same procedure defined in Spriggs & Busch (2002). Specifically, a replacement coefficient (r_{75}) is first calculated for a right cylinder of height and diameter 0.75 inches. A second replacement coefficient (r_{50}) is then calculated for a right cylinder of height and diameter 0.50 inches. The zero volume replacement coefficient is estimated by extrapolating to an infinitesimal right cylinder

$$r_0 = r_{75} - 3 \cdot (r_{75} - r_{50}). \tag{3}$$

The assumption here is that the replacement coefficient is a linear function of the radius and length of the cylinder. This arises from consideration of second order perturbation theory describing the influence of finite sample size on r (Hansen & Maier 1953).

For Godiva and Jezebel there are careful measurements of replacement coefficients for some 40 different materials placed at various radii in these assemblies. In general the experimental errors on the measured values of the replacement coefficients are quite small, typically of order a few tenths of a cent per mole. This is better than the numerical accuracy of our calculations.

3. Tests of ENDL 99 and and of Livermore's ENDF/B-V translation

3.1. $k_{\rm eff}$ values for critical assemblies

Table 2 gives experimental and calculated results for the assemblies in our suite. Two sets of calculations done with ENDF/B-V are presented. The first comes from Frankle (1999) and uses NJOY-processed ENDF data and the MCNP code Monte Carlo code. The second comes from Livermore's translation of ENDF/B-V and is calculated by AMTRAN. A set of calculations using ENDL 99 is also presented.

The experimental results and the calculations by Los Alamos include the contribution of β-delayed neutrons emitted following fission to $k_{\rm eff}$. Our calculations with AMTRAN do not. To enable a comparison we have added estimates of the contribution of β-delayed neutrons to our calculations. For the Pu metal assemblies we took $\delta k = 0.00202$. This is the experimental value for the Jezebel critical assembly. For the uranium assemblies enriched in ^{235}U we adopted $\delta k = 0.00688$. This is the experimental value for Godiva and is also close to the value found for intermediate enriched assemblies (van der Marck 2005). For the

^{233}U assemblies we adopted δk=0.0029, the experimentally determined value for U233-MET-FAST-001. It is estimated that our approximate account of β_{eff} may introduce an error as large as 0.001 in calculations of $k_{\rm eff}$ for some assemblies, but larger errors do not seem likely.

Regarding the quality of translations from ENDF into ENDL, we see from Table 2 that with a few exceptions there is good agreement between our calculations and Los Alamos' calculations. The most notable exceptions occur for HEU-MET-FAST-003l (a nickel reflected sphere) and HEU-MET-FAST-005 (a steel reflected sphere). Frankle's calculations showed that ENDF/B-V predicts both of these to be rather super-critical, with $k_{\rm eff} \approx 1.01$. Our calculations using translated ENDF/B-V also find these to be quite supercritical. But there is a discrepancy of about 0.025 between our results and Frankle's. This is far larger than can be accounted for by statistical error or errors in β_{eff}. Because both iron and nickel have high lying resonances and because we neglect self shielding there is a possibility that the discrepancy is an artifact. To test this idea we ran Monte Carlo calculations for IEU-MET-FAST-005 and HEU-MET-FAST-003 using ENDL 99. These calculations found that $k_{\rm eff} = 1.0056 \pm 0.0001$ for HEU-MET-FAST-003 and $k_{\rm eff} = 0.9978 \pm 0.0001$ for IEU-MET-FAST-005. This seems to confirm that the discrepancy results from the calculational method rather than troubles with the data. The other two assemblies for which calculations using Livermore-translated ENDF data disagree with those using NJOY-processed ENDF data both have significant water content. Because our calculations do not include $S_{\alpha\beta}$ corrections or an account of self-shielding, a discrepancy for these is not surprising. Overall, the comparisons speak well of Livermore's data translation, at least for the fissile isotopes most important in these assemblies.

As far as the quality of the ENDL 99 data is concerned, Table 2 shows that ENDL does a rather good job of reproducing experimental $k_{\rm eff}$'s for ^{233}U assemblies. For 233-MET-FAST-001 there is an approximately two standard deviation discrepancy between calculation and experiment. This is still better than the deviation found with ENDF/B-V data.

For assemblies enriched in ^{235}U, ENDL 99 data does a good job of reproducing experimental values for the bare metal assembly, for the poly-reflected assembly and for the natural uranium-reflected assembly. Agreement between calculation and experiment is marginally poor (at the 3 standard deviation level) for the graphite reflected assembly and just awful for the nickel and steel reflected assemblies. For the graphite reflected assembly one may be tempted to think that the discrepancy arises from our neglect of $S_{\alpha\beta}$ corrections. This seems unlikely since our calculations using translated ENDF/B-V (which do not include molecular effects) are in such close agreement with Frankle's calculations (which do include $S_{\alpha\beta}$ corrections). In the next section we show comparisons between experimental and calculated replacement coefficients for Carbon, and the agreement is quite good. For this reason there

doesn't seem to be a particular problem with data for the carbon cross section in ENDL 99. It was noted above that for the nickel and steel reflected assemblies our calculations using translated ENDF/B-V do not agree with those using untranslated data. That results using ENDL 99 are in almost implausibly large disagreement with experiment may be more evidence of trouble with the calculational method rather than the data.

An analysis of the quality of ENDL 99 for Pu systems is more complicated. For Jezebel, a bare metal assembly, the calculated k_{eff} is low by about 3 standard deviations relative to experiment. For PU-MET-FAST-002, also a bare assembly but with a large ^{240}Pu content, there is fine agreement between calculation and experiment. There is also fine agreement between calculation and experiment for the beryllium and thorium reflected assemblies. For the water-reflected assembly (PU-MET-FAST-011) the calculated k_{eff} is markedly low. As was noted above, our calculated value with ENDF data for the water-reflected assembly is also markedly high, whereas the Los Alamos calculation that includes corrections that we neglect is not. If these corrections are responsible for the discrepancy with the ENDF data, it implies that $S_{\alpha\beta}$ corrections account for a δk of about 0.025. With this correction, the ENDL-based calculation for the water-reflected assembly is in agreement with experiment. The only outstanding discrepancy then is for Jezebel.

3.1.1. What is the source of the discrepancy for Jezebel calculated with ENDL 99?

The most obvious guess is that the discrepancy has something to do with ^{239}Pu, the dominant isotope in Jezebel. To consider this in more detail and also to preview later results a little, we show in Figure 63 calculations and experiments for replacement coefficients for ^{239}Pu embedded in Jezebel. The agreement is rather good, certainly not worse than the agreement calculated with ENDF/B-V. This suggests that if there is a problem with ^{239}Pu it isn't related to cross sections for this isotope, but maybe instead to the post-fission neutron spectrum.

To check this conjecture about the problem with the prompt neutron spectrum in ENDL 99 we ran a few simple calculations. These involved substituting nuclear data (either the fission cross section, the prompt neutron spectrum, the number of prompt neutrons emitted in fission, or some combination of these) from one database into another. For example, in one case we took out the ^{239}Pu(n,f) cross section from ENDL and replaced it with that from ENDF, but kept all other data in ENDL unchanged. The results of these calculations are summarized in table 3. These results lend themselves to a simple approximate interpretation in terms of the relative contribution of data from ENDL and ENDF to k_{eff}. For the fission

cross section we see that

$$k_{\rm eff}(\text{ENDL99 cross section}) - k_{\rm eff}(\text{ENDFB5 cross section}) \approx +0.0020. \quad (4)$$

In other words, relative to the cross section in ENDF/B-V, the ENDL cross section tends to increase $k_{\rm eff}$ by about 0.002. For the prompt fission neutron spectrum table 3 shows that

$$k_{\rm eff}(\text{ENDL99 spectrum}) - k_{\rm eff}(\text{ENDFB5 spectrum}) \approx -0.0045, \quad (5)$$

i.e., relative to the spectrum found in ENDF/B-V, the spectrum in ENDL tends to decrease $k_{\rm eff}$ by about 0.0046. And the combined influence of inserting both the spectrum and cross section from one database into the other accounts for a change in k of about $0.0046 - 0.002 = 0.0026$. There are also differences between ENDL and ENDF in the account of $\bar{\nu}$ (the number of prompt neutrons emitted following fission). It is seen from table 3 that these have a modest impact, they change k_{eff} by about 0.01.

So, an explanation of the discrepancy between different calculations for Jezebel is relatively complicated. On one hand, it is true that differences in the account of the prompt neutron spectrum between ENDL 99 and ENDF/B-V are large enough by themselves to explain the discrepancy in calculations for $k_{\rm eff}$. But on the other hand, differences in the account of the cross section between the two databases tend to undo differences caused by the neutron spectrum.

3.2. Replacement Coefficients

Figures 3 to 63 show replacement coefficients for different materials embedded in the Godiva and Jezebel assemblies. Three sets of results are shown - experimental values, results calculated with Livermore's translation of ENDF/B-V and results calculated using the ENDL 99 translation. Experimental results were taken from the evaluation by Spriggs & Busch (2002) of the original experiments by Engle, Hansen & Paxton (1960). Spriggs & Busch also present estimates of uncertainties in the replacement coefficients. With a single exception, and apart from an overall $\sim 2\%$ normalization uncertainty associated with uncertainties in the contribution of β-delayed neutrons, all of the uncertainties in experimentally-determined replacement coefficients are smaller than 3 cents per mole. The exception is for Ho embedded in Godiva. The uncertainty for Ho placed at the center of Godiva is 14 cents/mole, while for Ho placed 1.78 inches from the center of Godiva the uncertainty is 3.6 cents/mole. The x axis in these plots (labeled "z index") corresponds to the radius at which material was embedded. A value of 1 corresponds to material placed at the center of the assembly while larger indices correspond to material placed further out. We refer the reader to Spriggs & Busch for a list of radii.

To aid in interpreting the many plots we summarize in figures 1 and 2 discrepancies between calculated and experimentally determined replacement coefficients. In these plots the several values shown for a given atomic number typically correspond to the different radii at which each material was embedded. In a few cases there is ambiguity about which isotope of an element is represented. This will be cleared up in the following for those cases where important discrepancies exist.

Before presenting a critical look at the discrepancies between calculated and experimental replacement coefficients, we note that there are a few sources of uncertainty associated with our calculations. The formal uncertainty associated with convergence of the calculation is small because we adopted a convergence criterion of 10^{-6}. For a typical sample containing 0.1 moles, this implies an uncertainty in the replacement coefficient of approximately 0.5 cents/mole for Jezebel and approximately 0.15 cents/mole for Godiva. Another source of uncertainty relates to the choice of group structure used in the calculations. All of the replacement coefficients presented in this study were calculated using 17 neutron groups, which is the same number of groups (though likely not the same group structure) used by Spriggs & Busch. For a few cases we ran more expensive calculations using 87 neutron groups. The differences were found to be quite small, typically less that 1 cent/mole for this limited set of tests. Another possible source of uncertainty relates to the choice for zoning. We tried factors of two finer and coarser zoning and found non-negligible differences in some cases. For ^{239}Pu in Jezebel, for example, changes in how the problem is zoned can change calculated replacement coefficients by about 20 cents/mole out of $\sim$ 1500 (a 1.3% change). A third potential source of uncertainty relates to the extrapolation procedure used for estimating zero-volume coefficients. In a sense Spriggs & Busch avoided such uncertainties by using the same factor to extrapolate both their calculations and the experimental results. Since we do not use our calculated extrapolation factor in determining extrapolated values for the experimental results (we use the values from Spriggs & Busch), there is the possibility for some error in our extrapolation procedure. Uncertainties associated with extrapolation and with problem zoning will be discussed in more detail for specific cases below. As a rough estimate, the various uncertainties typically amount to an uncertainty in calculated replacement coefficients of about two cents per mole for Godiva and about 10 cents per mole for Jezebel.

3.2.1. Godiva Replacement Coefficients

For the Godiva assembly it is seen from figure 1 that the discrepancy between calculated and experimental replacement coefficients is smaller than about 3 cents/mole for most

materials. However, there are some notable discrepancies. For calculations using ENDL 99 the largest discrepancies occur for the following isotopes:

- ^{10}B: values calculated with ENDL 99 are systematically high. The discrepancy for boron embedded at the center of the Godiva assembly is about 10 cents/mole.

- ^{23}Na: values calculated with ENDL 99 are systematically high. The discrepancy for sodium embedded at the center of the Godiva assembly is about 10 cents/mole. Part of this is a consequence of our estimating a different slope for the replacement coefficient than was estimated by Spriggs and Busch. Our estimate for the central replacement coefficient for a finite (1/2 in by 1/2 in) cylinder is 5.0 cents/mole. The experimental value for this finite coefficient is 1.05 cents/mole. Still, Na has somewhat too large a worth in ENDL 99.

- In (natural): values calculated with ENDL 99 are low by about 9 cents/mole for indium placed at the center of Godiva. This discrepancy also holds for the finite volume replacement coefficient, so it is not a consequence of our incorrectly estimating the slope. There are no measurements for indium at other radii.

- W (natural): values calculated with ENDL 99 are high by about 10 cents/mole for tungsten placed at the center of Godiva. Part of this is a consequence of our estimating a different slope for the replacement coefficient than was estimated by Spriggs and Busch. Our estimate for the central replacement coefficient for a finite (1/2 in by 1/2 in) cylinder is 2.4 cents/mole. The experimental value for this finite coefficient is -3.3 cents/mole. Still, tungsten has too large a worth in ENDL 99. There are no measurements for tungsten at other radii.

- ^{240}Pu: values calculated with ENDL 99 are high by about 10 cents/mole for ^{240}Pu placed at the center of Godiva. This seems to be mostly an artifact of our estimating a different slope for the replacement coefficient than was estimated by Spriggs and Busch. Our estimate for the central replacement coefficient for a finite (1/2 in by 1/2 in) cylinder is 171 cents/mole. This is in relatively close agreement with the experimental value of 168 cents/mole for this finite coefficient. There are no measurements for ^{240}Pu at other radii.

For calculations using Livermore's translation of ENDF/B-V the largest discrepancies between calculation and experiment occur for

- ^{1}H: values calculated with ENDF/B-V are systematically low. The discrepancy between calculation and experiment for hydrogen placed at the center of Godiva is about

9 cents/mole, for hydrogen placed at larger radii the discrepancy is smaller. Calculations by Spriggs & Busch find similar results.

- ^{10}B: values calculated with ENDF/B-V are systematically high. For boron placed at the center of Godiva the discrepancy is about 10 cents/mole, for boron placed at larger radii the discrepancy is smaller. Calculations by Spriggs & Busch find similar results.

- W (natural): values calculated with ENDF/B-V are high by about 8 cents/mole for material placed at the center of Godiva. There are no experimental results for tungsten placed at larger radii. Spriggs & Busch found that with ENDF/B-V the discrepancy between the calculated and experimental replacement coefficient is about 3.5 cents/mole. Most of the disagreement between our calculations using ENDF and their calculations come from differences in our estimates of the slope of the replacement coefficient. Spriggs & Busch estimate that $r_0 - r_{50} \approx -1.1$cents/mole for tungsten at the center of Godiva. Our calculations give $r_0 - r_{50} \approx +2.4$cents/mole. If we adopt the Spriggs & Busch estimate for the slope our calculation for the zero volume replacement coefficient becomes 4.5 cents/mole, which is in better agreement with experiment and in close agreement with the value calculated using untranslated ENDF.

- ^{238}U: values calculated with ENDF/B-V are high relative to experimental values by about 10 cents/mole for material placed at the center of Godiva. This is in pronounced disagreement with calculations by Spriggs & Busch, who find that values calculated with ENDF/B-V agree well with experiment. We do not have the value of the slope of the replacement coefficient used by Spriggs & Busch. To test if differences in computational methods might be responsible for the difference we re-ran our calculations using 87 neutron groups and somewhat coarser problem zoning. The replacement coefficients calculated this way are found to be in good agreement with experiment and with calculations by Spriggs & Busch.

3.2.2. Jezebel Replacement Coefficients

From figure 2 it is seen that the mean discrepancy between calculated and experimental results for Jezebel is about four times larger than the mean discrepancy for materials embedded in Godiva. This can be partly understood from eq. 2, which defines a replacement coefficient as the difference between two k_{eff} values divided by the value of the delayed neutron fraction β characterizing the assembly. Since the value of β for Jezebel is about 3.4 times smaller than the delayed neutron fraction for Godiva, comparable discrepancies between calculated k values for the two assemblies will result in discrepancies in replacement

which are about 3.4 times larger for Jezebel than for Godiva.

The discrepancy between calculated and experimentally-determined replacement coefficients for Jezebel is smaller than about 20 cents/mole for most materials. For calculations using ENDL 99 the largest discrepancies occur for

- Ti (natural): the value calculated with ENDL 99 is too high relative to experiment by about 27 cents/mole for titanium placed at the center of Jezebel. This discrepancy also holds for the finite volume replacement coefficient, so it is not a consequence of our incorrectly estimating the slope. For titanium placed at larger radii the agreement is good.

- ^{165}Ho: the value calculated with ENDL 99 is too high relative to experiment by about 30 cents/mole for holmium placed at the center of Jezebel. Since the uncertainty in this experimental replacement coefficient is about 14 cents/mole, this is regarded as fair agreement.

- W (natural): the value calculated with ENDL 99 is high by about 34 cents/mole for tungsten placed at the center of Jezebel. This discrepancy also holds for the finite volume replacement coefficient, so it is not a consequence of our incorrectly estimating the slope. For tungsten placed at larger radii agreement between calculation and experiment is better.

- ^{233}U: for ^{233}U embedded in the hole with the next-to-largest radius in Jezebel the value calculated with ENDL 99 is too small relative to experiment by about 64 cents/mole. At other radii the agreement between calculation and experiment is better.

- ^{235}U: values calculated with ENDL 99 are systematically low. For ^{235}U placed at the center of Jezebel the discrepancy is about 25 cents/mole.

- ^{237}Np: the value calculated with ENDL 99 is too high relative to experiment by about 80 cents/mole for neptunium placed at the center of Jezebel. Part of this is a consequence of our estimating a different slope for the replacement coefficient than was estimated by Spriggs and Busch. Our estimate for the central replacement coefficient for a finite (1/2 in by 1/2 in) cylinder is 704 cents/mole. The experimental value for this finite coefficient is 669 cents/mole. Still, neptunium has too large a worth in ENDL 99. There are no experimental results for neptunium placed at other radii.

- ^{239}Pu: values calculated with ENDL 99 are too low by about 25 cents/mole for plutonium placed near the center of Jezebel. Note that there is a sizable uncertainty in our

calculation (about 10 cents per mole), and also that the uncertainty in β_{eff} for Jezebel implies an uncertainty in this replacement coefficient of approximately 30 cents/mole.

For calculations using ENDF/B-V the largest discrepancies occur for

- Ti (natural): the value calculated with ENDF/B-V is too high relative to experiment by about 27 cents/mole for titanium placed at the center of Jezebel. For titanium placed at larger radii the agreement is good. The discrepancy for titanium at the center of Jezebel is in marked disagreement with results calculated by Spriggs & Busch. Those authors find that the replacement coefficient near the center of the assembly is about 8 cents/mole too high. Most of the disagreement between our calculations using ENDF and their calculations come from differences in our estimates of the slope of the replacement coefficient. Spriggs & Busch estimate that $r_0 - r_{50} \approx -3.8$cents/mole for titanium at the center of Jezebel. Our calculations give $r_0 - r_{50} \approx +6.8$cents/mole. If we adopt the Spriggs & Busch estimate for the slope, our estimate for the zero volume replacement coefficient decreases by about 10 cents/mole. This improves agreement between our estimate and that calculated by Spriggs & Busch, though the calculated replacement coefficient for titanium is still high relative to experiment.

- W (natural): the value calculated with ENDF/B-V is high by about 33 cents/mole for tungsten placed at the center of Jezebel. For tungsten placed at larger radii agreement between calculation and experiment is better. Spriggs & Busch calculate a replacement coefficient that is about 10 cents/mole too high for tungsten at the center of Godiva. The discrepancy between our results and theirs is not accounted for by consideration of the slope of the replacement coefficient. To test if differences in computational methods might be responsible for the difference we re-ran our calculations using 87 neutron groups and somewhat coarser problem zoning. The replacement coefficients calculated this way are found to be in good agreement with experiment and with calculations by Spriggs & Busch.

- ^{233}U: for ^{233}U embedded in the hole with the next-to-largest radius in Jezebel the value calculated with ENDF/B-V is too small relative to experiment by about 64 cents/mole. At other radii the agreement between calculation and experiment is better. Spriggs and Busch calculate a replacement coefficient that is larger than experiment by about 25 cents/mole, though the precise value is hard to read from their plot. This discrepancy between our calculation and theirs is accounted for by differences in our estimates of the slope of the replacement coefficient. They find $r_0 - r_{50} \approx 97$cents/mole, whereas our calculations give $r_0 - r_{50} \approx 147$cents/mole - a difference of about 50.

- ^{237}Np: the value calculated with ENDF/B-V is too high relative to experiment by about 150 cents/mole for neptunium placed at the center of Jezebel. There are no experimental results for neptunium placed at other radii. Spriggs and Busch also find a value that is too high, by about 125 cents/mole.

- ^{239}Pu: values calculated with ENDF/B-V are too low by about 25 cents/mole for plutonium placed near the center of Jezebel. Spriggs & Busch find closer agreement, though the exact value is hard to tell from their plots. The discrepancy between calculations and experiments is within the $\sim 2\%$ uncertainty arising from the uncertainty associated with β for Jezebel.

4. Summary

We have developed a test suite based on S_n calculations of critical assemblies and replacement coefficients for materials embedded in the Godiva and Jezebel critical assemblies. This will be used to check the quality of data and the fidelity of translations from the ENDF format to the ENDL format. Currently there 15 assemblies in the test suite and it is likely that more will be added. As discussed in the appendix, the suite is driven by python classes and is quite easy to use. Checking all of the critical assemblies in the suite and calculating replacement coefficients for a great many materials can be done with a dozen or so simple lines of code.

As an illustration and first application of the tests we have examined the quality of data in ENDL 99 and the accuracy of a previous translation from ENDF/B-V to the ENDL format. Our study found a few potentially important shortcomings in the ENDL 99 data

- Calculations using ENDL 99 find that k_{eff} for Jezebel, a bare metal assembly and likely one of the most accurately characterized assemblies, is too low by about 0.006.

- For the Godiva assembly, calculations using ENDL 99 find sodium and tungsten to have replacement coefficients that are too large relative to experiment, while indium is found to have a replacement coefficient that is too small relative to experiment.

- For the Jezebel assembly, calculations with ENDL 99 find titanium, tungsten and neptunium to have replacement coefficients that are too large relative to experiment.

Our use of replacement coefficient calculations has been relatively crude. Because the worth measurements are associated with small errors, they could in principal be used to provide stringent constraints on different cross sections for different materials. We have

not really pursued this, but instead have just noted where the largest discrepancies exist. A better treatment would likely require us to carefully quantify and reduce uncertainties associated with our calculations. These efforts are now underway.

Regarding the quality of the ENDF/B-V → ENDL translation, our study found no significant problems apart from calculations for a steel reflected assembly and an iron reflected assembly. Discrepancies for these two assemblies seem most likely to arise from problems with our S_n calculations rather than problems with the data.

We would like to thank John Compton of B-division for helping us to get the AMTRAN tests running. We are also indebted to Chris Clouse for many patient discussions on the finer details of deterministic calculations and to M. Scott McKinley for doing MC calculations for the Fe and Ni reflected assemblies. Lastly, we thank Greg Spriggs for a series of lectures and many informative discussions about critical assemblies and the quality of measurements for them.

A. A brief users manual for the test suite

This test suite is a set of Python classes that "wrap" the AMTRAN S_n code and provide support for some calculations related to replacement coefficients. Because the test suite is presented in this way, it is simple to automate running critical assemblies, for example, as part of a larger data V&V testing project. In the next two subsections, we illustrate the use of the Python wrapper classes with examples found in the `examples/` subdirectory. Following this we detail the two main Python classes, `Amtran_Assembly` and `replacementProject` and how they interact with AMTRAN. Both of these classes allow the user to quickly run a simulation using any of the decks in the `decks/` subdirectory of this project.

A.1. Examples

For our first example, we illustrate the simplest use of the `Amtran_Assembly` wrapper class with the `runDeck.py` script found in the `examples/` subdirectory:

```
import sys
sys.path.append("/usr/gapps/data/nuclear/testSuite/Src")
from Assembly_Amtran import *
```

```
deckname="jezebel.in"
a=Amtran_Assembly(deckName=deckname)
a.setDeckValue("ixsecs","1")
a.setIdgroup("77")
a.runProblem()
print a.keff
a.clean()
```

In this example, the first three lines ensure that the main class, `Amtran_Assembly`, of the test suite is loaded correctly. The next line specifies the filename for the template for an assembly: `jezebel.in`. The next line actually loads the template into an instance of the class `Amtran_Assembly`. The next two lines set various parameters for this run. In the next line, we actually run the problem through AMTRAN, via the `runProblem()` call. At the end of this run, the k_{eff} and other run parameters are saved within the `Amtran_Assembly` instance with which we are working. We print k_{eff} on the next line. Finally, we clean up the temporary files produced while running this assembly.

In our second example, we illustrate the use of the `replacementProject` wrapper class. This is a more complicated example simply because each `replacementProject` instance creates and runs a list of `Amtran_Assembly` instances so that it can perform the extrapolation needed to extract the replacement coefficient. Below we give a simple driver script that calculates replacement coefficients for ^{238}U in Godiva.

```
import sys
sys.path.append("/usr/gapps/data/nuclear/testSuite/Src")
from replacementProject import *
deckname="godivaReplacement.in"
beta=0.00688
holeZList=[0.0*2.54, 1.242*2.54, 1.930*2.54, 2.512*2.54, 3.142*2.54, 3.206*2.54]
ixsecs=9

workDir="/g/g13/pruet1/testSuite/newReplacements/92238Godiva''
r=replacementProject(beta=beta,holeZList=holeZList,deckName=deckname,\
    workDir=workDir,ixsecs=ixsecs)

fillZA=92238
rs,rb,r0=r.getReplacement(fillZA,0)
rs,rb,r0=r.getReplacement(fillZA,1)
rs,rb,r0=r.getReplacement(fillZA,2)
```

```
rs,rb,r0=r.getReplacement(fillZA,3)
rs,rb,r0=r.getReplacement(fillZA,4)
rs,rb,r0=r.getReplacement(fillZA,5)
```

This example begins by importing the various Python components that we need for this problem. After this, we set `beta` for the Godiva assembly, the list of radii at which worth measurements were done for Godiva (in holeZList), and the flag to denote that we will use ENDF/B-V data (`ixsecs=9`). Next, the local variable `r` is set to our instance of the `replacementProject` class. The constructor just sets up the input decks and the workspace. It also does a sequence of calculations to find values of k_{eff} for Godiva with empty voids at the radii specified by holeZList. Following this the replacement coefficients for ^{238}U are found for each of the five radii. The `getReplacement` calculations return rs - the replacement coefficient for a small sample (1/2 in. by 1/2 in.), rb - the replacement coefficient for a large sample (3/4 in. by 3/4 in), and r0 - the extrapolated zero volume coefficient. These results are written to a subdirectory in the working directory to a file called "results".

A.2. The Python Project Files

`class Amtran_Assembly` This class provides a simple interface with AMTRAN. It can read and set nearly any parameter in an AMTRAN input deck, run a problem and return the results. Furthermore, it provides member functions that simplify creating cylindrical holes in an assembly for studying replacement coefficients.

`def __init__(self, deckName, ndfFile, workDir, codePath, deckPath):` Constructor for `Amtran_Assembly` class. Arguments are defined as follows:

`deckName` – Name of the deck to use as template for this run.

`ndfFile` – Location of the `ndf` file to use for the nuclear data.

`workDir` – Working directory name - Defaults to a file in the users TMP directory.

`codePath` – Path to the AMTRAN executable,
Defaults to /usr/gapps/data/nuclear/testSuite/gpsExecutable/amtran.kd0208.

`deckPath` – Path to the AMTRAN input decks,
Defaults to /usr/gapps/data/nuclear/testSuite/decks.

`def clean(self):` Clean the work directory `workDir`.

`def collectResults(self):` Parse the results read in the `readResults()` member function.

`def getValueFromDeck(self, itemName):` Gets the value of a given quantity from the input deck. Returns `None` if it can't find it.

`def initializeDeck(self):` Reads the input deck template.

`def makeScript(self):` Create the script that controls running the problem.

`def readResults(self):` Read the output files created when running the problem.

`def runProblem(self):` Main driver routine. Runs the problem, parses the results then cleans up the work directory.

`def runScript(self):` Execute the script created by the `makeScript()` member function.

`def setDeckValue(self, itemName, itemValue):` Sets the value of `itemName` to `itemValue` in deck. If the deck does not initially contain a variable named `itemName` then this returns a 0 and does nothing. If the deck does contain a variable named `itemValue` this makes the replacement and returns 1.

`def setEmptyCylinder(self, zPosition, radius, length, density):`
Sets properties of the empty cylinder in the `cog` part of the input deck. This assumes that `cogc` begins the `cog` block, that `assign-md` begins the density part of this block, and that the filled cylinder corresponds to the first material.

`def setEmptyReplacement(self, zPosition, radius, length, density):`
Modifies deck to have an empty (well - of a nominal low density) material.

`def setFilledCylinder(self, zPosition, radius, length, density):`
Sets properties of the filled cylinder in the `cog` part of the input deck. This assumes that `cogc` begins the `cog` block, that `assign-md` begins the density part of this block, and that the filled cylinder corresponds to the first material.

`def setFilledReplacement(self, ZA, zPosition, radius, length, density):`
Modifies a deck to have a replacement material made of `ZA`. The replacement material is assumed to be a cylinder of radius `radius` and length `length` with its center at `zPosition`. It is assumed in the replacement deck that the first `isofrac` corresponds to the cylinder.

`def setIdgroup(self, idgroup):`
Sets the data set's id group

`def writeDeck(self):` Write out the deck to the `workDir`.

`class replacementProject:`

This automates the calculation of replacement coefficients. As we discuss in the main text, to compute the replacement coefficient of a material in a critical assembly, we must create a hole in an assembly, measure k_{eff} and then extrapolate to find the value of k_{eff} in a zero radius hole. Almost all of this is done internally within `replacementProject`.

`def __init__(self, beta, holeZList, deckName, smallRadius=0.635, smallLength=1.27, ndfFile=None, workDir=None, codePath=None, deckPath=None, ixsecs=None, idgroup=None, k0Small=None, k0Big=None):`

`replacementProject` class constructor. Arguments are as follows:

`beta` – Contribution of delayed neutrons to the k_{eff} for the assembly under consideration.

`holeZList` – List of radii (in cm) at which replacement coefficients are to be calculated.

`deckName` – Name of the deck to use as template for this run (at present only godivaReplacement and jezebelReplacement are available).

`smallRadius` – Radius of the smallest holes. Default is 1/2 in.

`bigRadius` – Radius of the largest holes. Default is 3/4 in.

`ndfFile` – Location of the `ndf` file to use for the nuclear data.

`workDir` – Working directory name. Defaults to a place in the users TMP directory.

`codePath` – Path to the AMTRAN executable.
Default is /usr/gapps/data/nuclear/testSuite/gpsExecutable/amtran.kd0208.

`deckPath` – Path to the AMTRAN input decks.
Defaults is /usr/gapps/data/nuclear/testSuite/decks/.

`ixsecs` – Chooses cross section database (see AMTRAN notes below).

`idgroup` – Data set's id group (see `Amtran_Assembly` documentation).

`def getAmtranDeck(self):` Sets up and returns an `Amtran_Assembly` for part of the problem.

`def getKeff(self, fillZA, zIndex, smallOrBig):` Gets keff for the named `za`, at the z position `zindex` if `smallOrBig = "small"`, then it gets keff for the small hole if `smallOrBig = "big"`, then it gets keff for the big hole.

`def getr0(self, rcSmall, rcBig):` Calculates zero volume replacement coefficient by assuming the coefficient to be a linear function of the effective radius (see report by Spriggs and Busch).

`def getReplacement(self, fillZA, zIndex):` Gets replacement coefficient for the `filledZA`, at the z position `zindex` the scale factor applies to all dimensions of the filled cylinder and can be used to estimate zero volume replacement coefficients.

`def getSubWorkDir(self):` Makes a work directory branched from `self.workDir` to calculate things – uses `workIterator` to iterate name.

`def initizializek0(self, smallOrBig):` Get the list of $k_{\rm eff}$'s for the different empty holes in the critical assembly.

A.3. AMTRAN input deck basics

AMTRAN is the S_n transport code that we use to model the critical assemblies we consider. The best source for information about AMTRAN is the "AMTRAN Users Manual" AMTRAN (2005), included in the AMTRAN code distribution. Table 4 lists a few basic control parameters. For data validation work the user need only know about the few parameters for the amtran and replacement coefficient classes described above.

REFERENCES

The AMTRAN Users Guide, 2005, can be found in /usr/gapps/amtran/doc/amtran.htm on the LC computing machines.

Cross Section Evaluation Working Group 1991, "Cross Section Evaluation Working Group Benchmark Specifications", ENDF-202, BNL 19302.

Engle, L. B., Hansen, G. E. & Paxton, H. C. 1960, "Reactivity Contributions of Various Materials in Topsy, Godiva, and Jezebel", Nucl. Sci. Eng. 8, 543.

Frankle, S. 1999, "A Suite of Criticality Benchmarks for Validating Nuclear Data", LA-13594.

Frankle, S. 1999, "Criticality Benchmark Results Using Various MCNP Data Libraries", LA-13627.

Hansen, G. E. & Maier, C. 1953, "Material Replacement Experiments: Theory and Measurements for the Lady Godiva Assembly", LA-1525.

Hansen, G. E. & Maier, C. 1960, "Perturbation theory for fast neutron systems", Nucl. Science & Eng. 8, 515.

T. Hill, G. Hedstrom, B. Beck, C. Hagmann, D. McNabb, 2003, "Final Release of ENDF/B-V for Use with LLNL Codes," LLNL Report UCRL-ID-152901.

NEA Nuclear Science Committee 1998, "International Handbook of Evaluated Criticality Safety Benchmark Experiments", NEA/NSC/DOC(95)03, 1998 edition.

Spriggs, G. D. & Busch, R. D. 2002, "Evaluation of MENDF5 and MENDF6 using measured integral parameters in Godiva-I and Jezebel", LANL Report LA-UR-02-1809.

van der Marck, S.C., 2005, "β_{eff} calculations using ENDF/B-VII nuclear data", NRG.

Table 1. Critical Assemblies in the current Test Suite

assembly name	fissile material	reflector	input deck name
Jezebel	Pu (92% 239)	none	`jezebel.inp`
Godiva	U (94% 235)	none	`godiva.inp`
U233-MET-FAST-001	U (98 % 233)	none	`u233metfast001.inp`
U233-MET-FAST-002	U (98 % 233)	HEU (93% 235)	`u233metfast002.inp`
U233-MET-FAST-004	U (98 % 233)	tungsten	`u233metfast004.inp`
HEU-MET-FAST-003l	U (94% 235)	nickel	`heumetfast003.inp`
IEU-MET-FAST-005	U (36% 235)	steel	`ieumetfast005.inp`
HEU-MET-FAST-019	U (87% 235)	graphite	`heumetfast019.inp`
HEU-MET-FAST-020	U (87% 235)	poly	`heumetfast020.inp`
HEU-MET-FAST-028	U (93% 235)	uranium (99% 238)	`heumetfast028.inp`
PU-MET-FAST-002	Pu (74% 239, 14% 240)	none	`pumetfast002.inp`
PU-MET-FAST-008a	Pu (91% 239)	thorium	`pumetfast008a.inp`
PU-MET-FAST-011	Pu (95% 239)	water	`pumetfast011.inp`
PU-MET-FAST-018	Pu (92 % 239)	Be	`pumetfast018.inp`
PU-SOL-THERM-011a	Pu (96% 239)	[solution assembly]	`pusotherm011.inp`

Table 2. Calculated and Experimental Results for Assemblies in the Test Suite

assembly name	experimental $k_{\rm eff}$	ENDF/B-V $k_{\rm eff}$[a]	ENDF/B-V $k_{\rm eff}$[b]	ENDL 99 $k_{\rm eff}$[c]
Jezebel[d]	1.000 ± 0.002	0.9982 ± 0.0011	0.9978	0.9938
Godiva[e]	1.000 ± 0.001	0.9969 ± 0.0012	0.9988	1.0008
U233-MET-FAST-001[f]	1.000 ± 0.001	0.9942 ± 0.0011	0.9933	0.9977
U233-MET-FAST-002[f]	1.000 ± 0.001	0.9952 ± 0.0011	0.9956	1.0008
U233-MET-FAST-004[f]	1.000 ± 0.0007	1.0037 ± 0.0012	1.0041	0.9988
HEU-MET-FAST-003l[e,*]	1.000 ± 0.003	1.0148 ± 0.0013	1.0486	1.0296
IEU-MET-FAST-005[e,*]	1.000 ± 0.0021	1.0112 ± 0.0011	1.0374	1.0256
HEU-MET-FAST-019[e]	1.000 ± 0.003	1.0040 ± 0.0012	1.0045	1.0088
HEU-MET-FAST-020[e]	1.000 ± 0.003	0.9958 ± 0.0013	0.9956	0.9989
HEU-MET-FAST-028[e]	1.000 ± 0.003	1.003 ± 0.001	1.0044	0.9981
PU-MET-FAST-002[d]	1.000 ± 0.002	0.9979 ± 0.0011	0.9999	0.9982
PU-MET-FAST-008a[d]	1.000 ± 0.003	1.0042 ± 0.0012	1.0062	0.9985
PU-MET-FAST-011[d]	1.000 ± 0.001	1.0009 ± 0.0014	0.9748	0.9745
PU-MET-FAST-018 [d]	1.000 ± 0.003	0.9999 ± 0.0013	0.9966	0.9974
PU-SOL-THERM-011a[g]	1.000 ± 0.0052	1.0019 ± 0.0011	1.0305	1.0278

[a] Taken from Frankle (1999b). This $k_{\rm eff}$ was calculated using an untranslated version of ENDF/B-V and MCNP. These MCNP calculations include $S_{\alpha\beta}$ corrections to neutron scattering.

[b] Calculated using Livermore's translation of ENDF/B-V and the AMTRAN S_n code. None of the AMTRAN calculations include $S_{\alpha\beta}$ corrections.

[c] Calculated using ENDL 99 and the AMTRAN S_n code.

[d] For the plutonium metal assemblies the delayed neutron fraction was approximated to be $\beta_{eff} = 0.00202$, the value appropriate for Jezebel.

[e] For the HEU assemblies the delayed neutron fraction was approximated as $\beta_{eff} = 0.00688$, the value appropriate for Godiva. This same value was adopted for the intermediate-enriched assembly IEU-MET-FAST-005. The delayed neutron fraction for Big Ten (an IEU assembly with 10% enrichment) is estimated as $\beta_{eff} = 0.0072 \pm 0.0001$, indicating that the difference in delayed neutron fractions between HEU and IEU is not appreciable for our purposes.

[f] For U233-MET-FAST-001 the measured value of the delayed neutron fraction is $\beta_{eff} = 0.0029 \pm 0.0001$. We adopted a value of $\beta_{eff} = 0.0029$ for all ^{233}U assemblies.

[g] No β_{eff} correction was made for this. As discussed in the text, our neglect of self-shielding and $S_{\alpha\beta}$ corrections renders calculations for thermal assemblies unreliable.

[*] As discussed in the text, our S_n calculations for these two assemblies seem unreliable. Both iron and nickel have high lying resonances which can cause trouble for calculations like ours that do not include self shielding. Monte Carlo calculations using ENDL 99 for IEU-MET-FAST-005, for example, found $k_{\rm eff} = 0.9978 \pm 0.0001$, while Monte Carlo calculations using ENDL 99 found $k_{\rm eff} = 1.0056$ for IEU-MET-FAST-005.

Table 3. A closer look at Jezebel

data used	k_{eff}
ENDL99	0.9938
ENDL99 with cross section from ENDFB5	0.9921
ENDL99 with spectrum from ENDFB5	0.9987
ENDL99 with $\bar{\nu}$ from ENDFB5	0.9948
ENDL99 with cross section and spectrum from ENDFB5	0.9964
ENDL99 with c.s. and spectrum and $\bar{\nu}$ from ENDFB5	0.9973
ENDFB5	0.9978
ENDFB5 with cross section from ENDL99	1.0000
ENDFB5 with spectrum from ENDL99	0.9935
ENDFB5 with $\bar{\nu}$ from ENDL99	0.9969
ENDFB5 with cross section and spectrum from ENDL99	0.9952
ENDFB5 with c.s. and spectrum and $\bar{\nu}$ from ENDFB5	0.9943

Table 4. AMTRAN input deck options relevant to the test suite.

option	type	meaning
		General options
`probname`	`str`	Problem name
`probinfo`	`str`	Problem description
		Nuclear data set options
`idgroup`	`int`	Specifies predefined sets of energy group boundaries and number of energy groups. When running NDF, idgroup 4 is an 87 group set, idgroup 6 is a 175 group set, and idgroup 7 is 230 group set.
`ndffid`	`str`	Specifies whether to use the older 87 group NDF data files or the newer 175 or 230 group files. Valid values are "230", "175" and "87".
`ievt`	`int`	What kind of calculation to do (`ievt`=1 means do k_{eff} calculation).
`ixsecs`	`int`	Chooses cross section database. 0 and 3 are special 2 group sets, 1 is NDF, 2 is RSIC, and 9 corresponds use ENDF/B-V
`ndflib`	`str`	Directory in `/usr/gapps/data/nuclear` in which to grab data, defaults to `endl`
`ndfuse`	`str`	Subdirectory of `ndflib` to look for data
		Problem geometry options
`nmat`	`int`	Number of materials in the problem.
`isofrac[`i`]`	`array`	Material in the i^{th} region. The array is `isofrac[nm][`i`][2]` where `nm` is the material number and should vary from 0 to `nmats`-1, i is the isotope number, starting at 0, and the final index holds the clyde number and atom fraction respectively.
`bigr[`i`]`	`array`	Array of radial points in i^{th} region (smallest to largest).
`rhoi[`i`]`	`array`	Array of densities at the radial points given in `bigr[`i`]`. Densities are linearly interpolated between points.
`iregsphr[`i`]`	`int`	Material number to be used the i^{th} region.
		Temperature options
`temp_effects`	`bool`	Turn on/off zone dependent temperatures.
`tempi[`i`]`	`float`	Temperature of i^{th} region, in MeV (e.g. 2.58e-8 is room temperature).

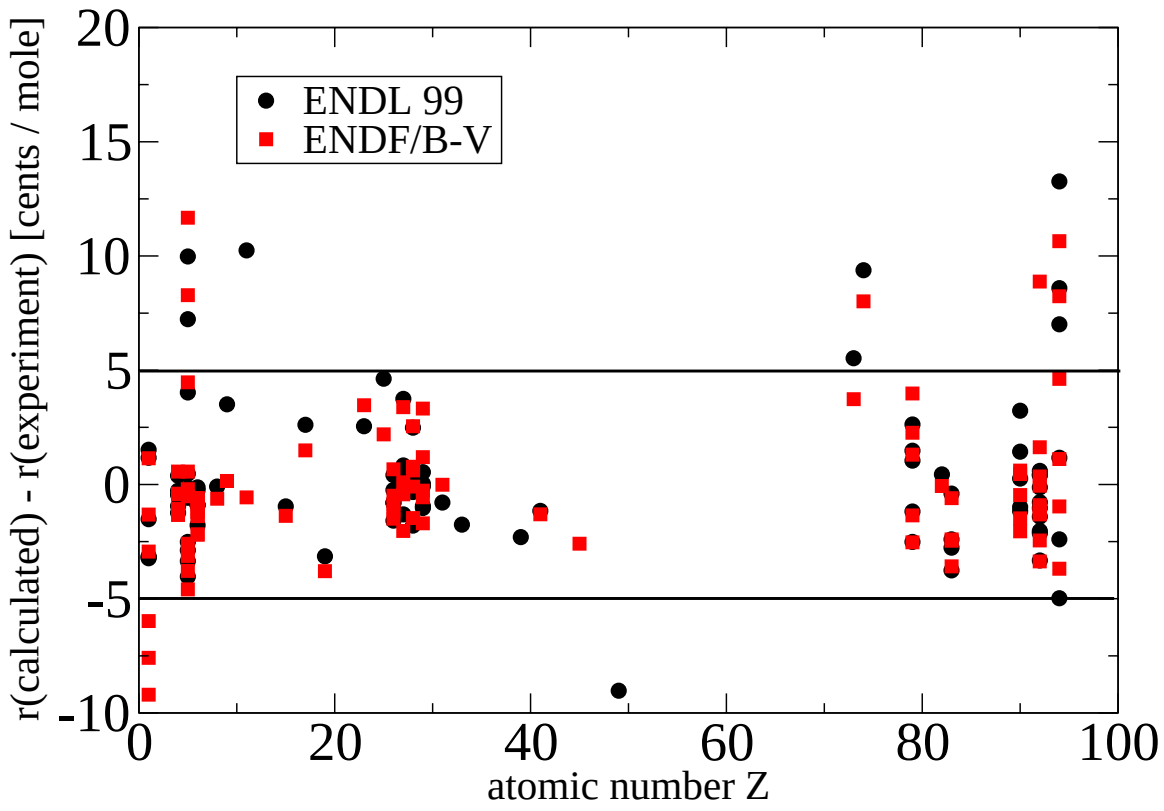

Fig. 1.— Comparison between calculated and experimental replacement coefficients for materials in the Godiva assembly. Values calculated using both ENDL 99 and Livermore's translation of ENDF B/V are shown. The black lines here delimit a range of ±5 cents/mole.

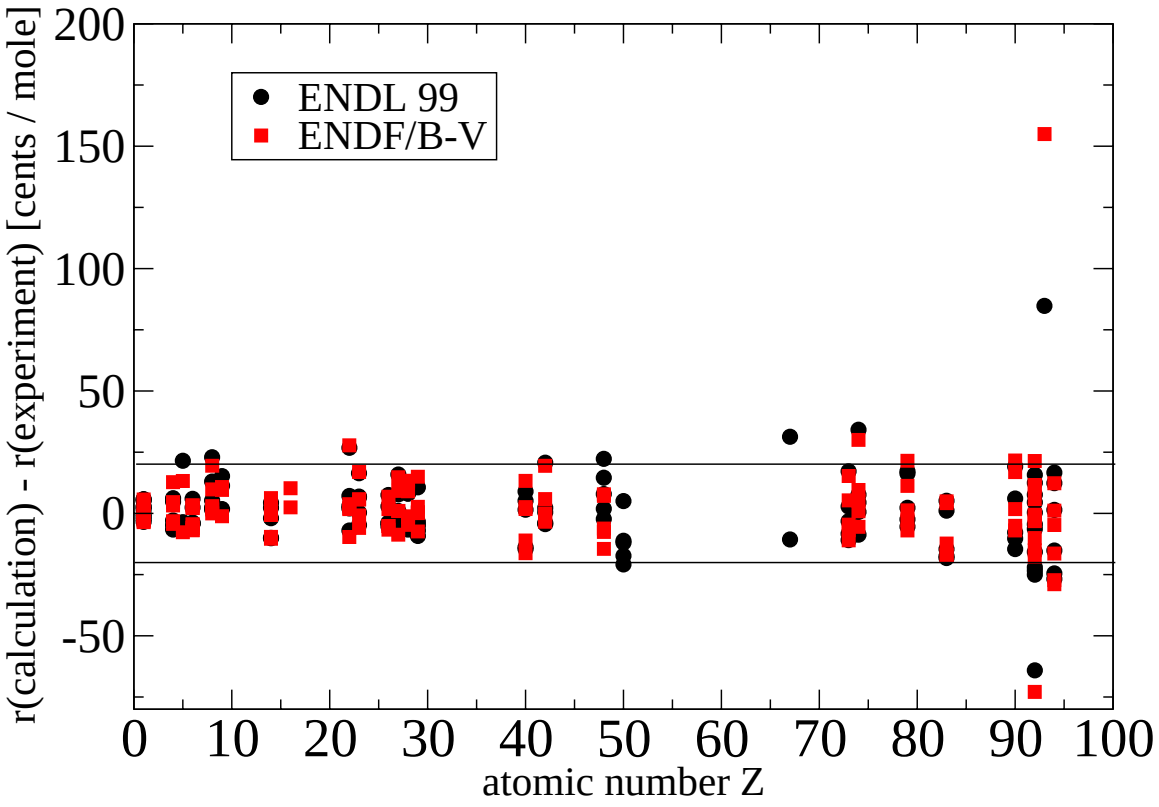

Fig. 2.— Comparison between calculated and experimental replacement coefficients for materials in the Jezebel assembly. Values calculated using both ENDL 99 and Livermore's translation of ENDF B/V are shown. The black lines denote a range of ±20 cents/mole.

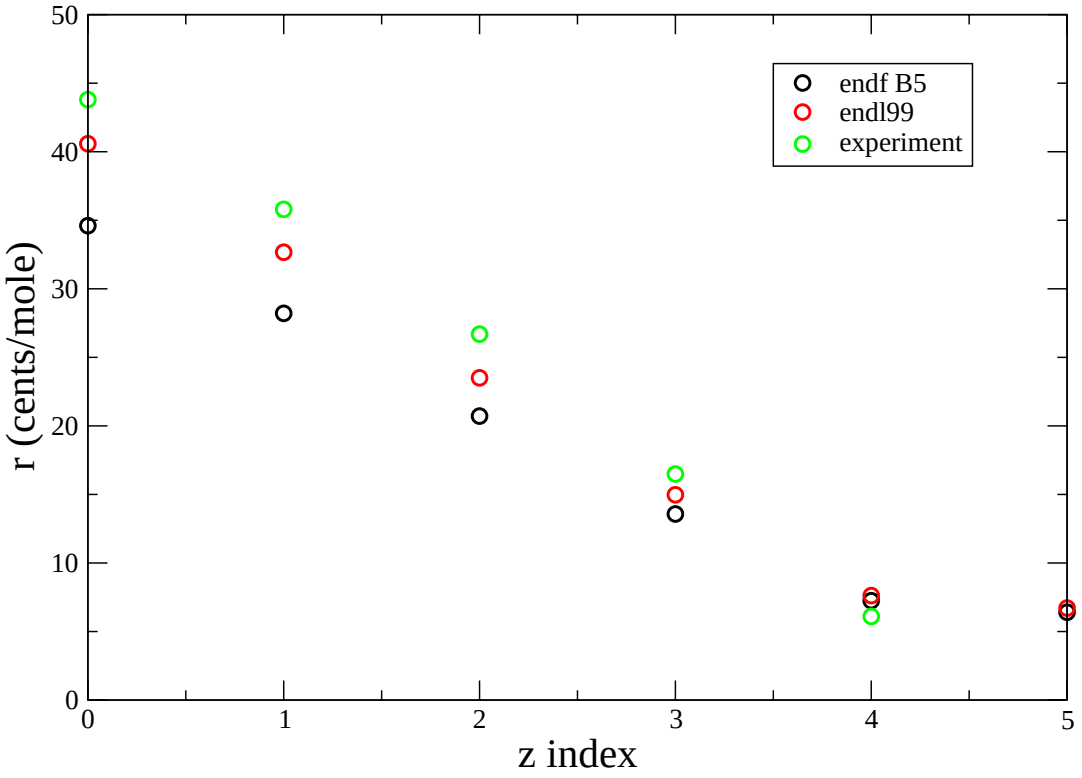

Fig. 3.— Replacement coefficients for ZA=1001 in the Godiva assembly.

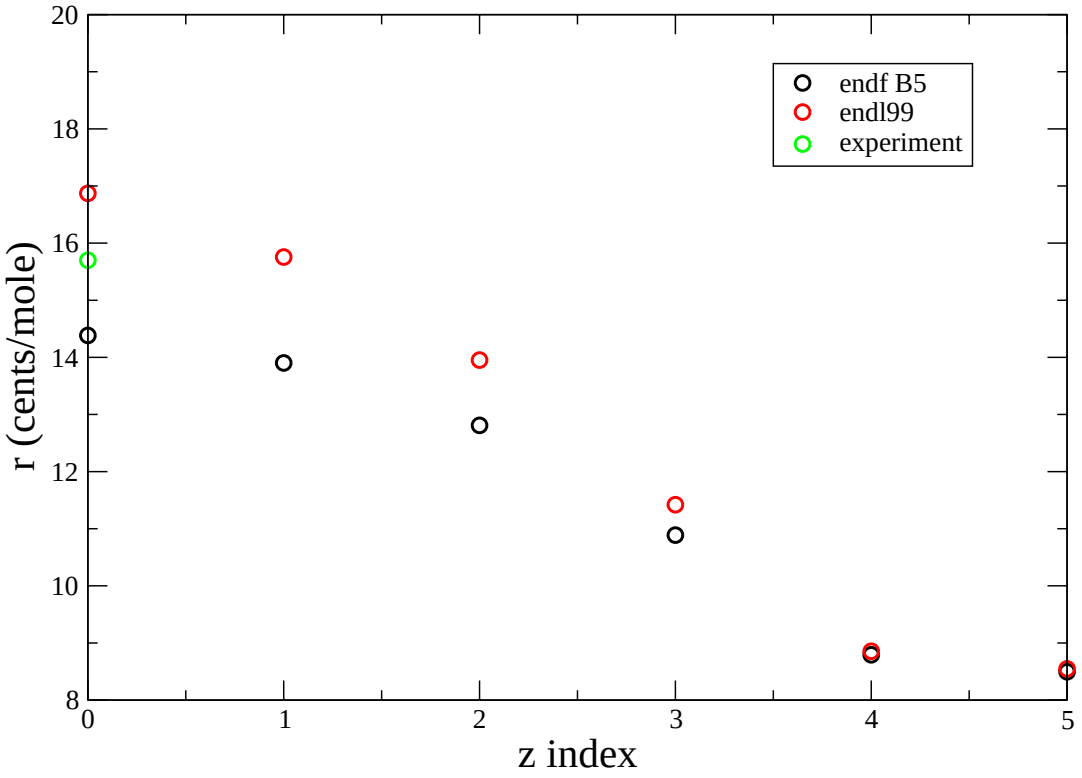

Fig. 4.— Replacement coefficients for ZA=1002 in the Godiva assembly.

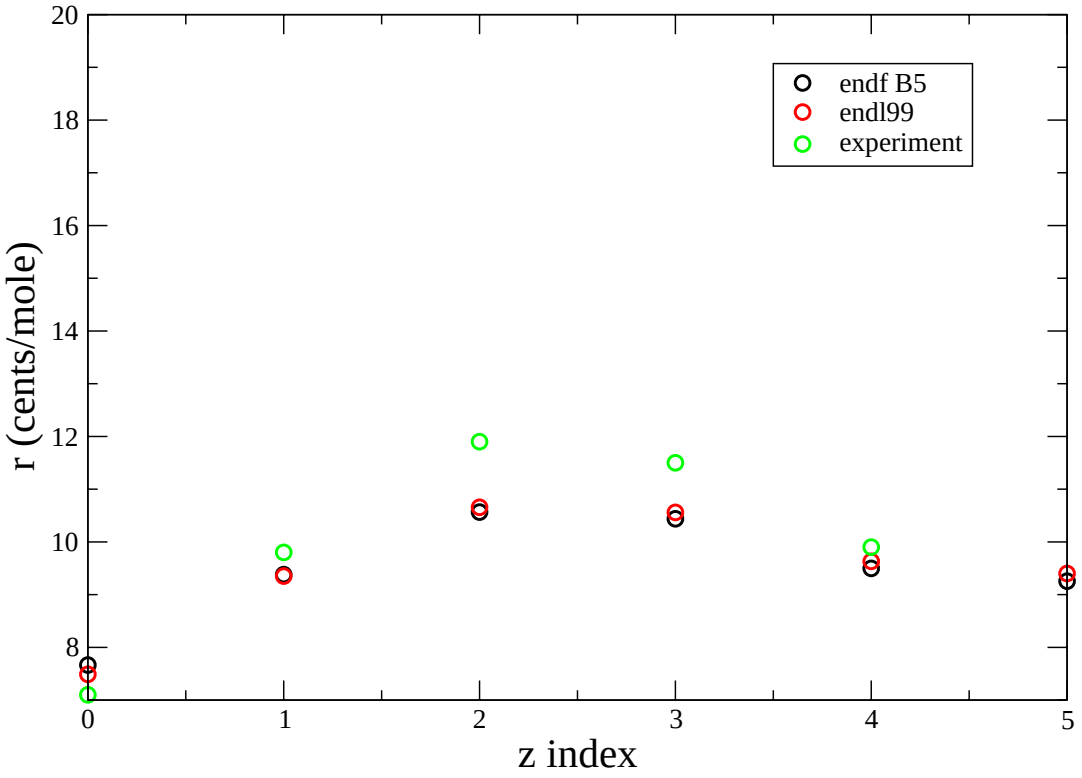

Fig. 5.— Replacement coefficients for ZA=4009 in the Godiva assembly.

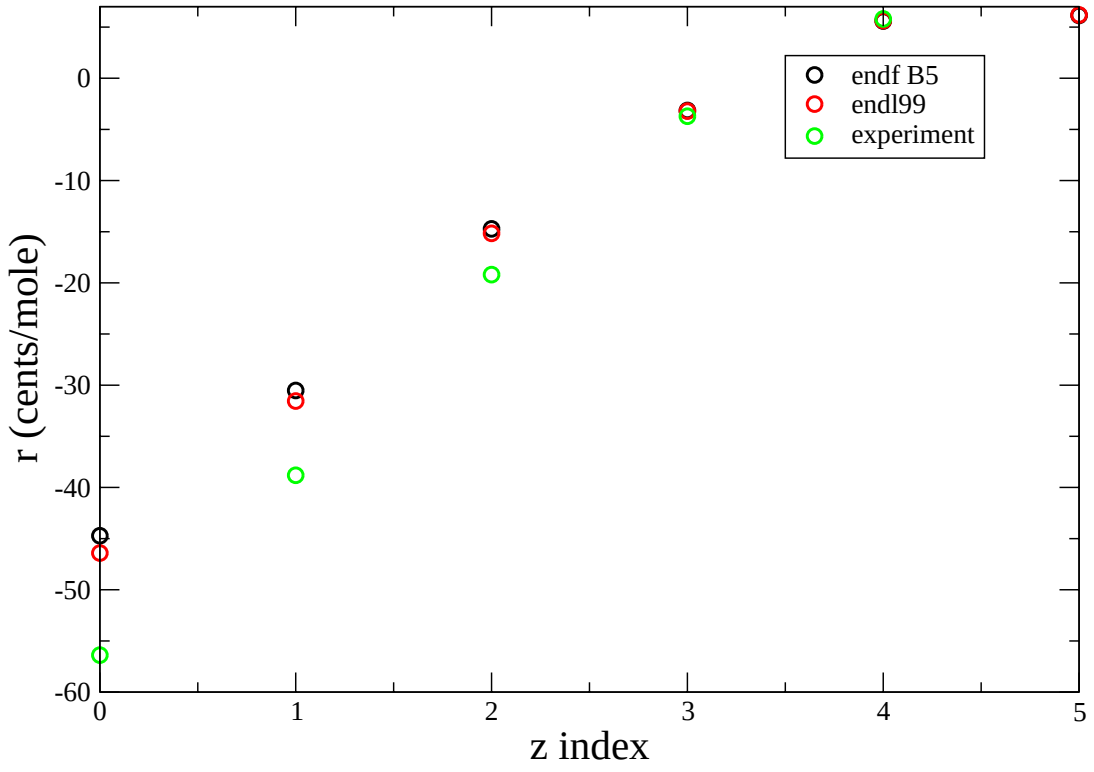

Fig. 6.— Replacement coefficients for ZA=5010 in the Godiva assembly.

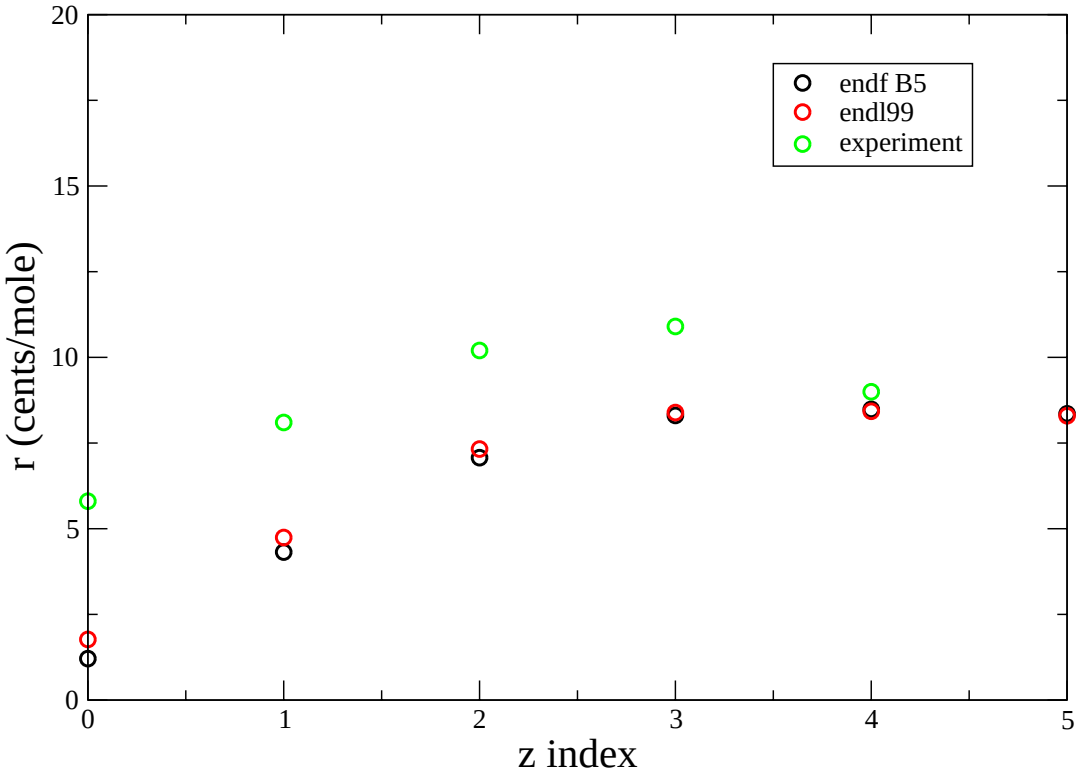

Fig. 7.— Replacement coefficients for ZA=5011 in the Godiva assembly.

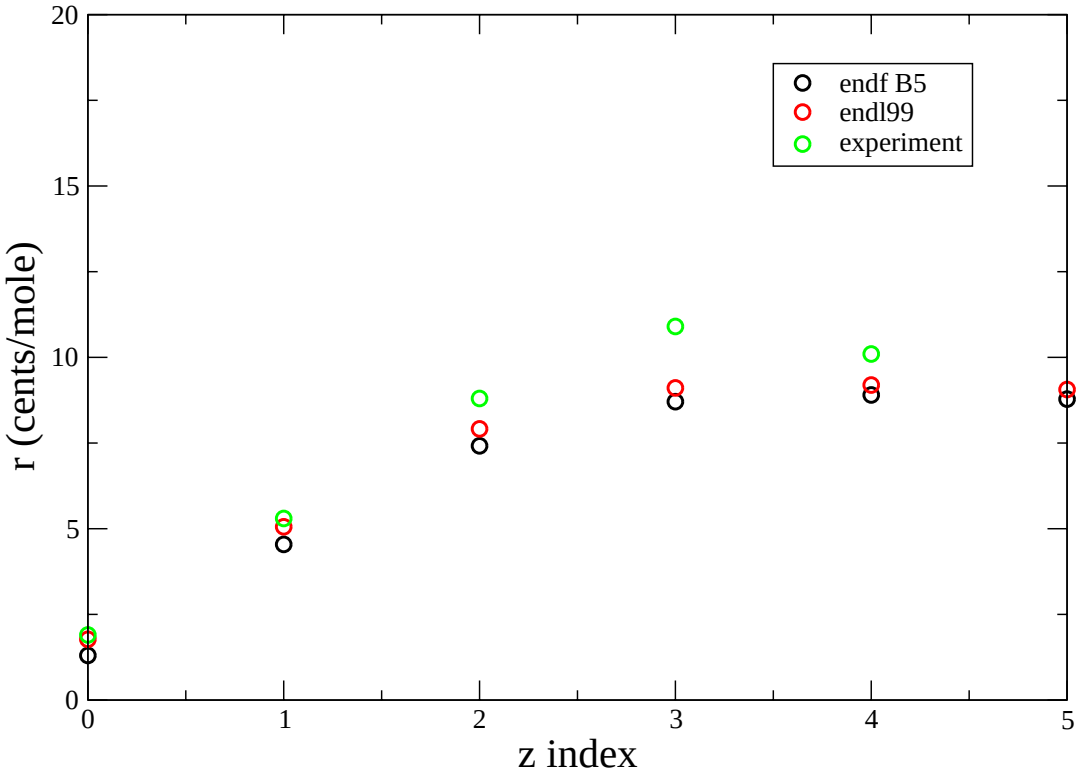

Fig. 8.— Replacement coefficients for ZA=6012 in the Godiva assembly.

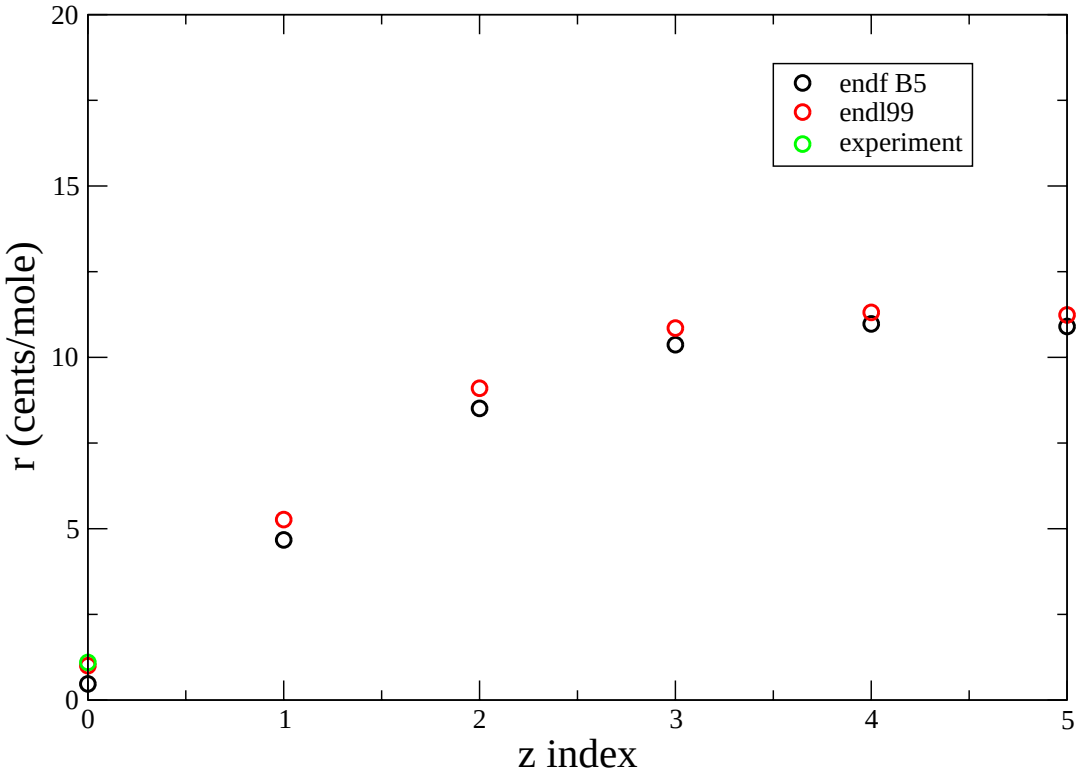

Fig. 9.— Replacement coefficients for ZA=8016 in the Godiva assembly.

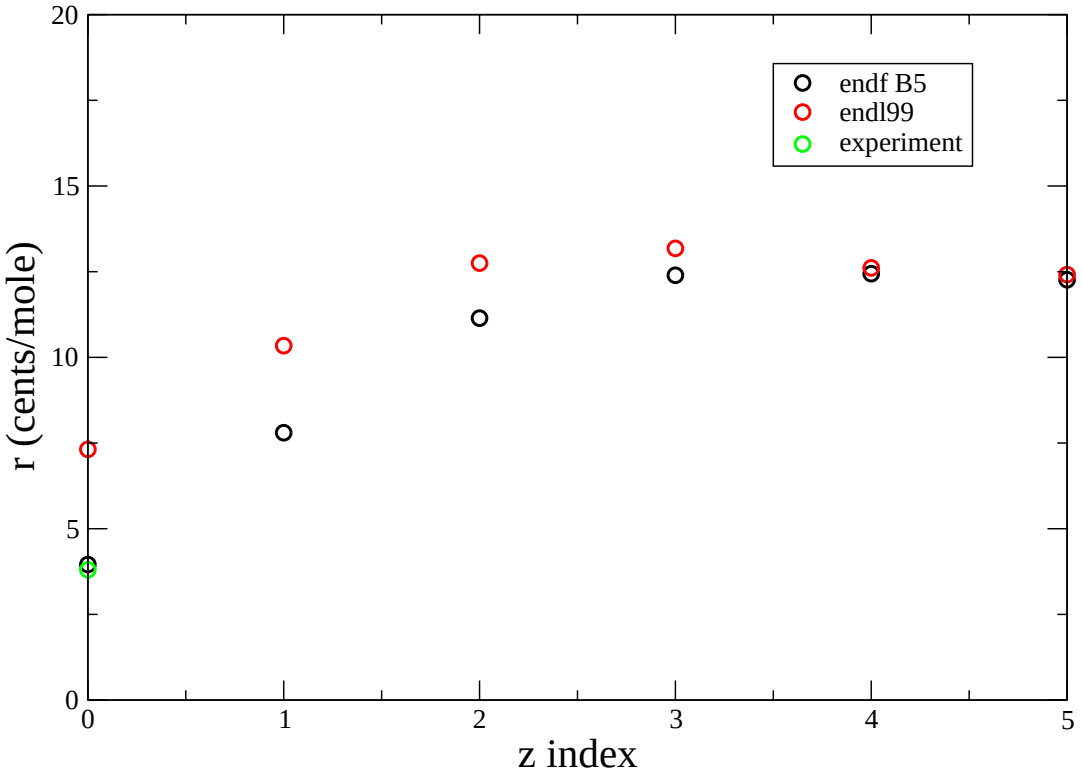

Fig. 10.— Replacement coefficients for ZA=9019 in the Godiva assembly.

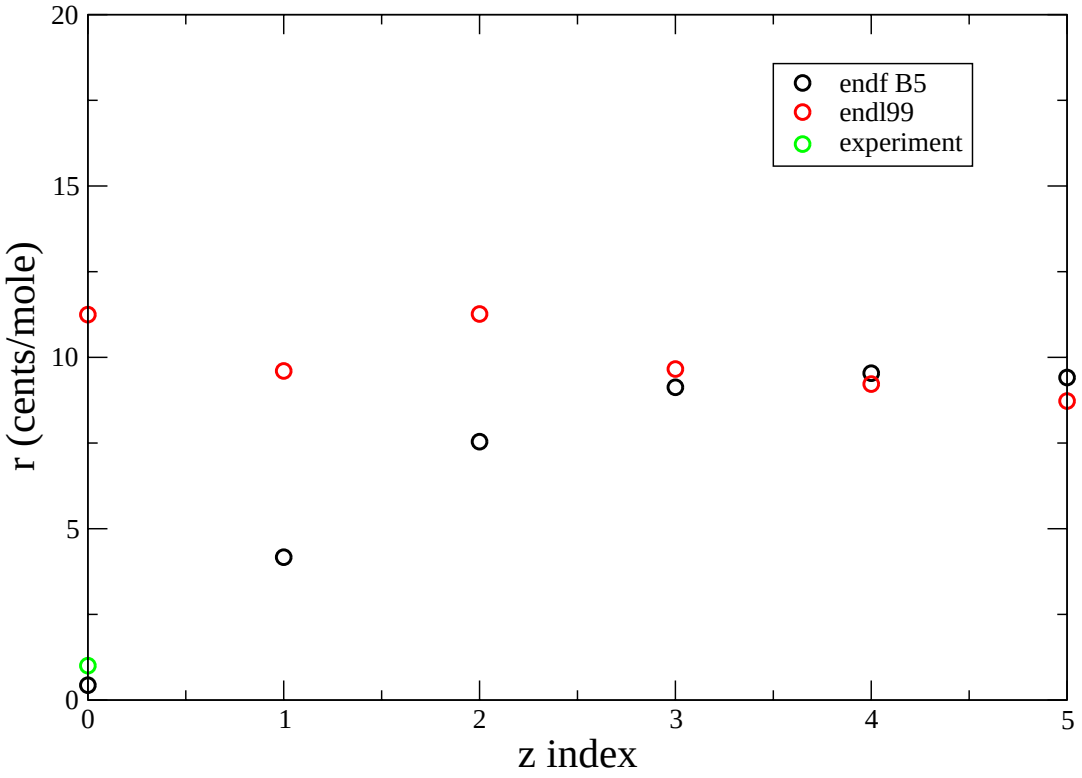

Fig. 11.— Replacement coefficients for ZA=11023 in the Godiva assembly.

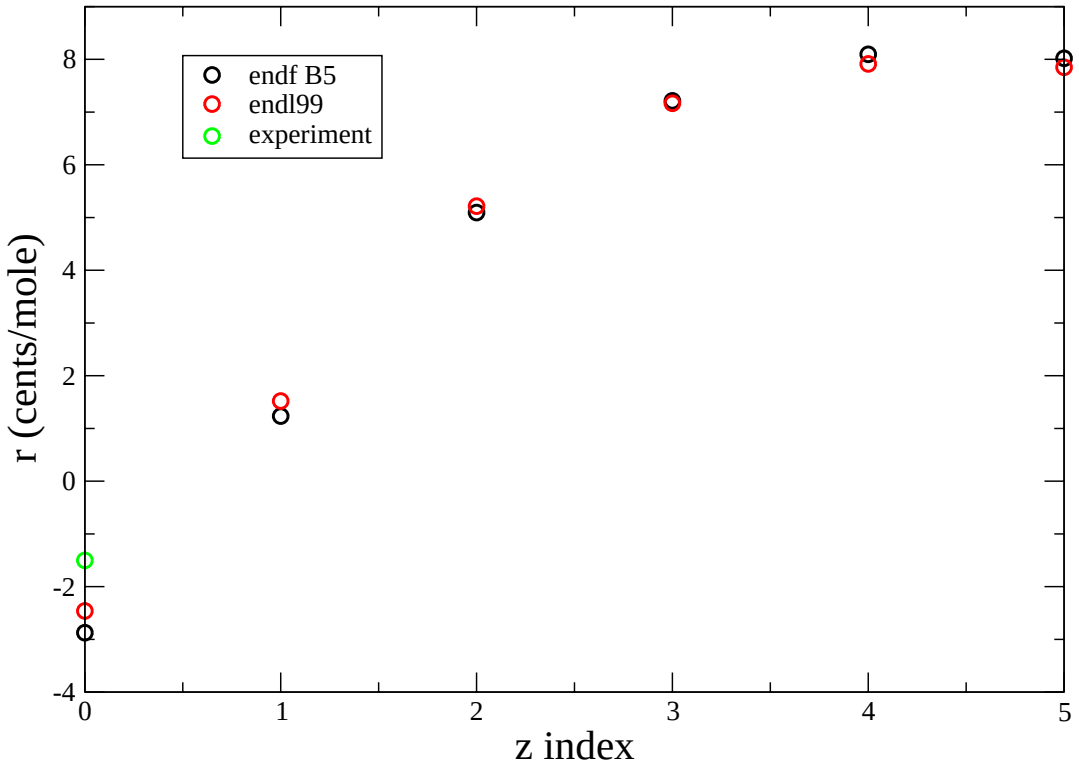

Fig. 12.— Replacement coefficients for ZA=15031 in the Godiva assembly.

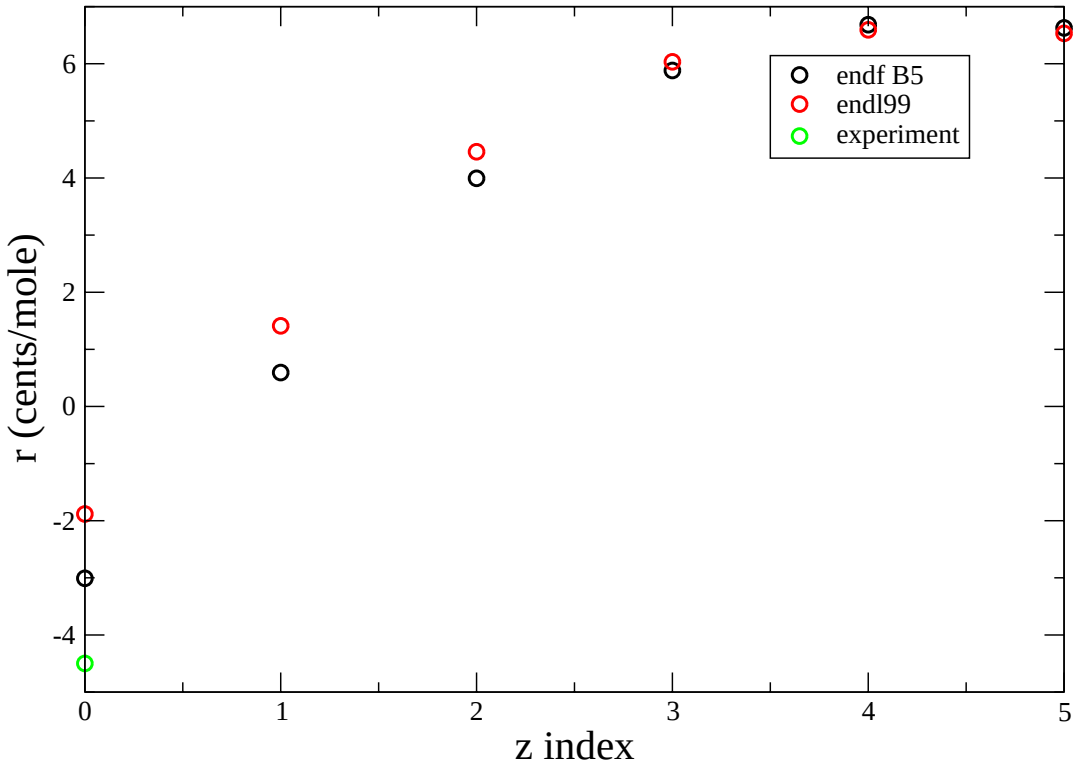

Fig. 13.— Replacement coefficients for ZA=17000 in the Godiva assembly.

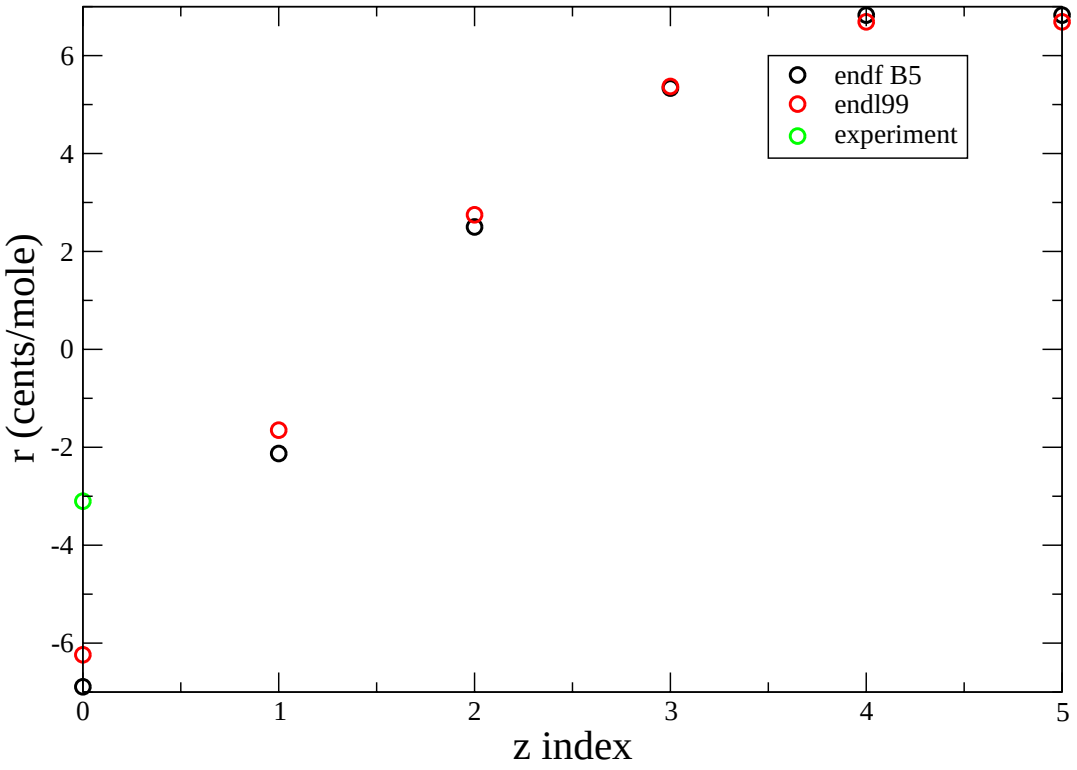

Fig. 14.— Replacement coefficients for ZA=19000 in the Godiva assembly.

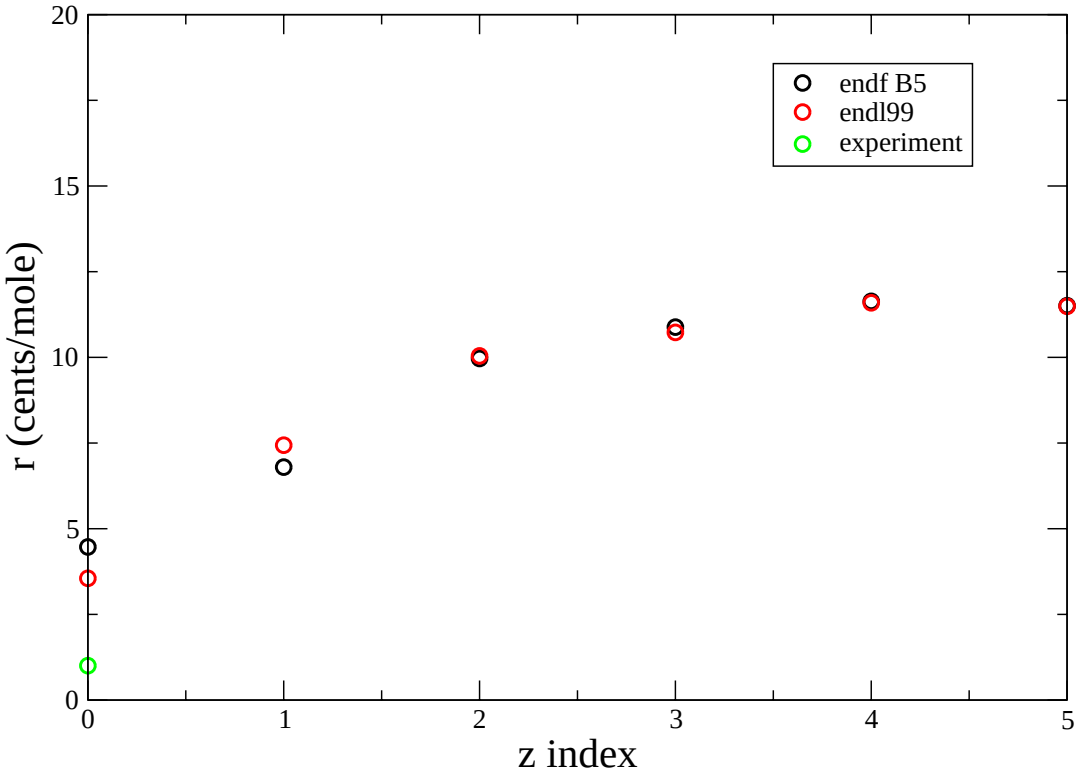

Fig. 15.— Replacement coefficients for ZA=23000 in the Godiva assembly.

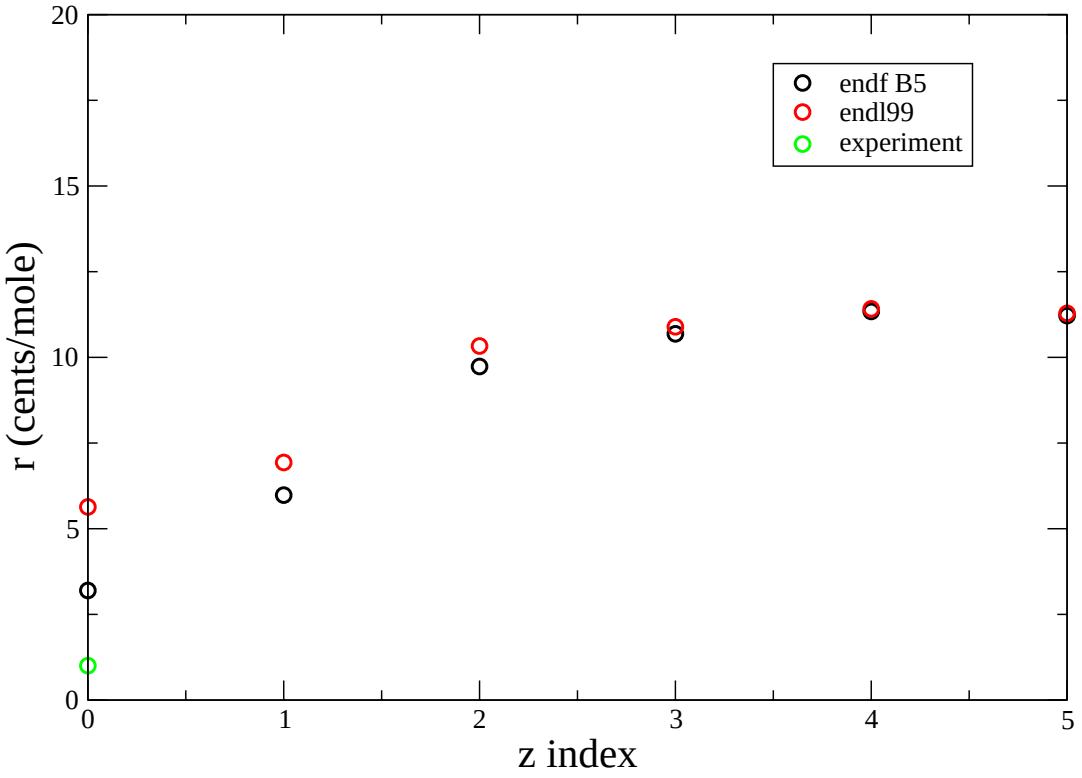

Fig. 16.— Replacement coefficients for ZA=25055 in the Godiva assembly.

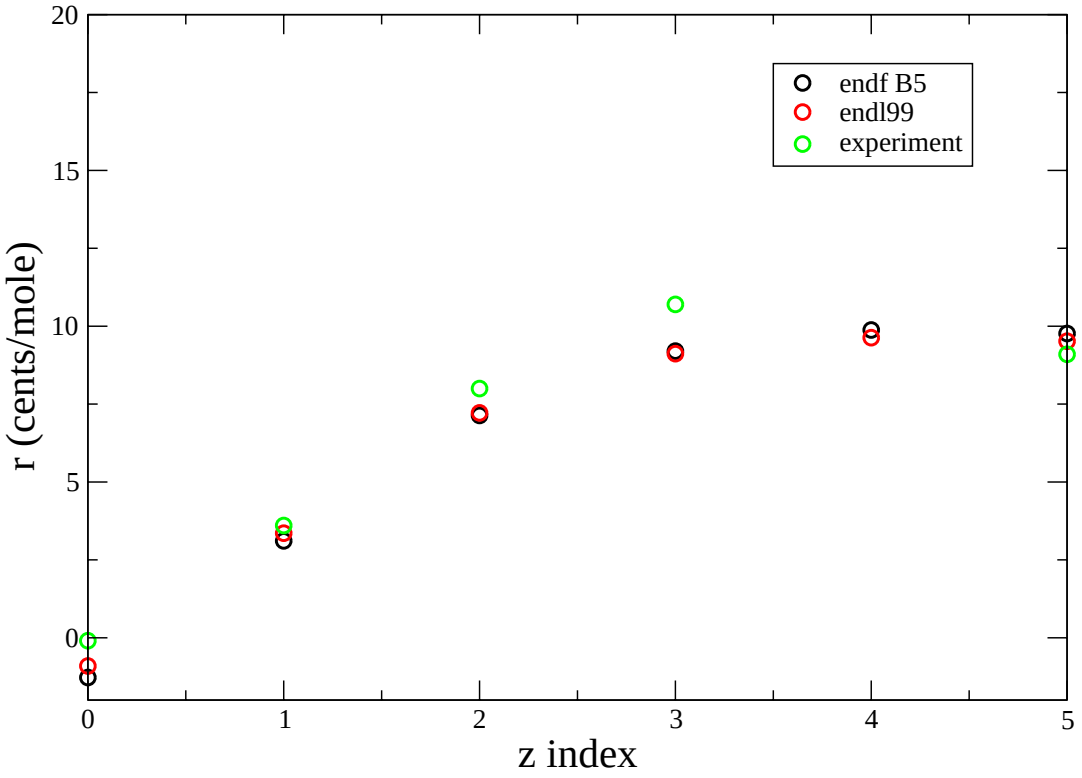

Fig. 17.— Replacement coefficients for ZA=26000 in the Godiva assembly.

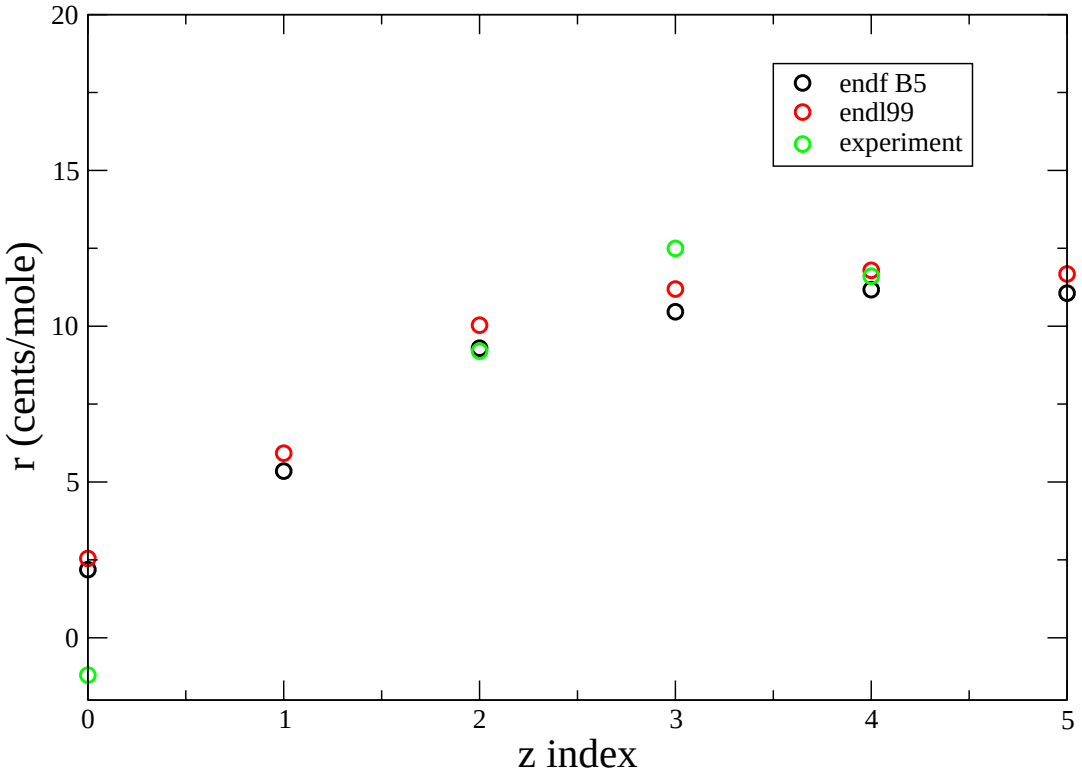

Fig. 18.— Replacement coefficients for ZA=27059 in the Godiva assembly.

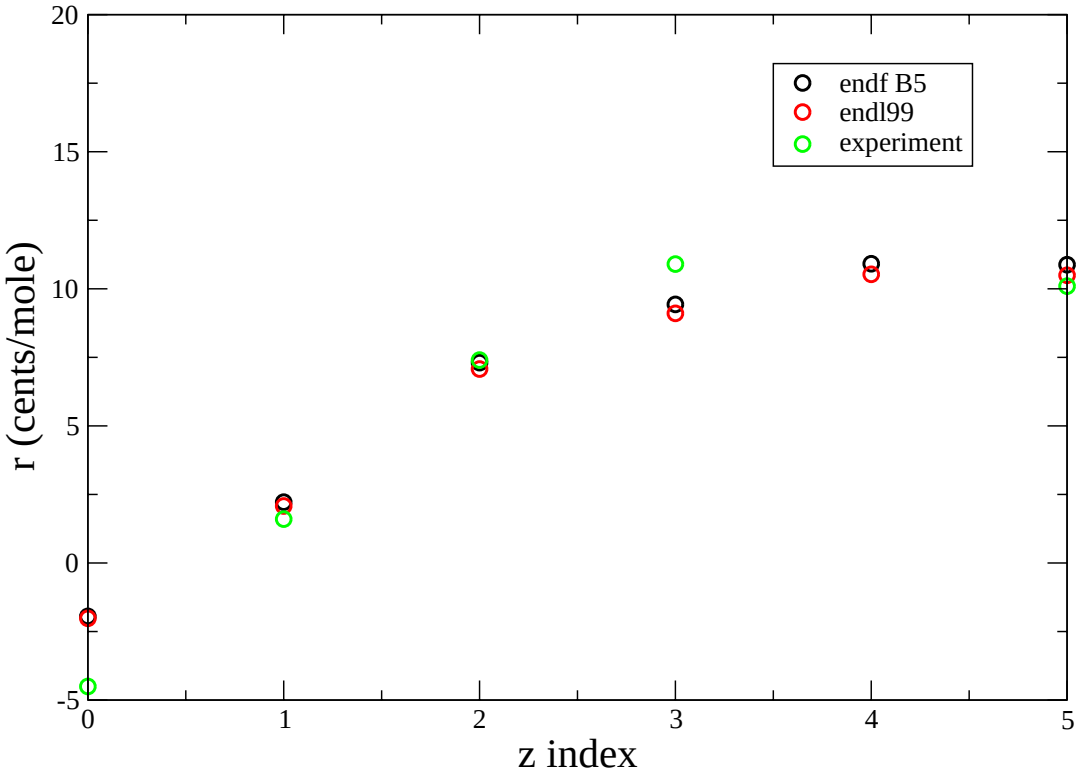

Fig. 19.— Replacement coefficients for ZA=28000 in the Godiva assembly.

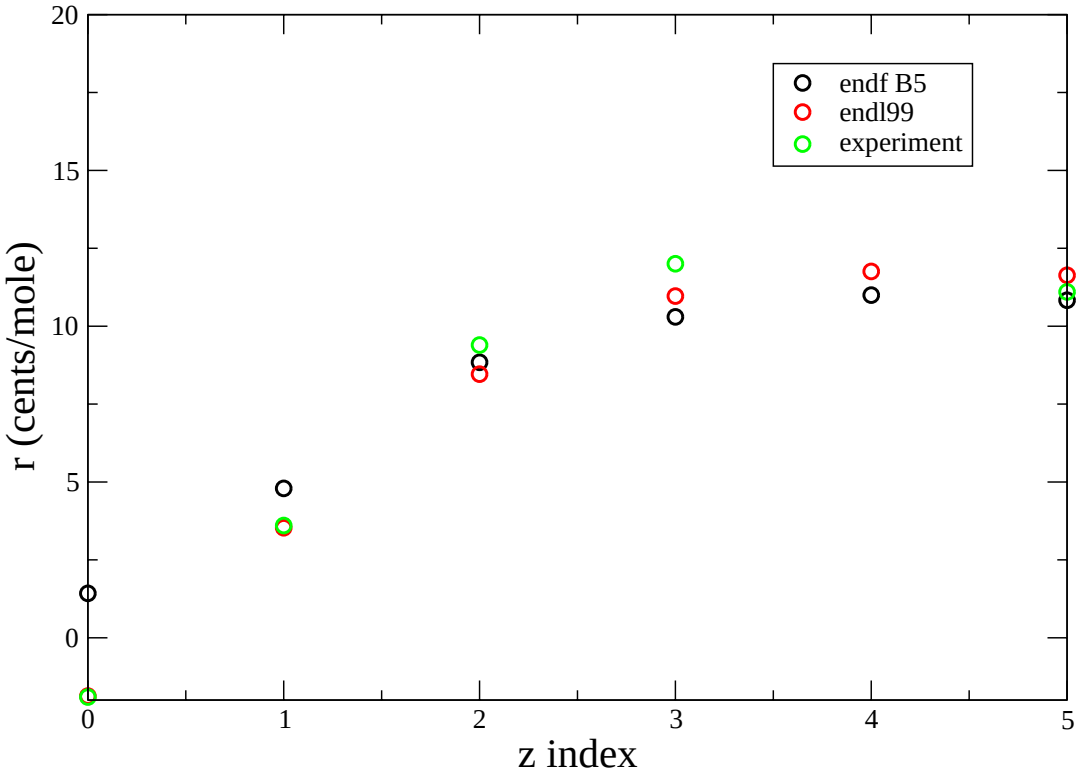

Fig. 20.— Replacement coefficients for ZA=29000 in the Godiva assembly.

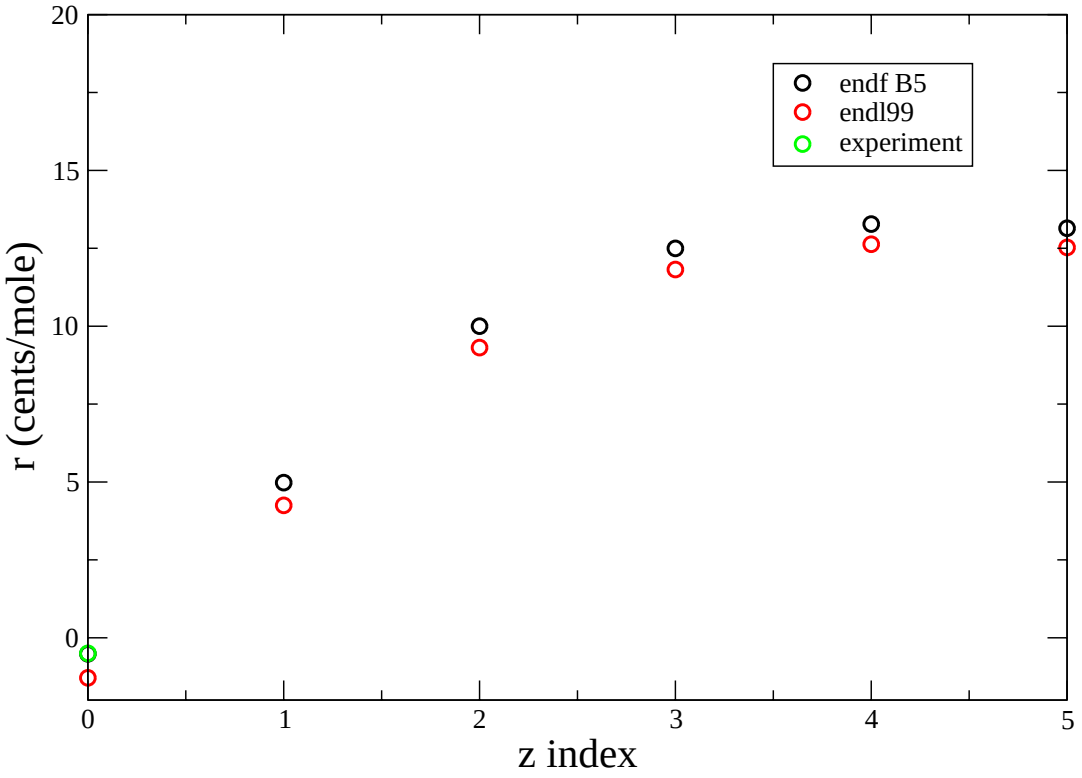

Fig. 21.— Replacement coefficients for ZA=31000 in the Godiva assembly.

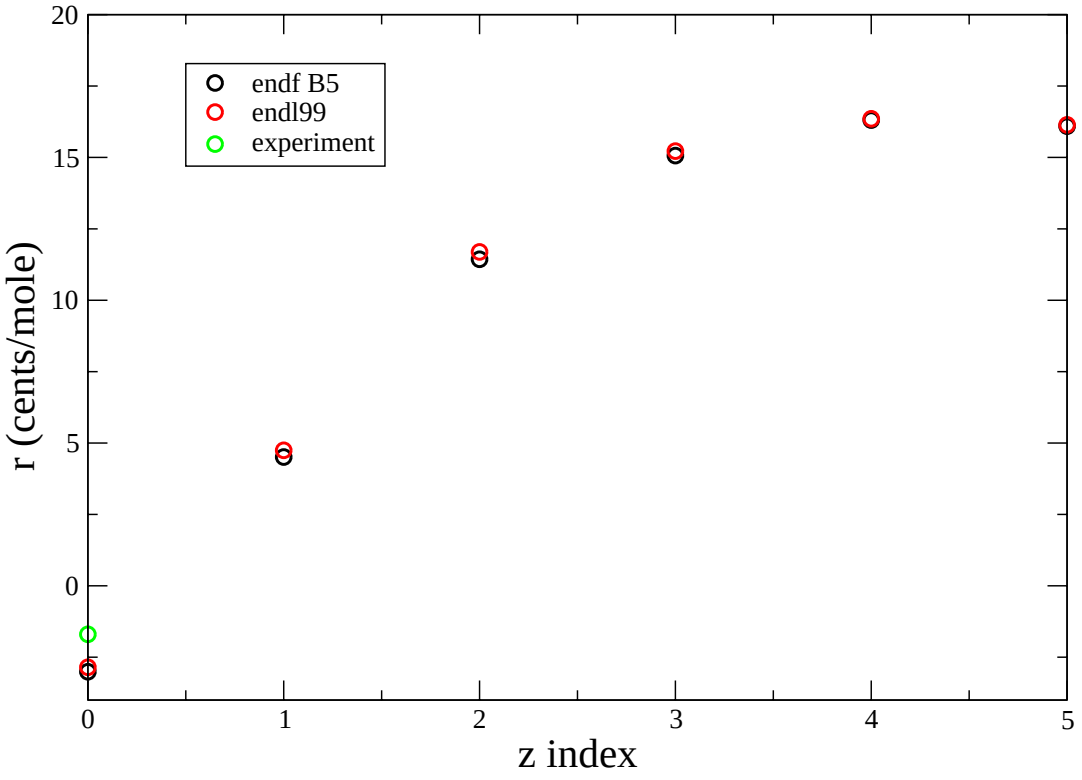

Fig. 22.— Replacement coefficients for ZA=41093 in the Godiva assembly.

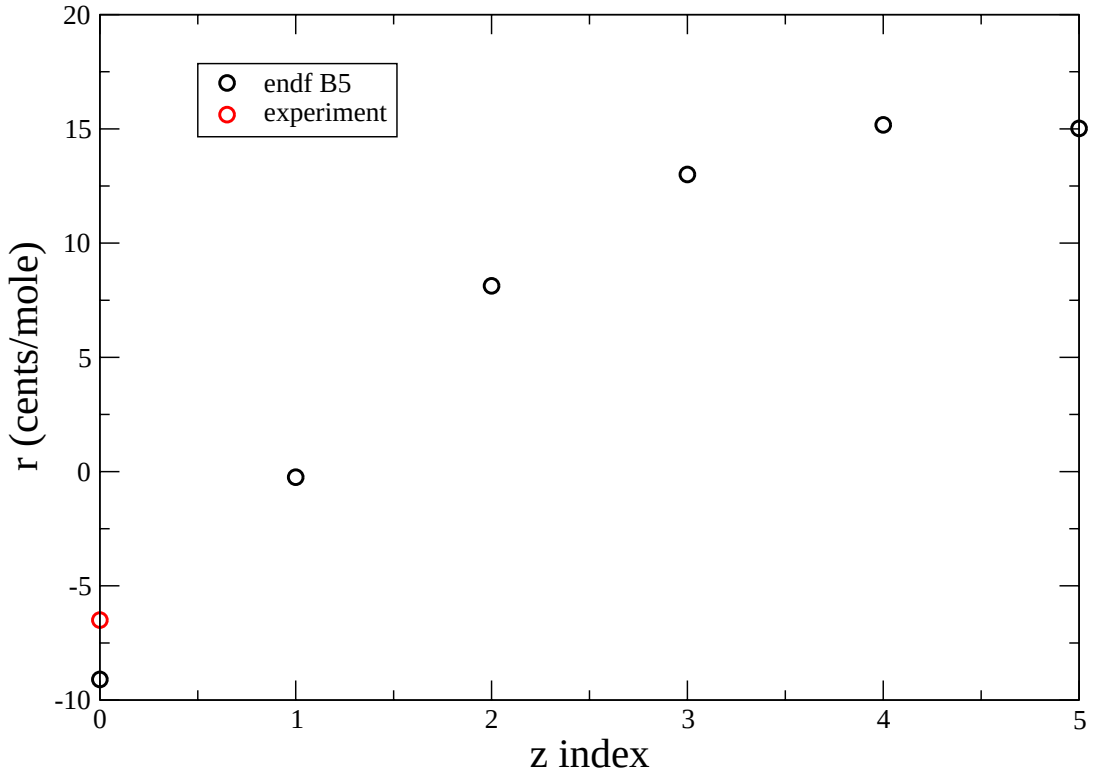

Fig. 23.— Replacement coefficients for ZA=45103 in the Godiva assembly.

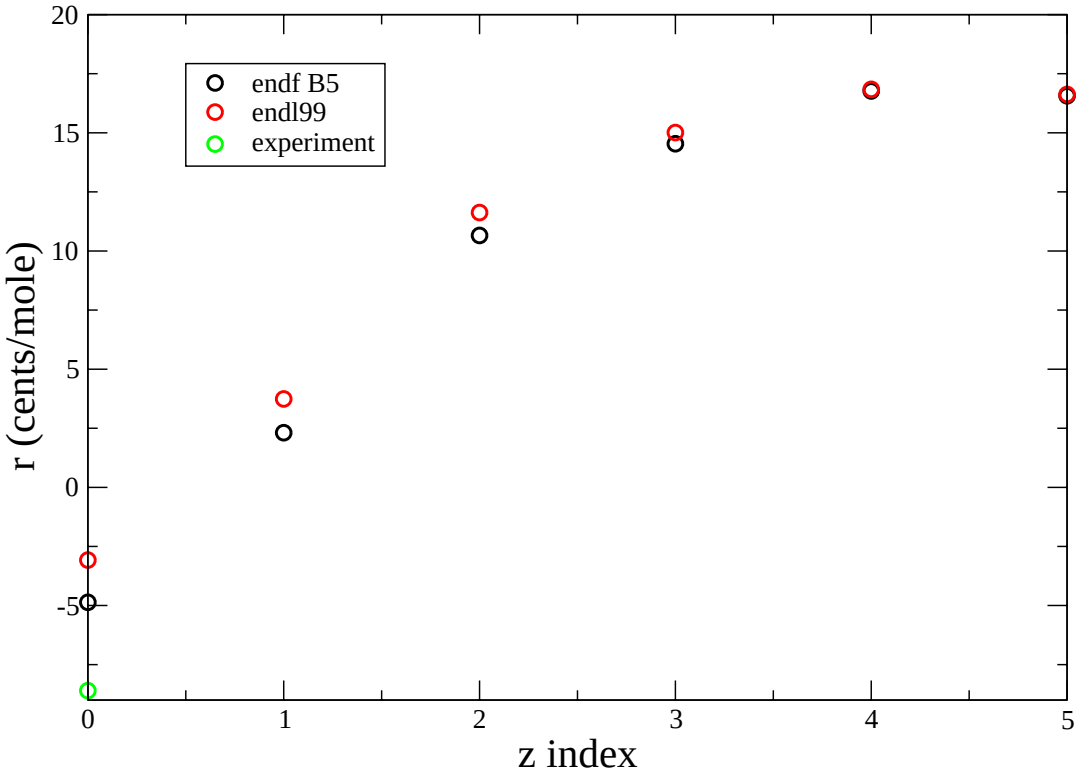

Fig. 24.— Replacement coefficients for ZA=73181 in the Godiva assembly.

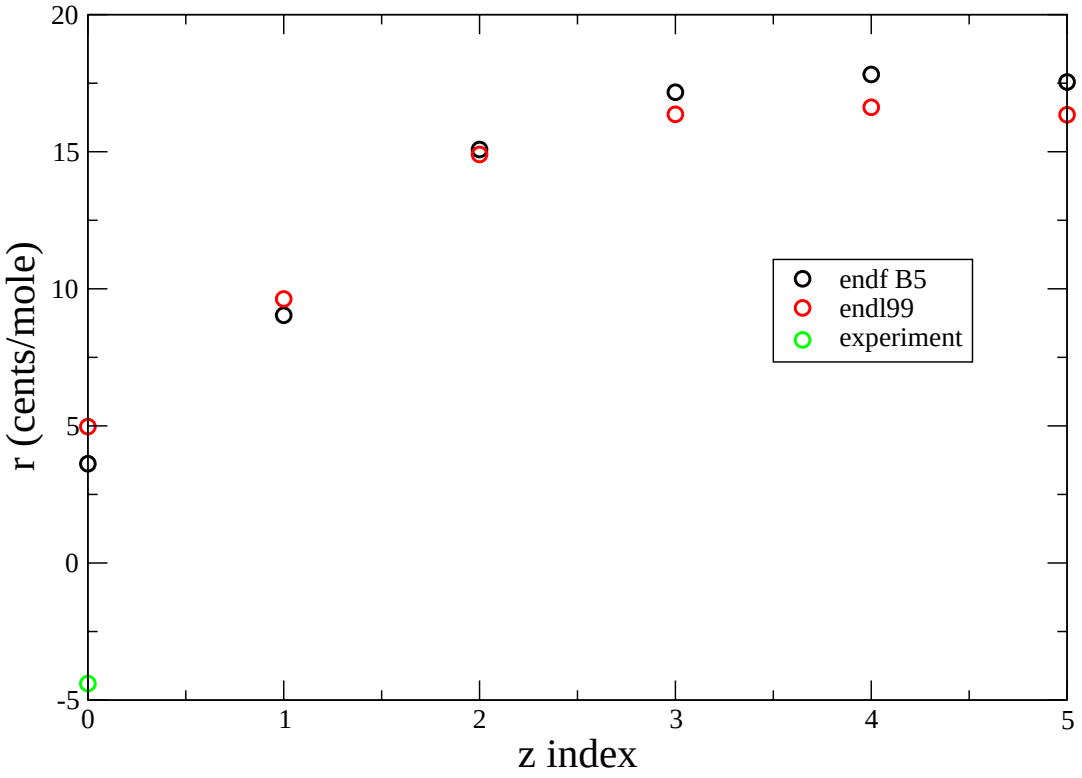

Fig. 25.— Replacement coefficients for ZA=74000 in the Godiva assembly.

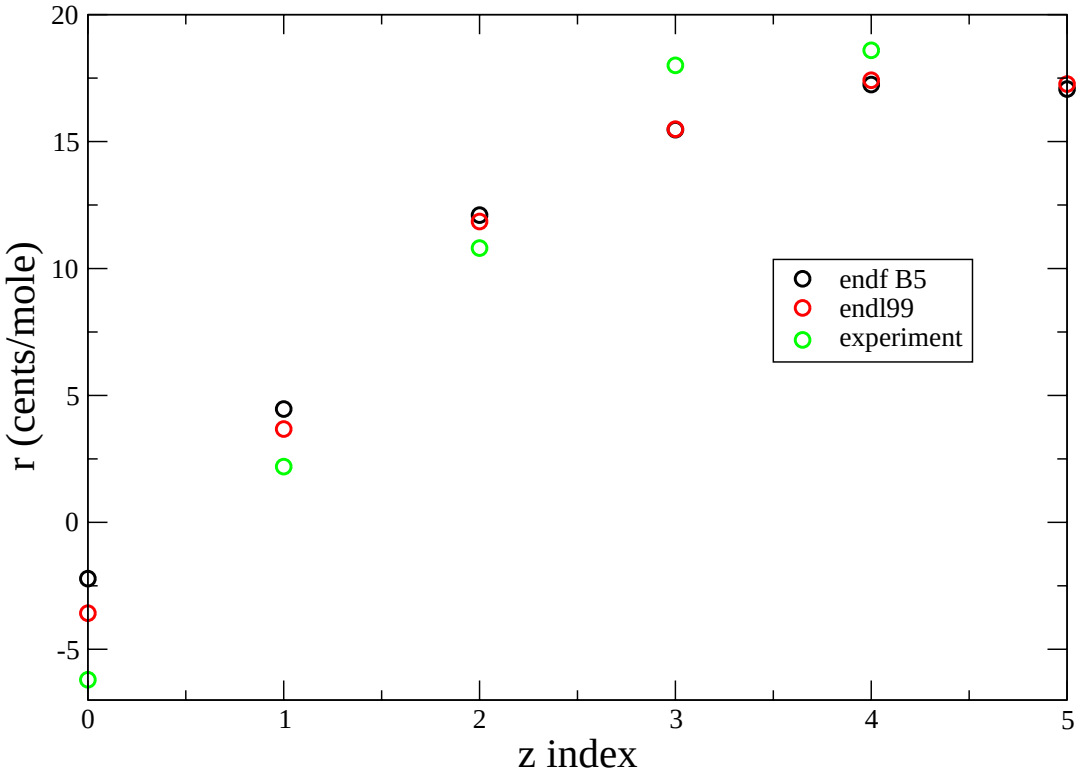

Fig. 26.— Replacement coefficients for ZA=79197 in the Godiva assembly.

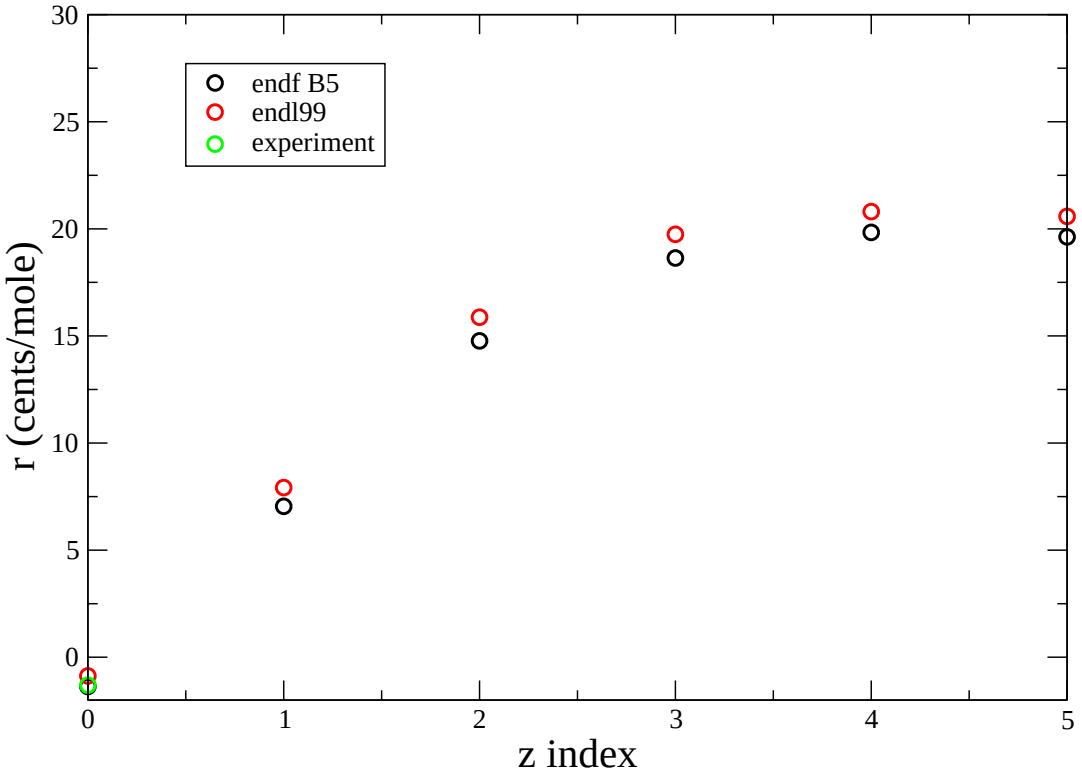

Fig. 27.— Replacement coefficients for ZA=82000 in the Godiva assembly.

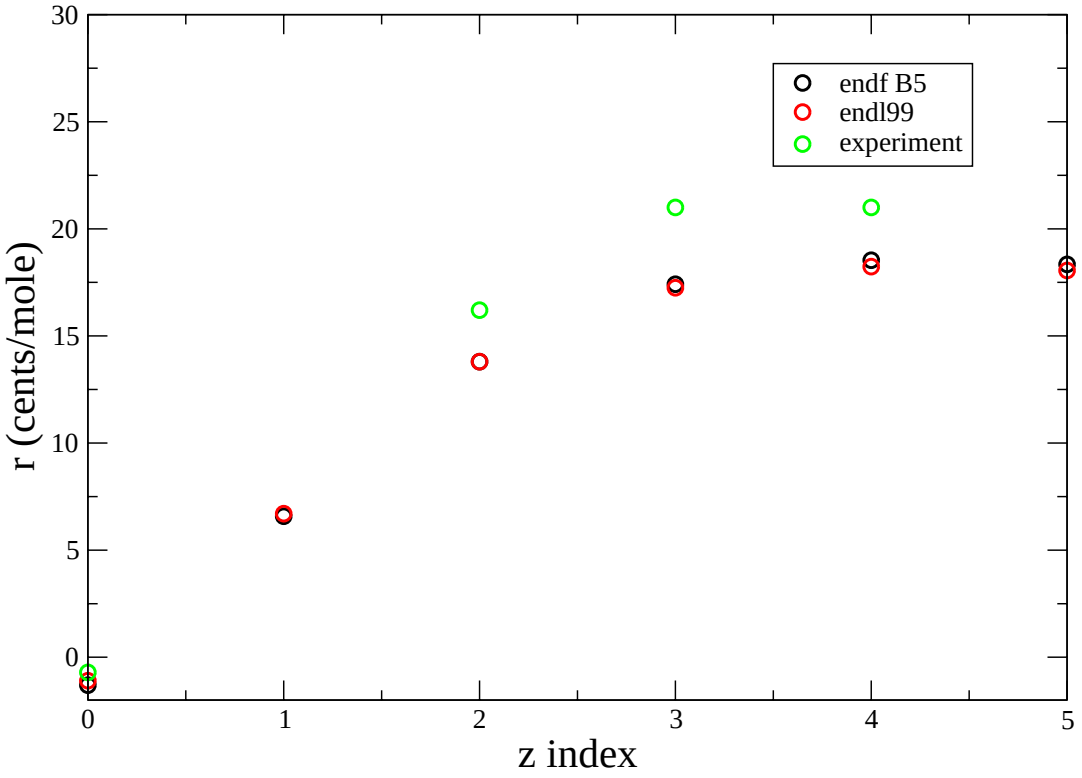

Fig. 28.— Replacement coefficients for ZA=83209 in the Godiva assembly.

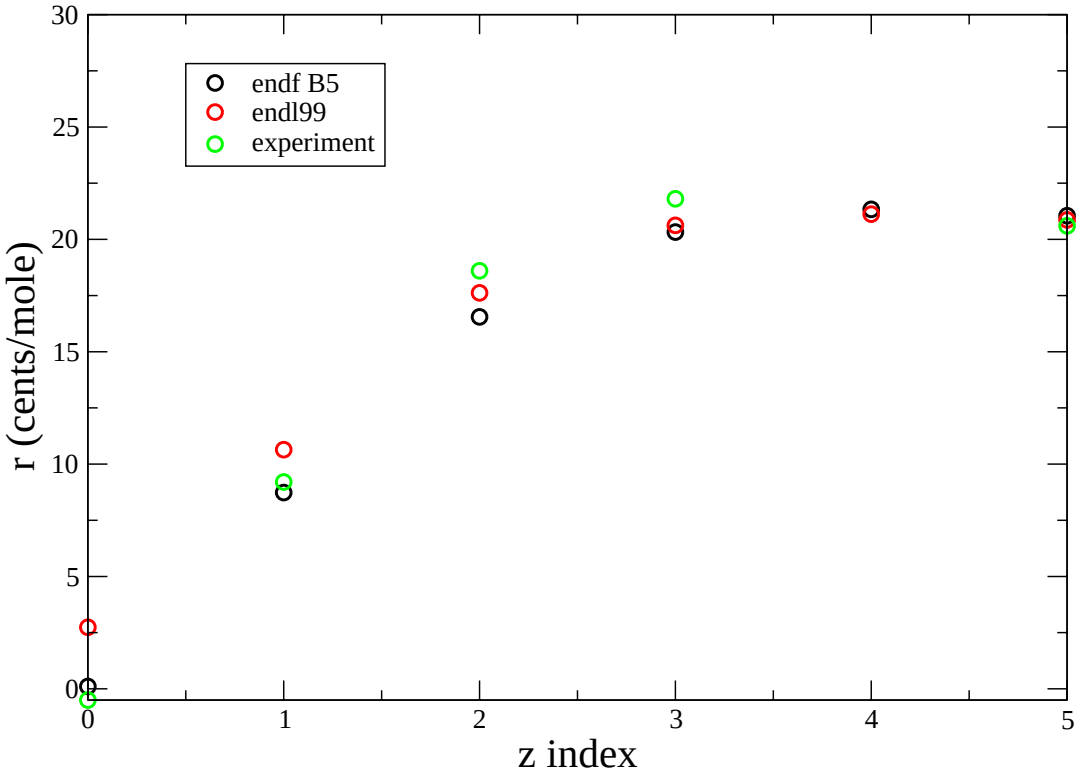

Fig. 29.— Replacement coefficients for ZA=90232 in the Godiva assembly.

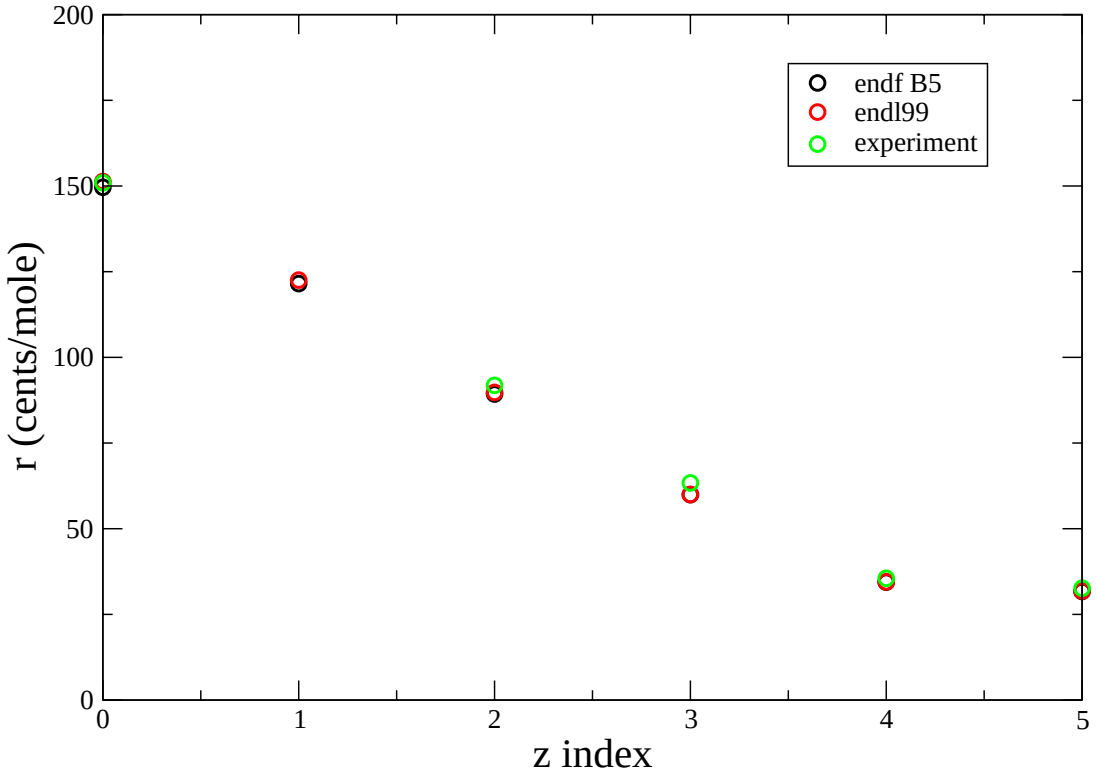

Fig. 30.— Replacement coefficients for ZA=92235 in the Godiva assembly.

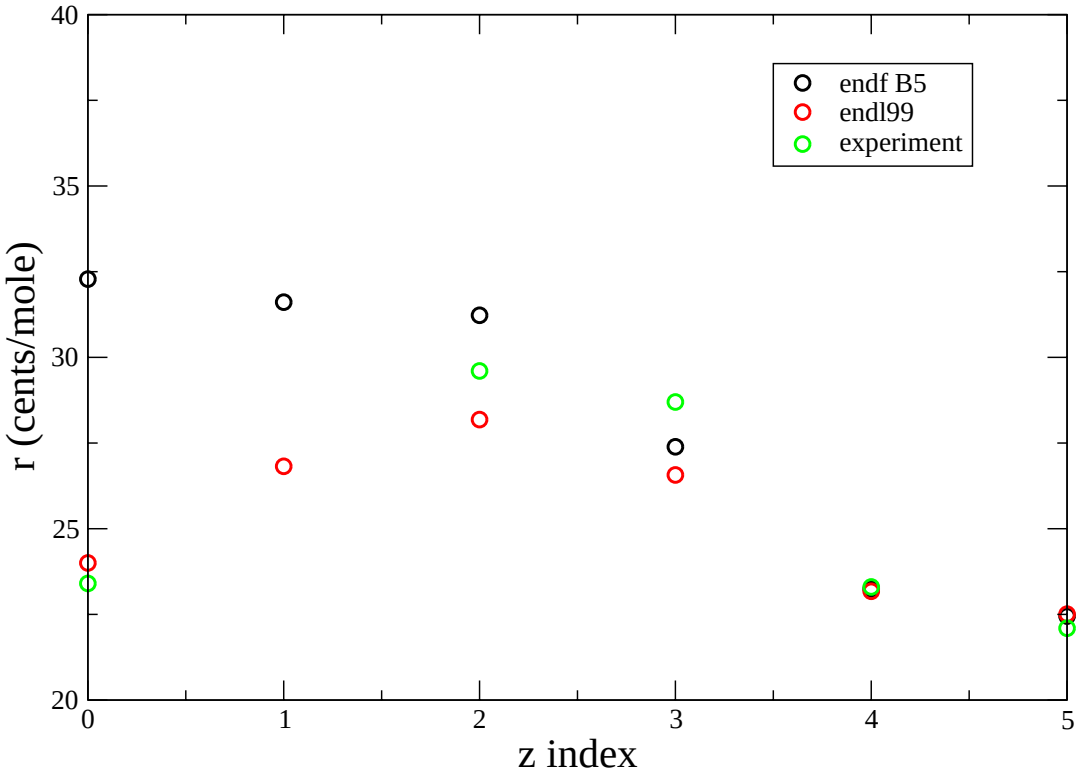

Fig. 31.— Replacement coefficients for ZA=92238 in the Godiva assembly.

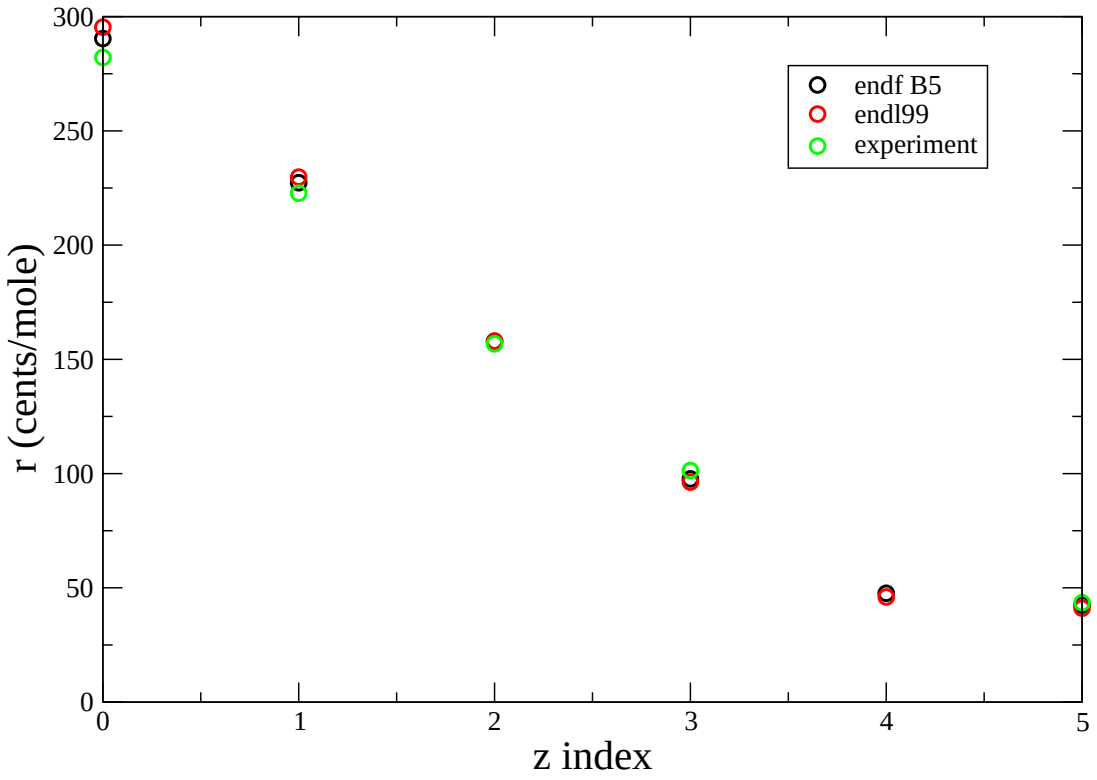

Fig. 32.— Replacement coefficients for ZA=94239 in the Godiva assembly.

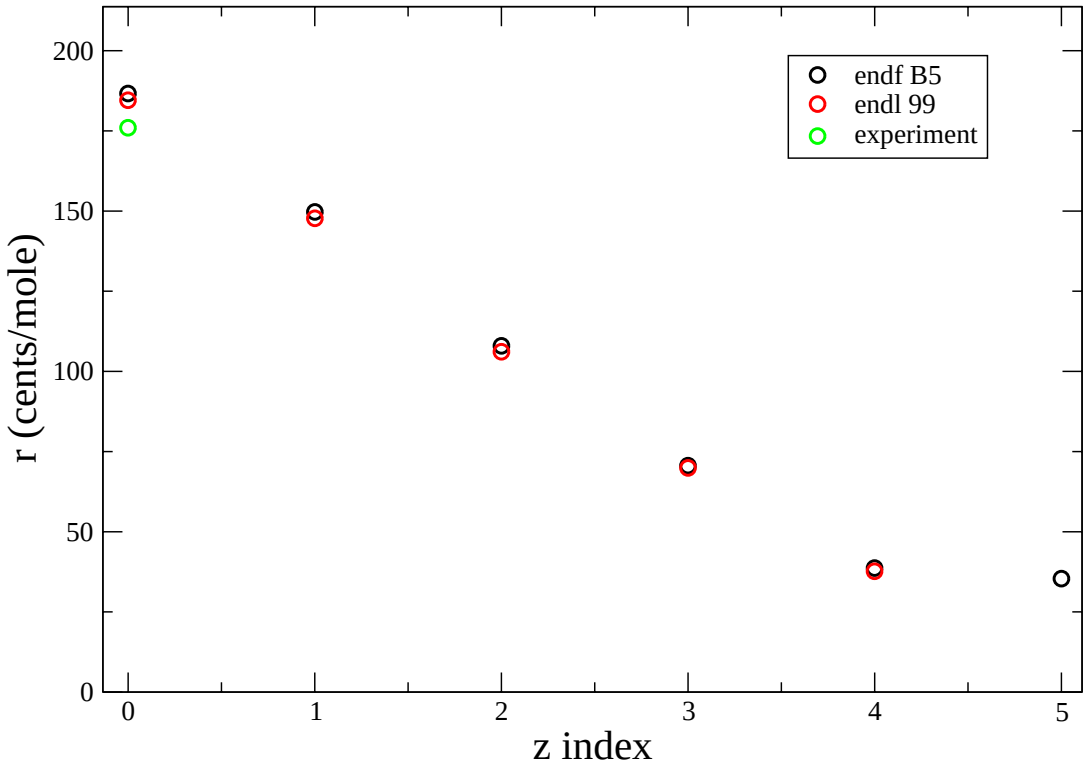

Fig. 33.— Replacement coefficients for ZA=94240 in the Godiva assembly.

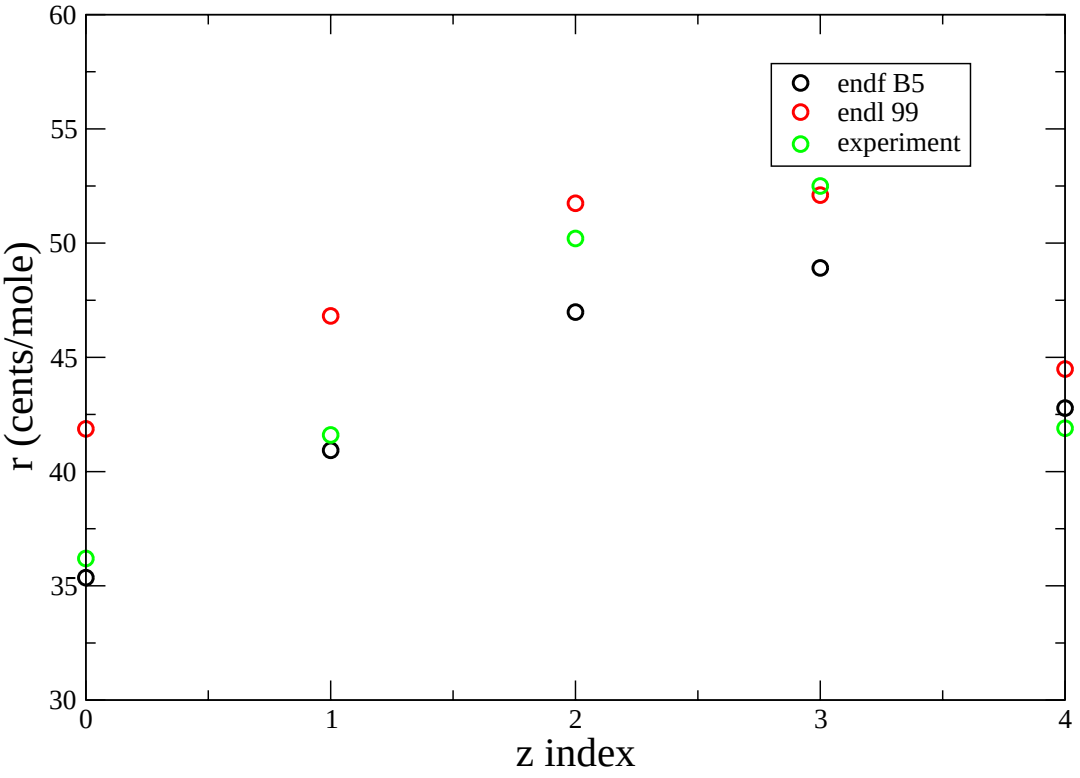

Fig. 34.— Replacement coefficients for ZA=1001 in the Jezebel assembly.

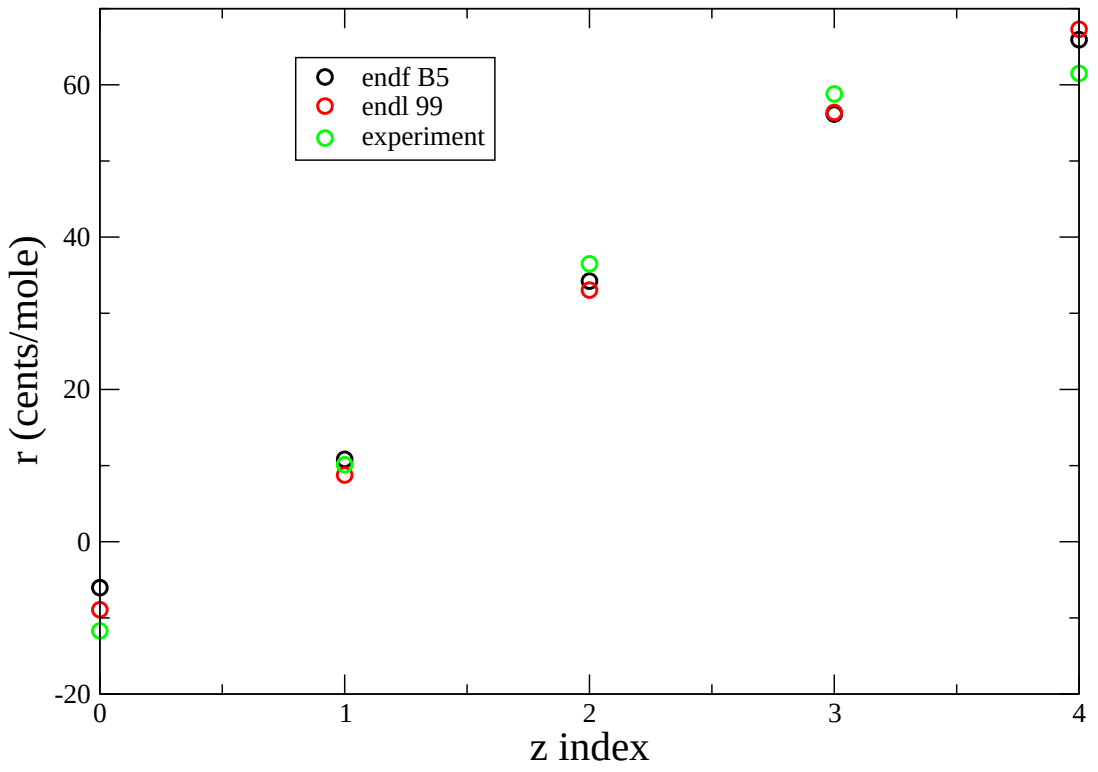

Fig. 35.— Replacement coefficients for ZA=1002 in the Jezebel assembly.

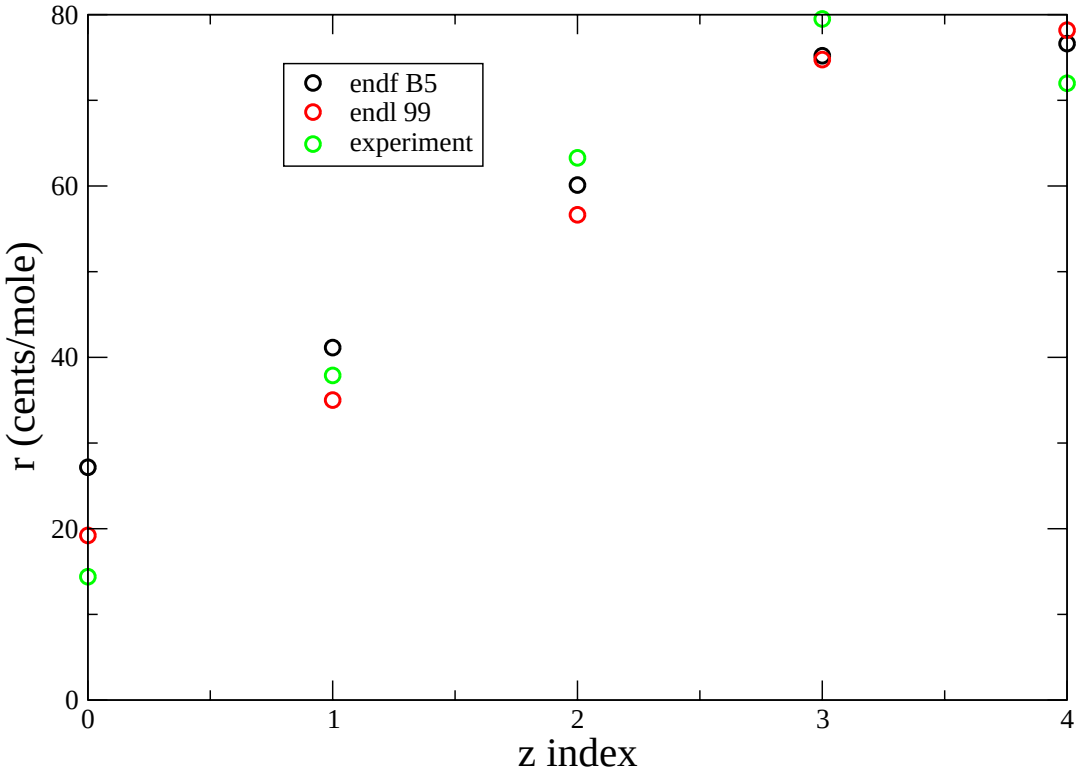

Fig. 36.— Replacement coefficients for ZA=4009 in the Jezebel assembly.

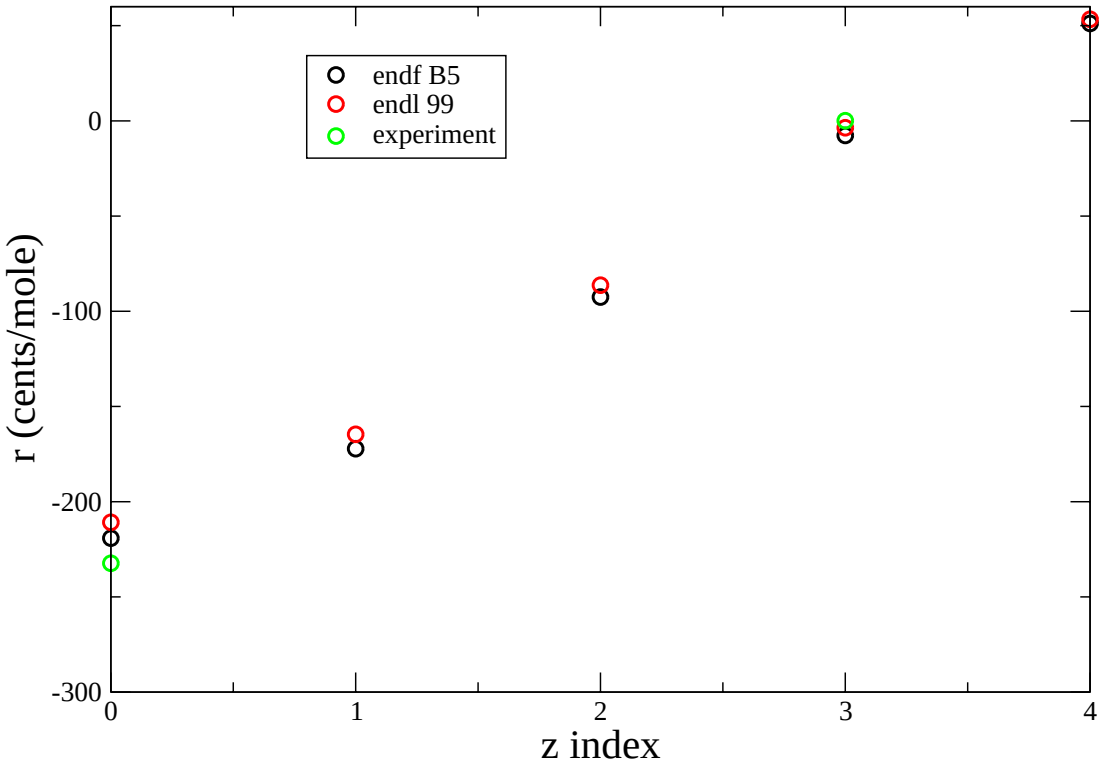

Fig. 37.— Replacement coefficients for ZA=5010 in the Jezebel assembly.

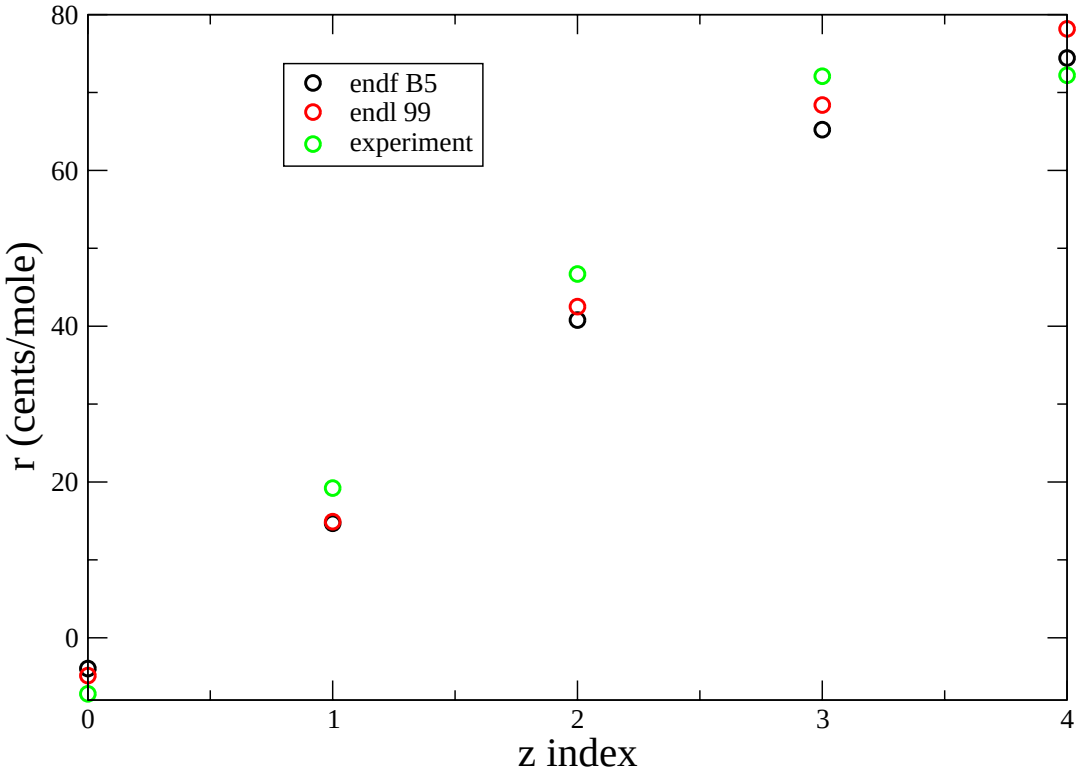

Fig. 38.— Replacement coefficients for ZA=6012 in the Jezebel assembly.

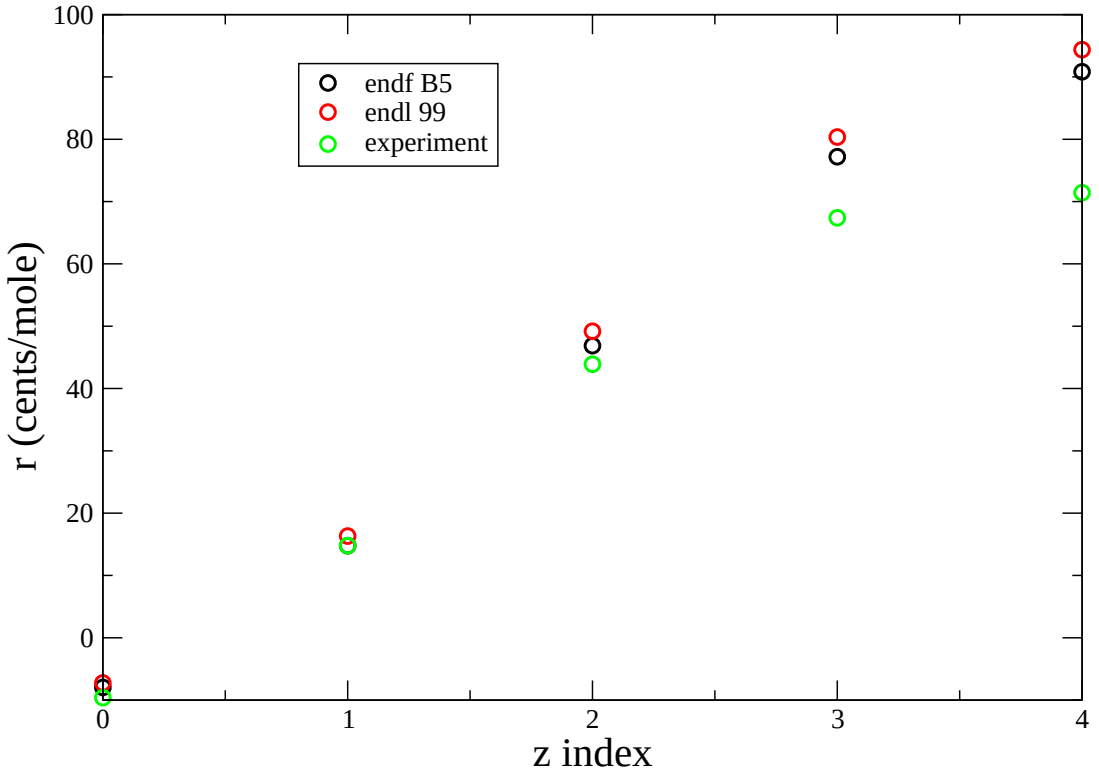

Fig. 39.— Replacement coefficients for ZA=8016 in the Jezebel assembly.

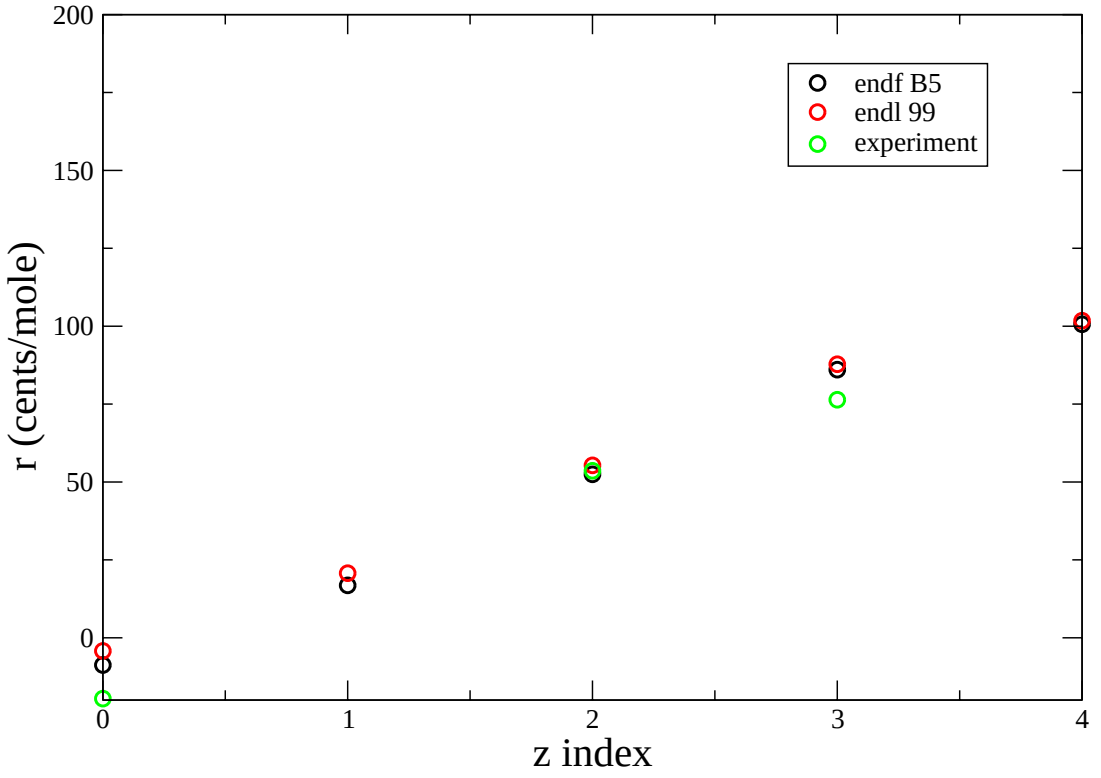

Fig. 40.— Replacement coefficients for ZA=9019 in the Jezebel assembly.

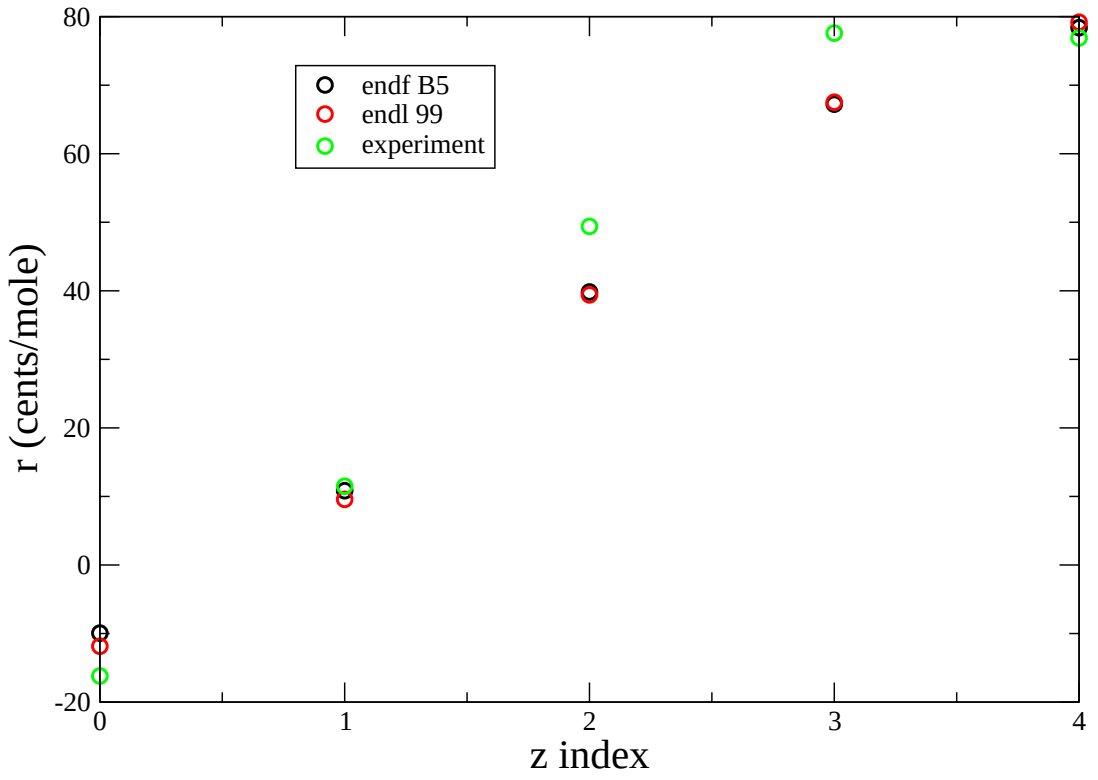

Fig. 41.— Replacement coefficients for ZA=14000 in the Jezebel assembly.

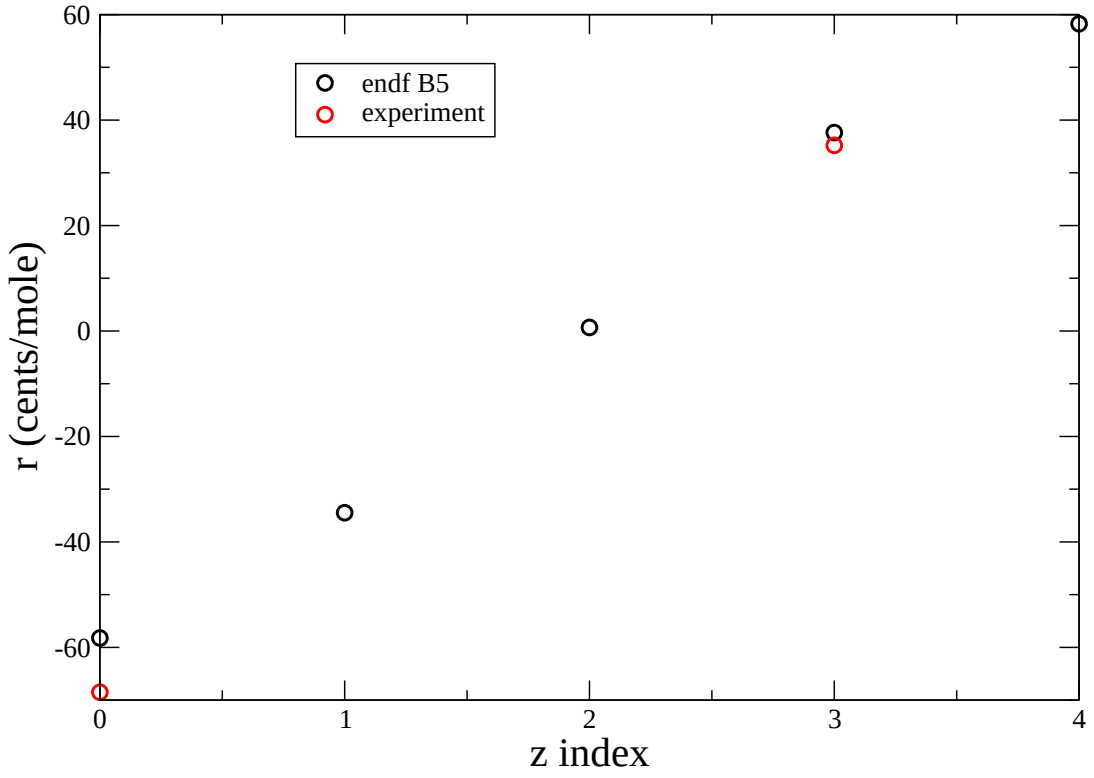

Fig. 42.— Replacement coefficients for ZA=16000 in the Jezebel assembly.

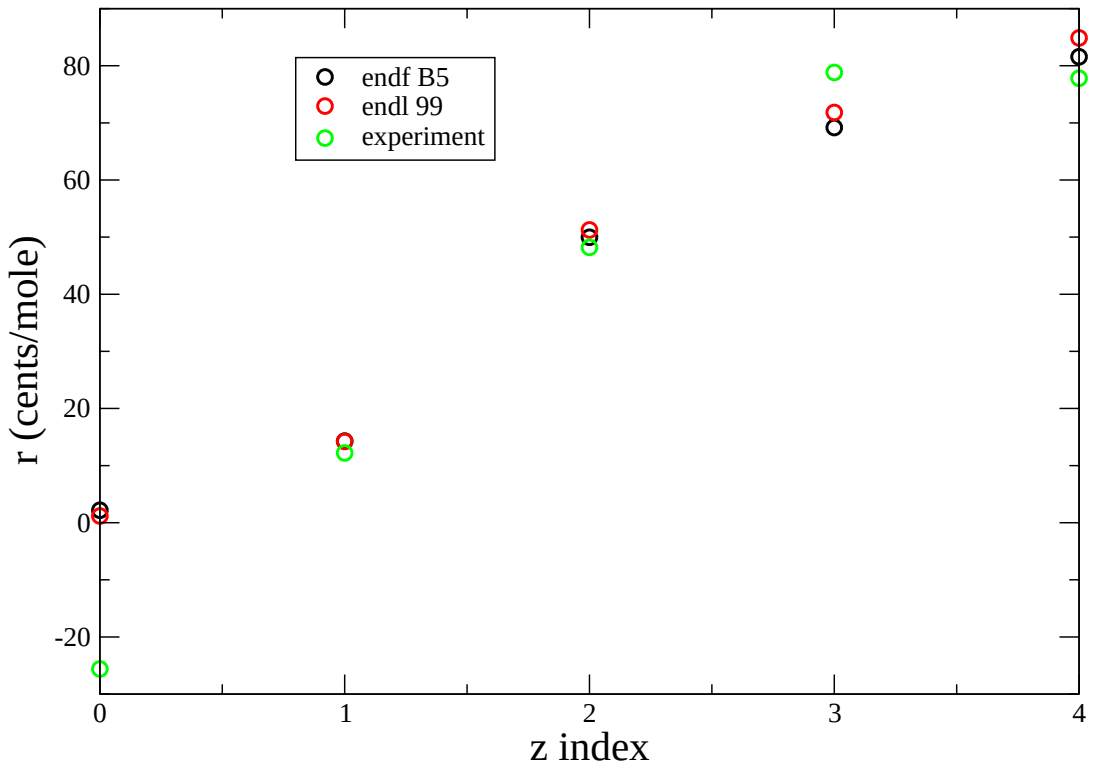

Fig. 43.— Replacement coefficients for ZA=22000 in the Jezebel assembly.

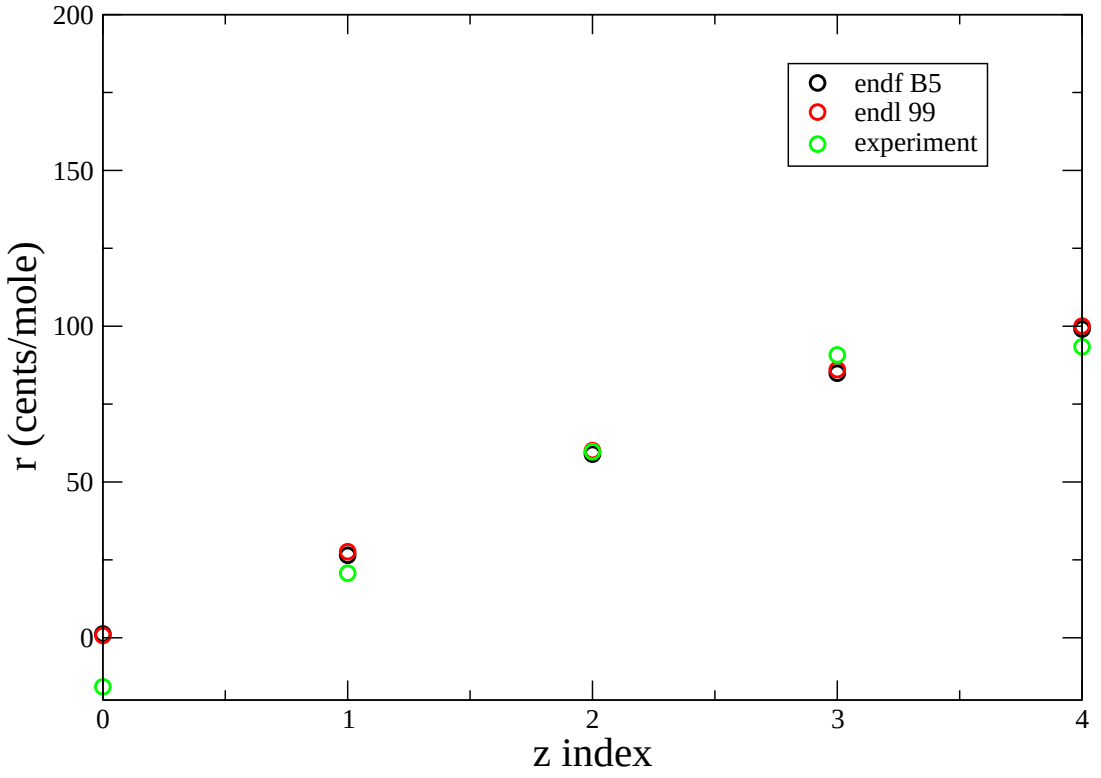

Fig. 44.— Replacement coefficients for ZA=23000 in the Jezebel assembly.

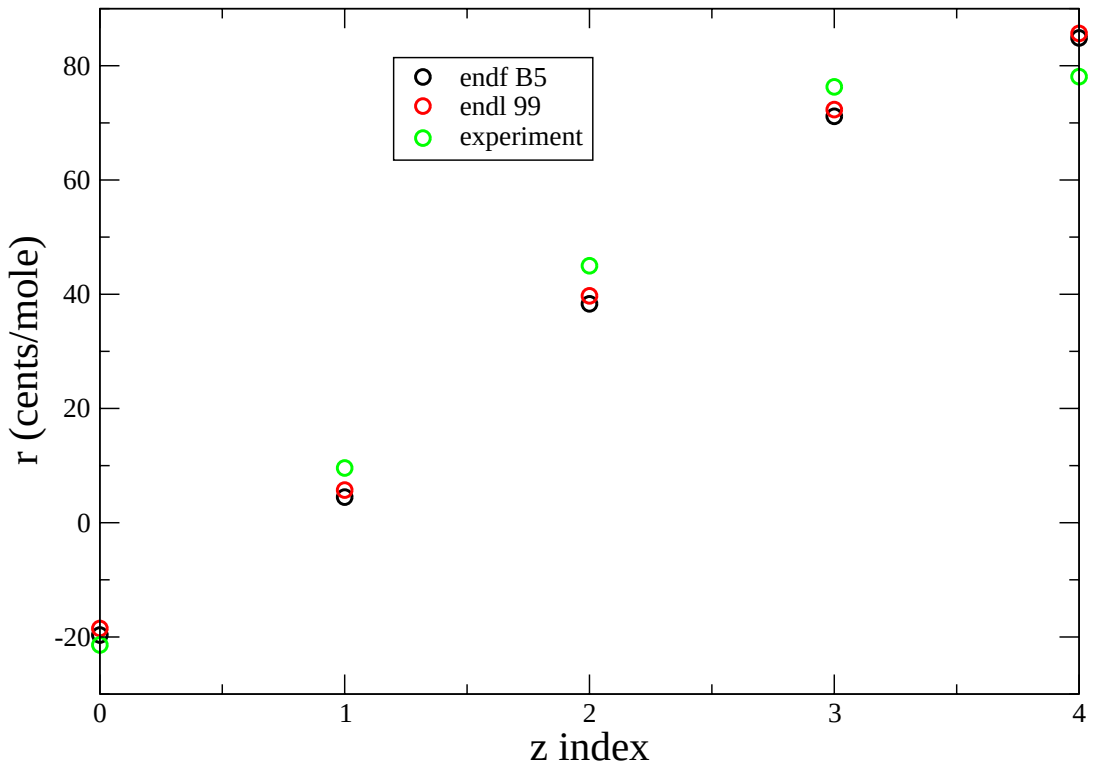

Fig. 45.— Replacement coefficients for ZA=26000 in the Jezebel assembly.

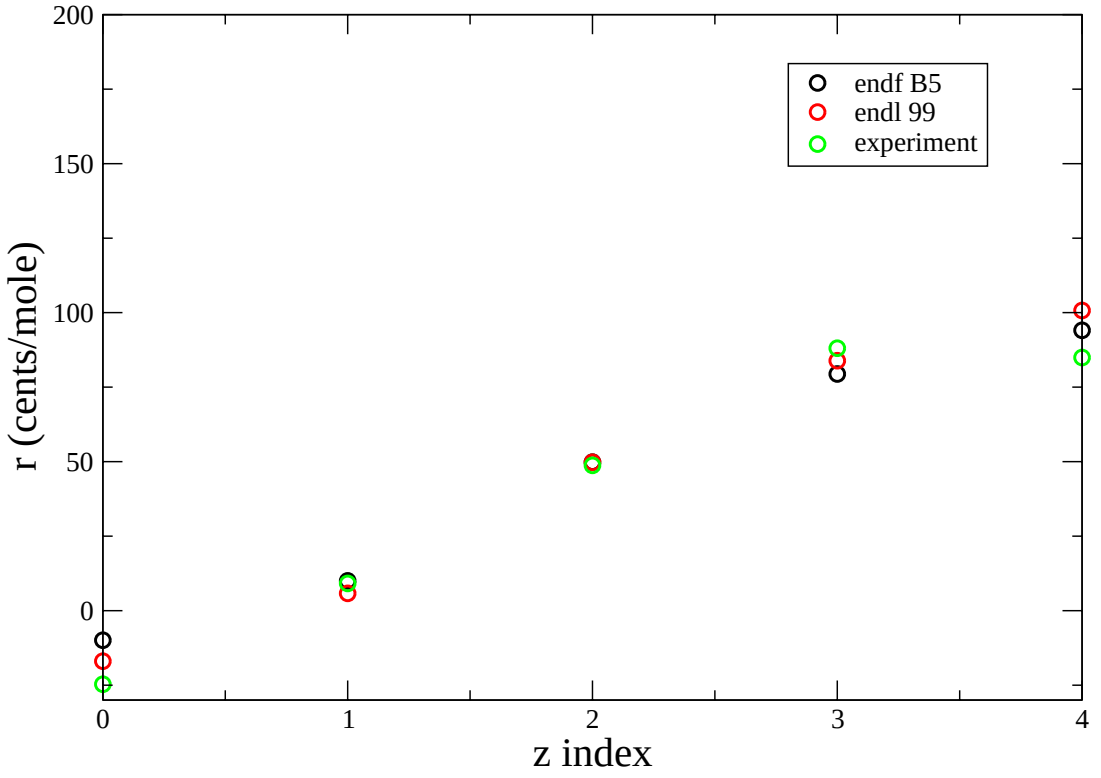

Fig. 46.— Replacement coefficients for ZA=27059 in the Jezebel assembly.

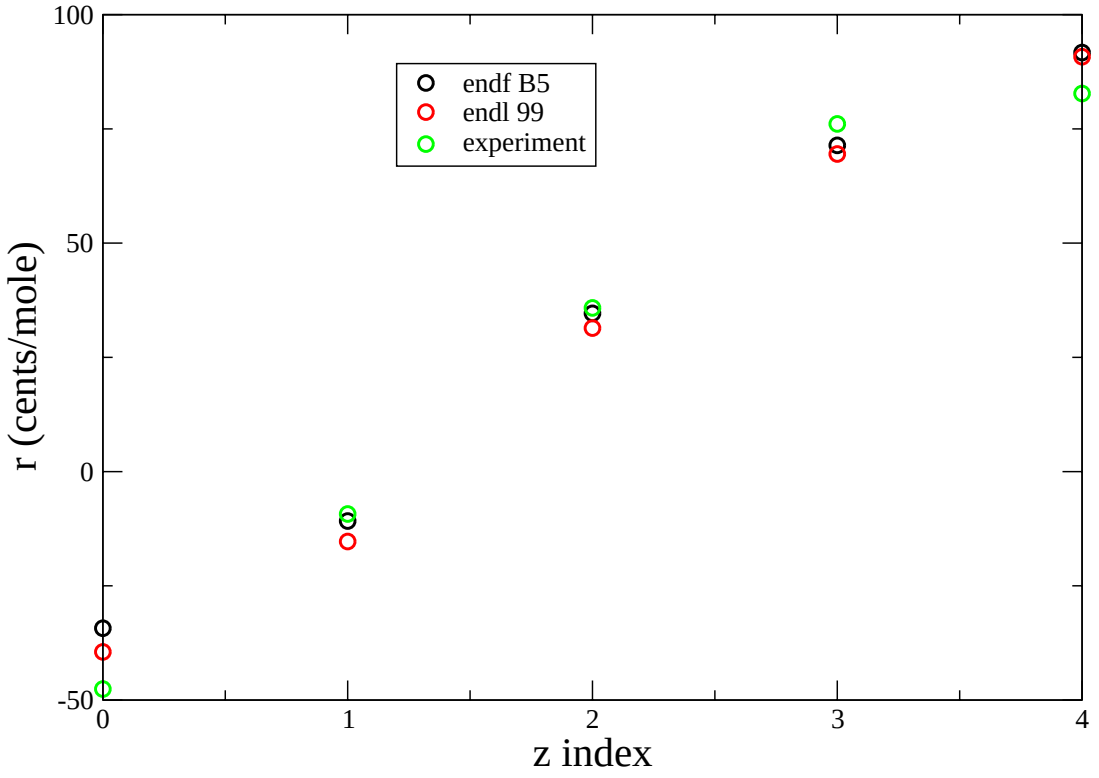

Fig. 47.— Replacement coefficients for ZA=28000 in the Jezebel assembly.

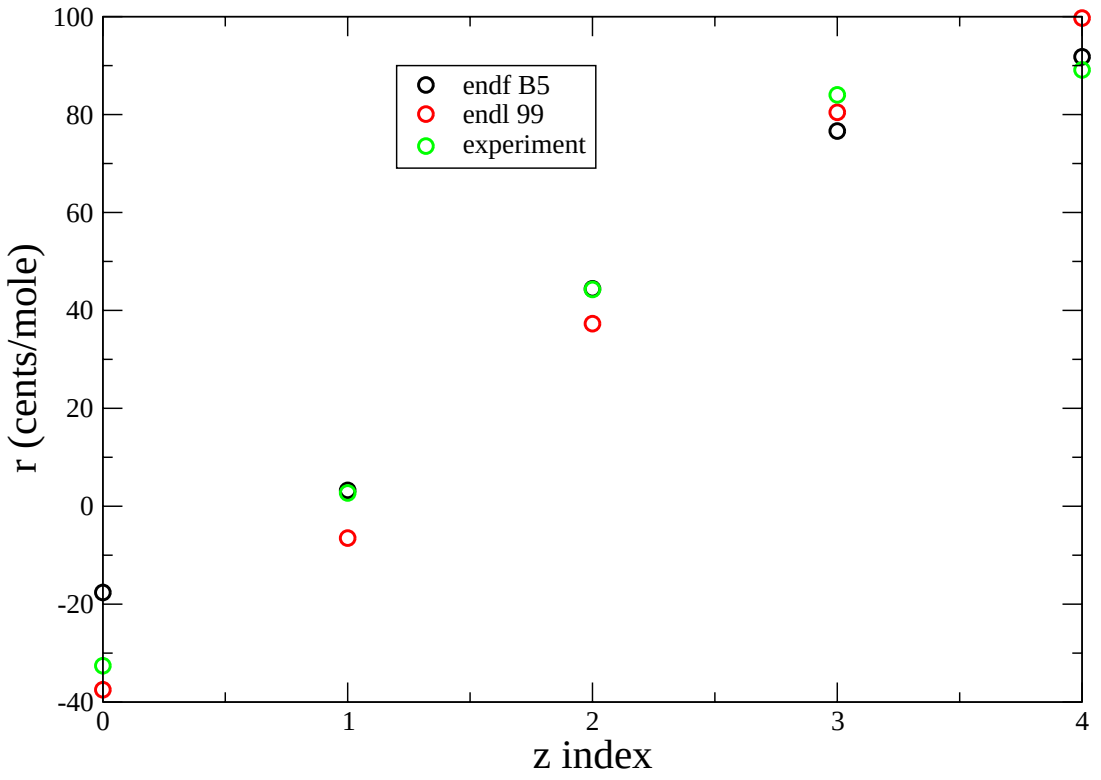

Fig. 48.— Replacement coefficients for ZA=29000 in the Jezebel assembly.

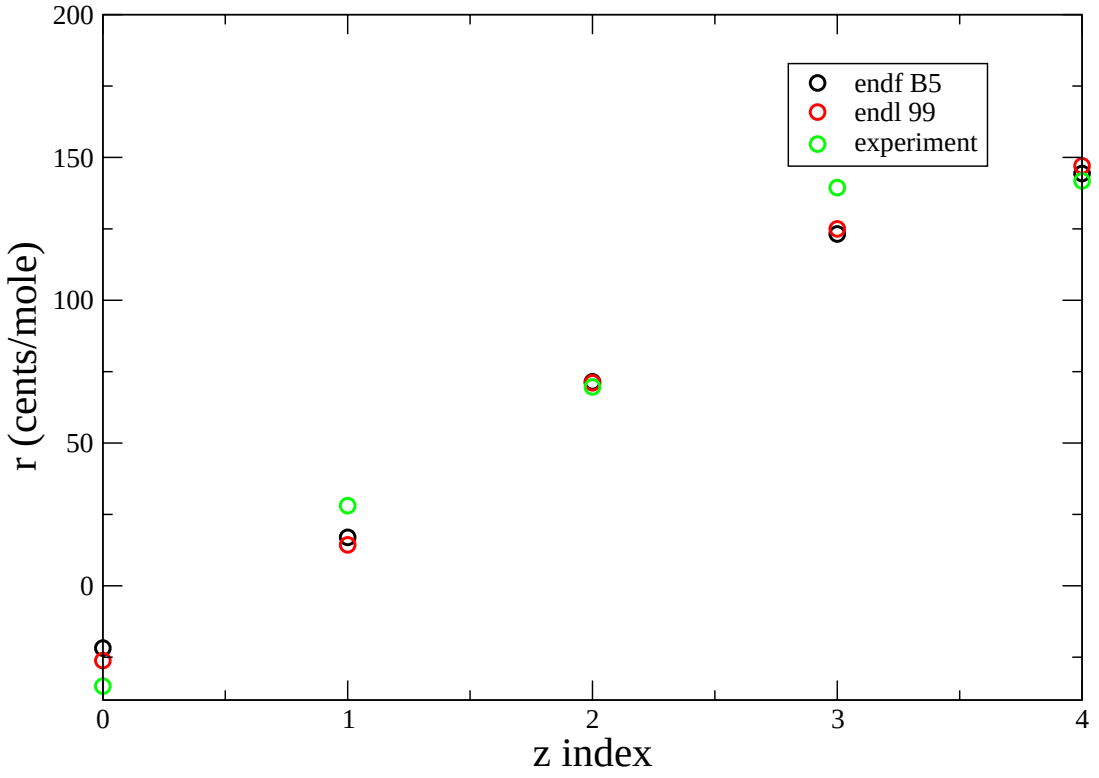

Fig. 49.— Replacement coefficients for ZA=40000 in the Jezebel assembly.

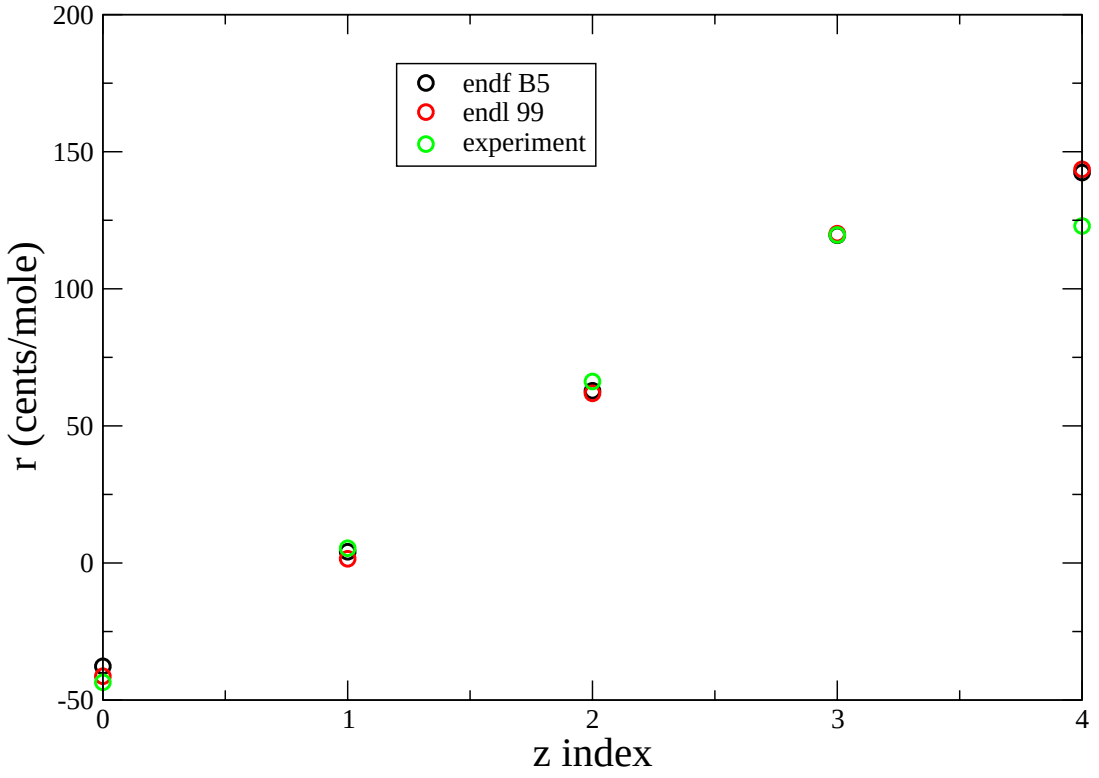

Fig. 50.— Replacement coefficients for ZA=42000 in the Jezebel assembly.

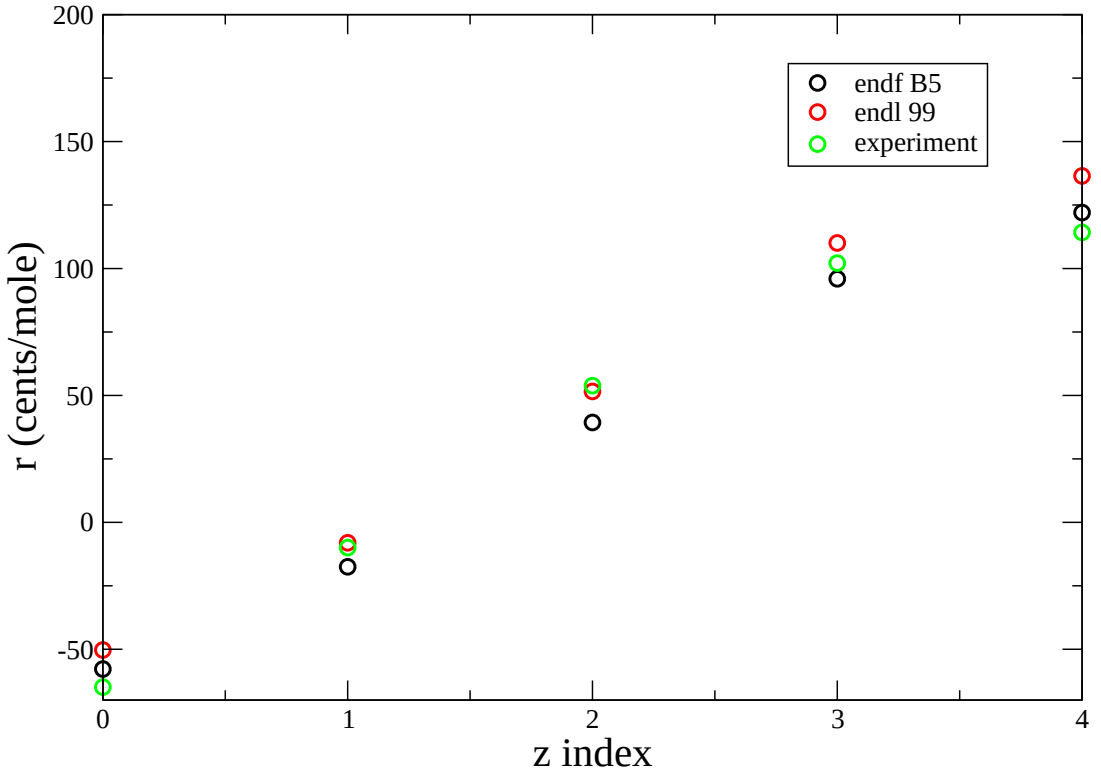

Fig. 51.— Replacement coefficients for ZA=48000 in the Jezebel assembly.

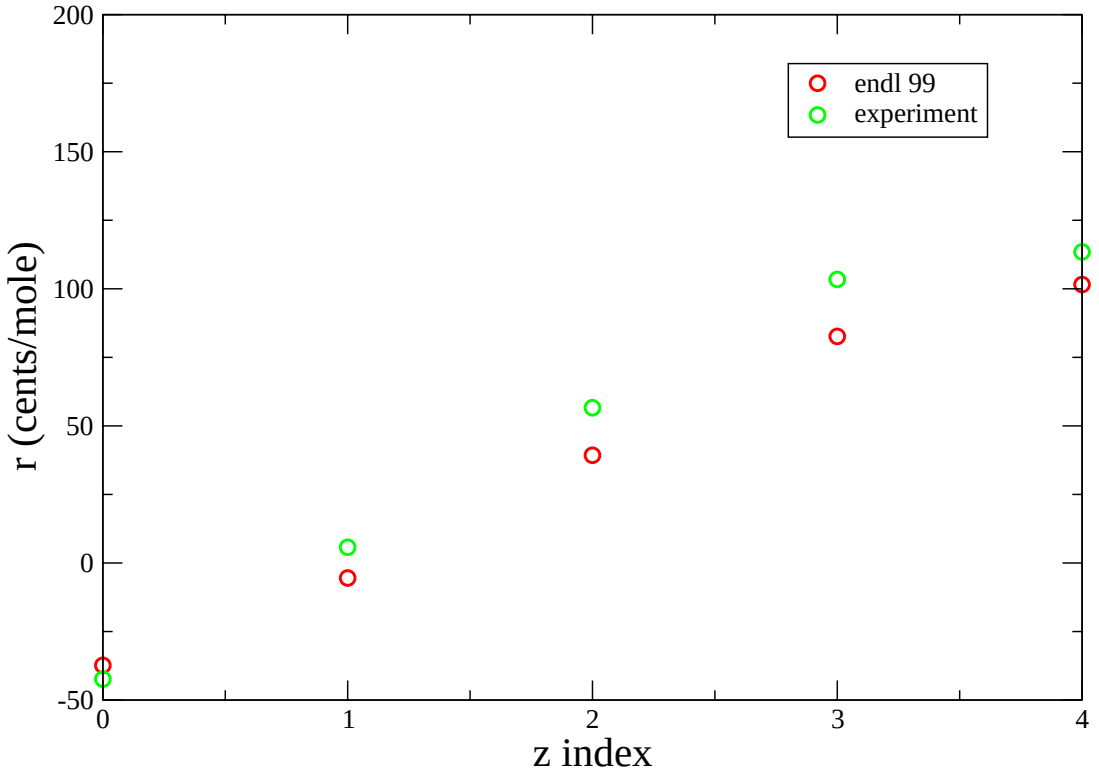

Fig. 52.— Replacement coefficients for ZA=50000 in the Jezebel assembly.

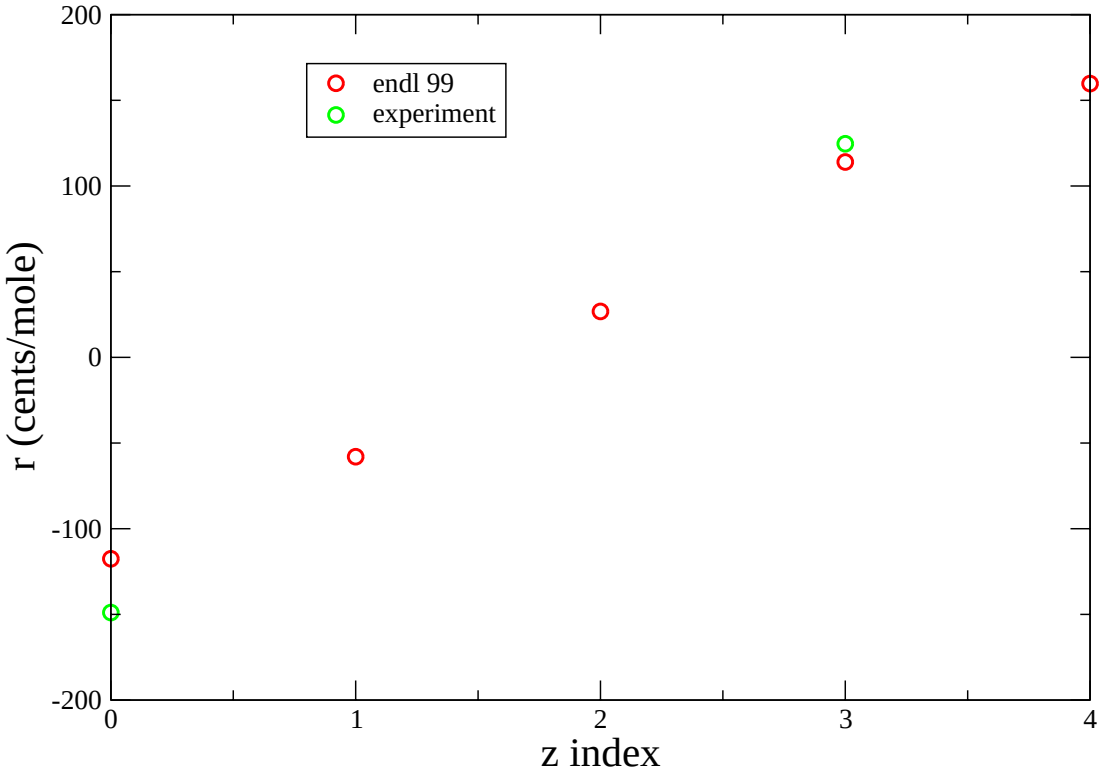

Fig. 53.— Replacement coefficients for ZA=67165 in the Jezebel assembly.

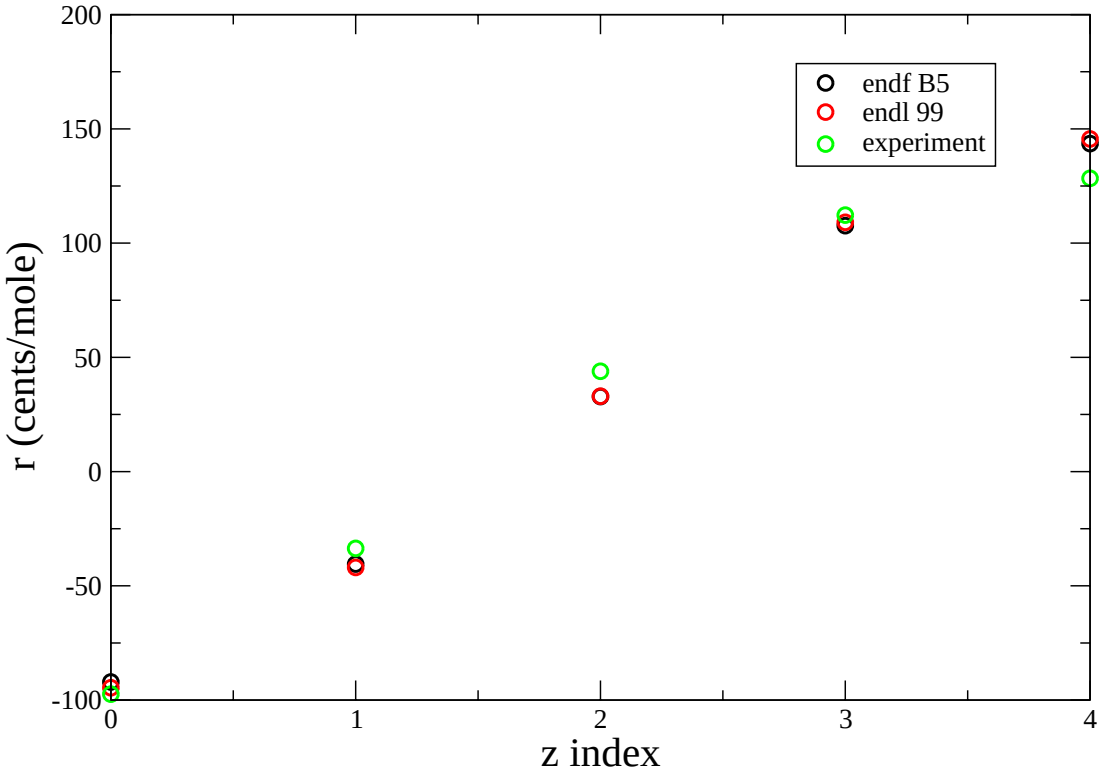

Fig. 54.— Replacement coefficients for ZA=73181 in the Jezebel assembly.

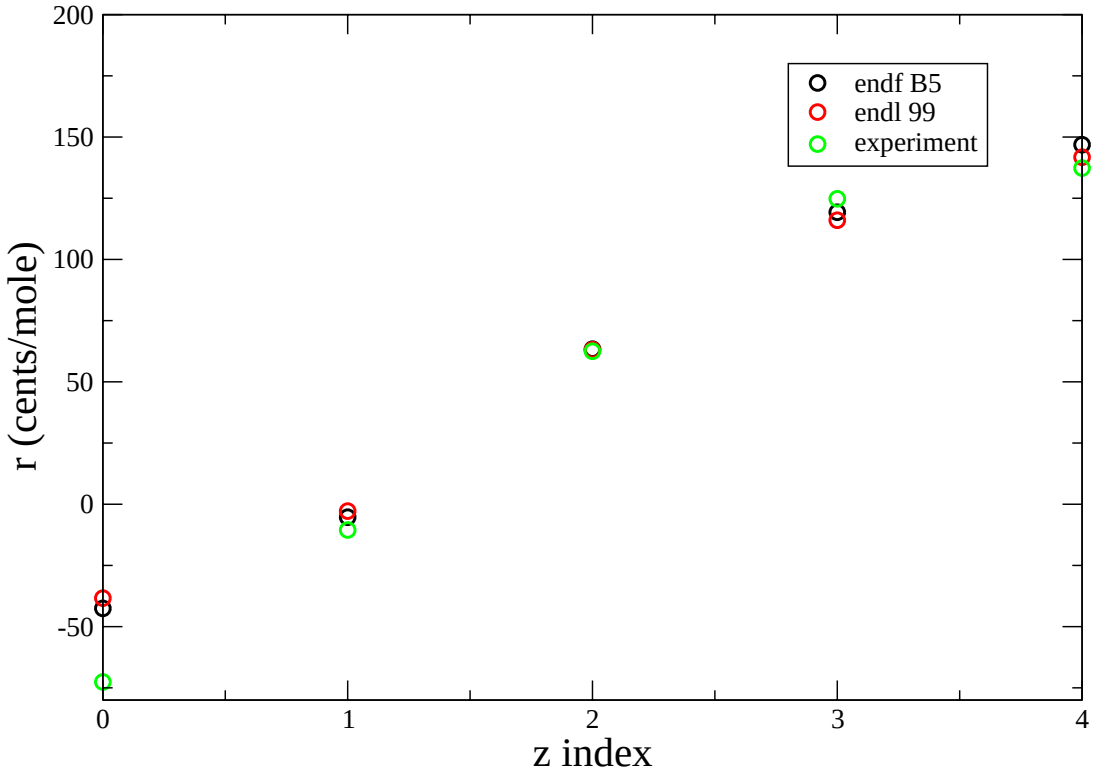

Fig. 55.— Replacement coefficients for ZA=74000 in the Jezebel assembly.

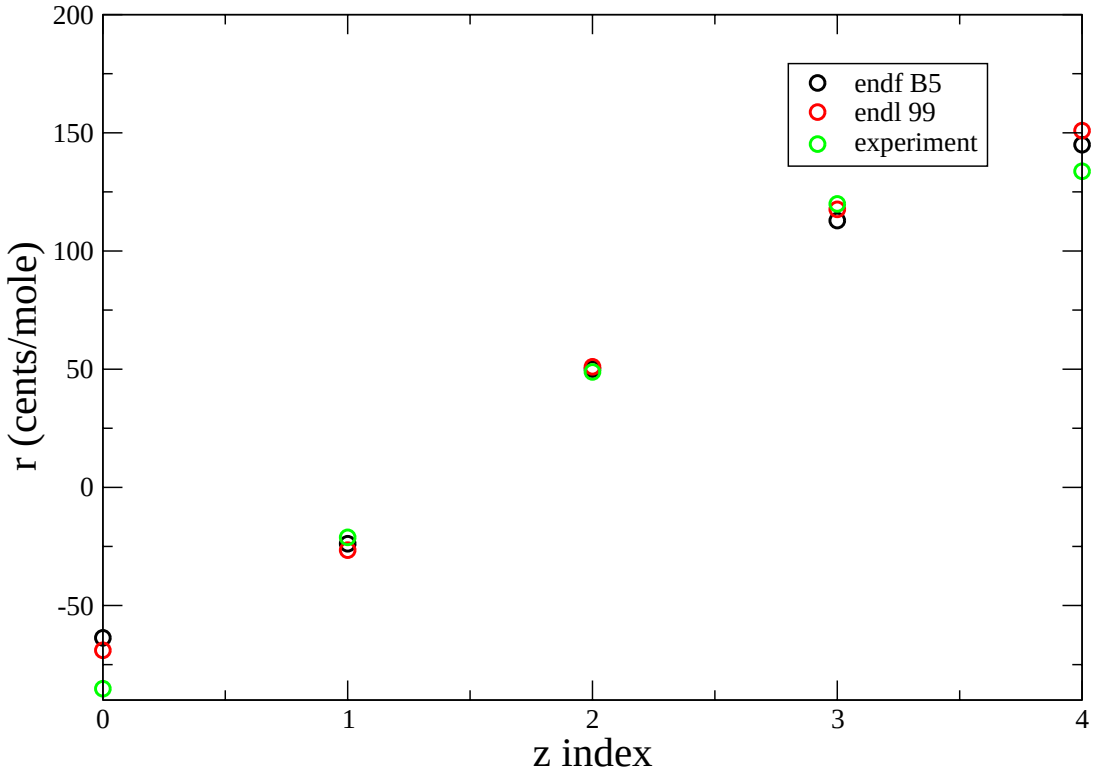

Fig. 56.— Replacement coefficients for ZA=79197 in the Jezebel assembly.

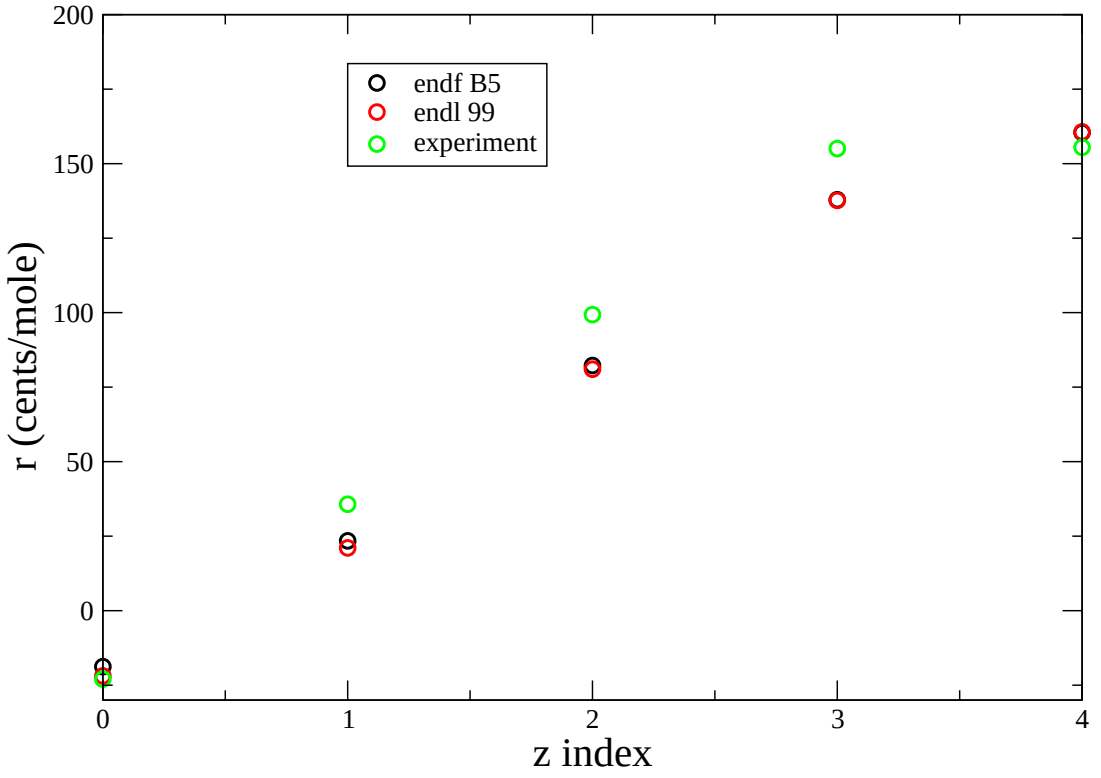

Fig. 57.— Replacement coefficients for ZA=83209 in the Jezebel assembly.

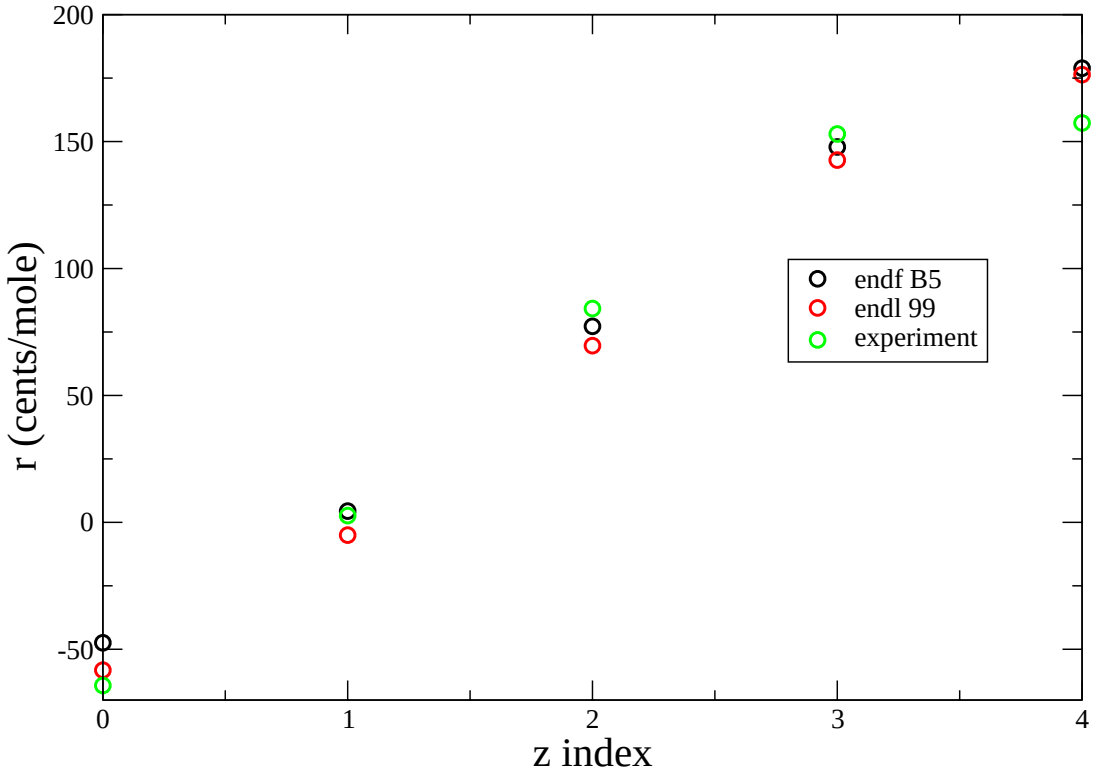

Fig. 58.— Replacement coefficients for ZA=90232 in the Jezebel assembly.

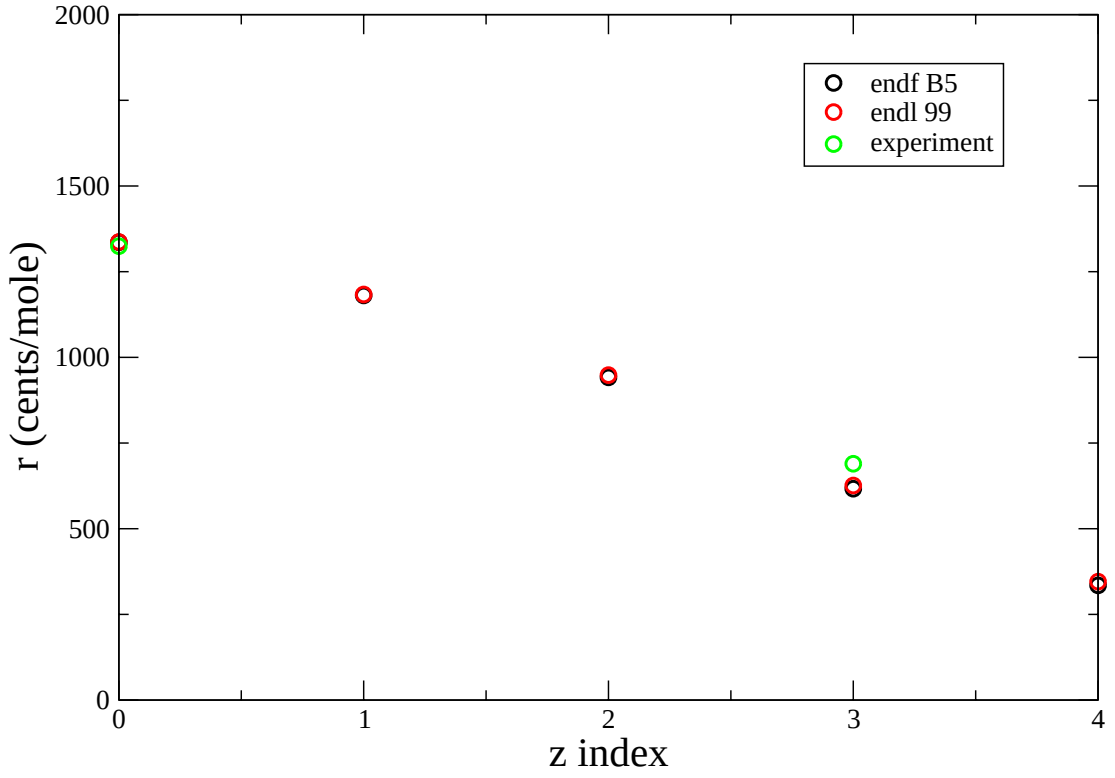

Fig. 59.— Replacement coefficients for ZA=92233 in the Jezebel assembly.

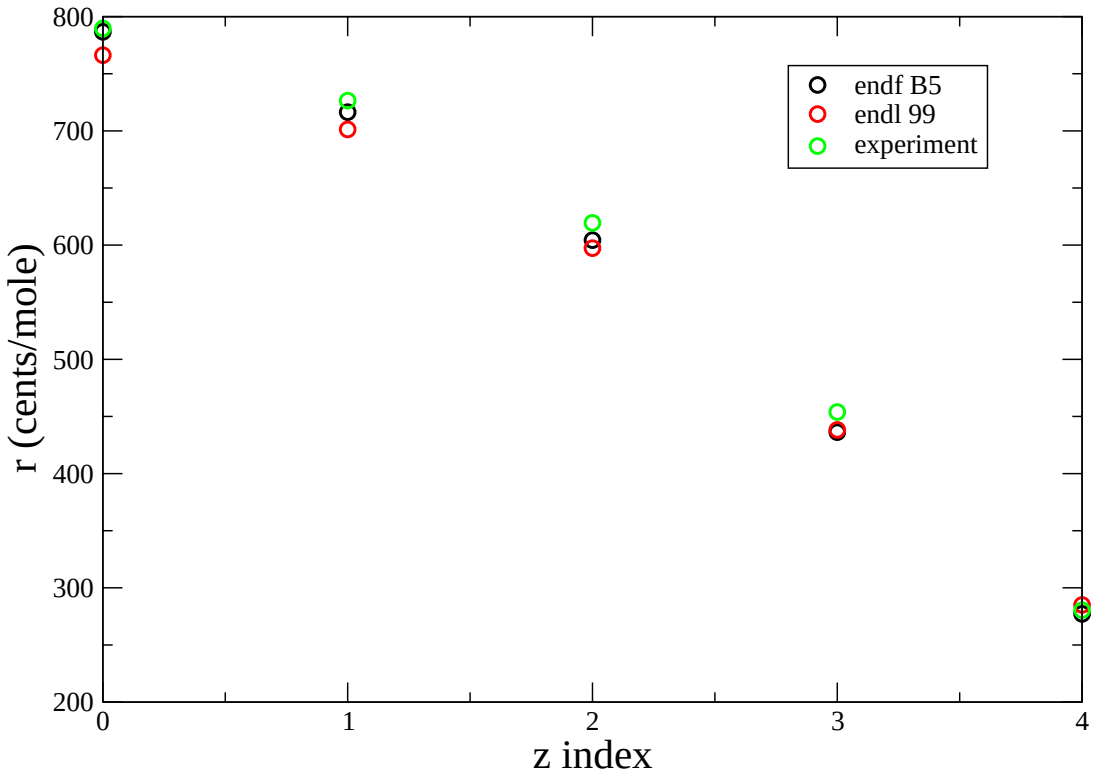

Fig. 60.— Replacement coefficients for ZA=92235 in the Jezebel assembly.

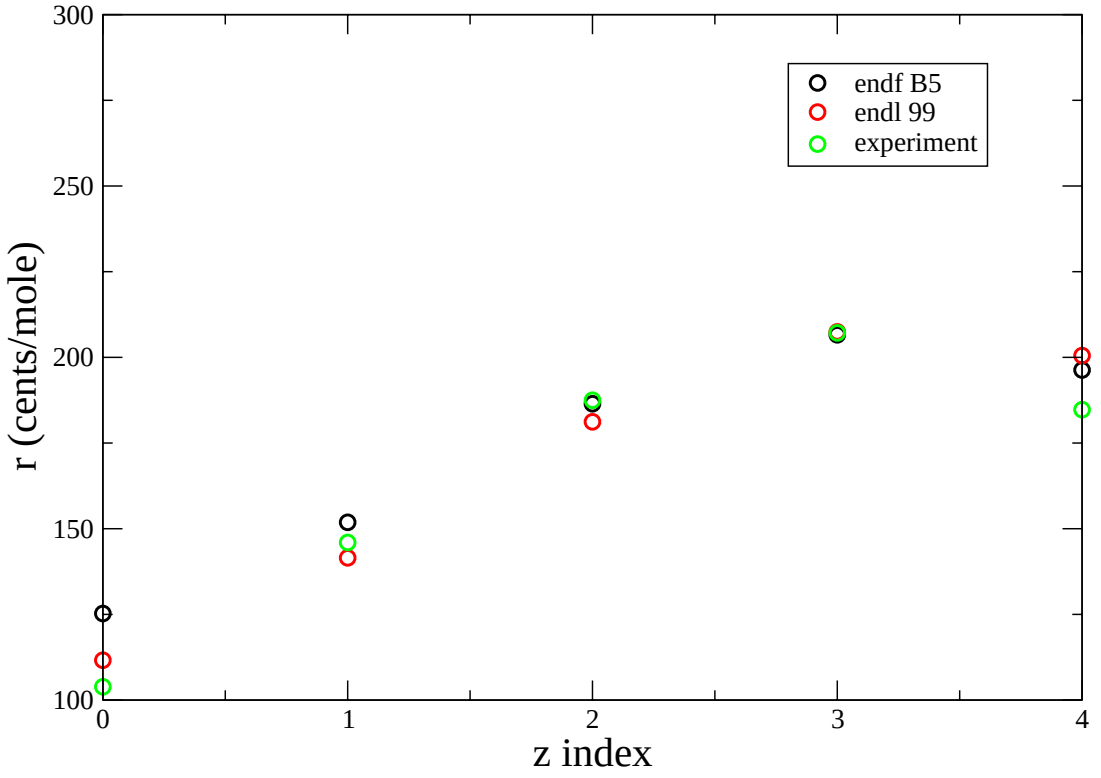

Fig. 61.— Replacement coefficients for ZA=92238 in the Jezebel assembly.

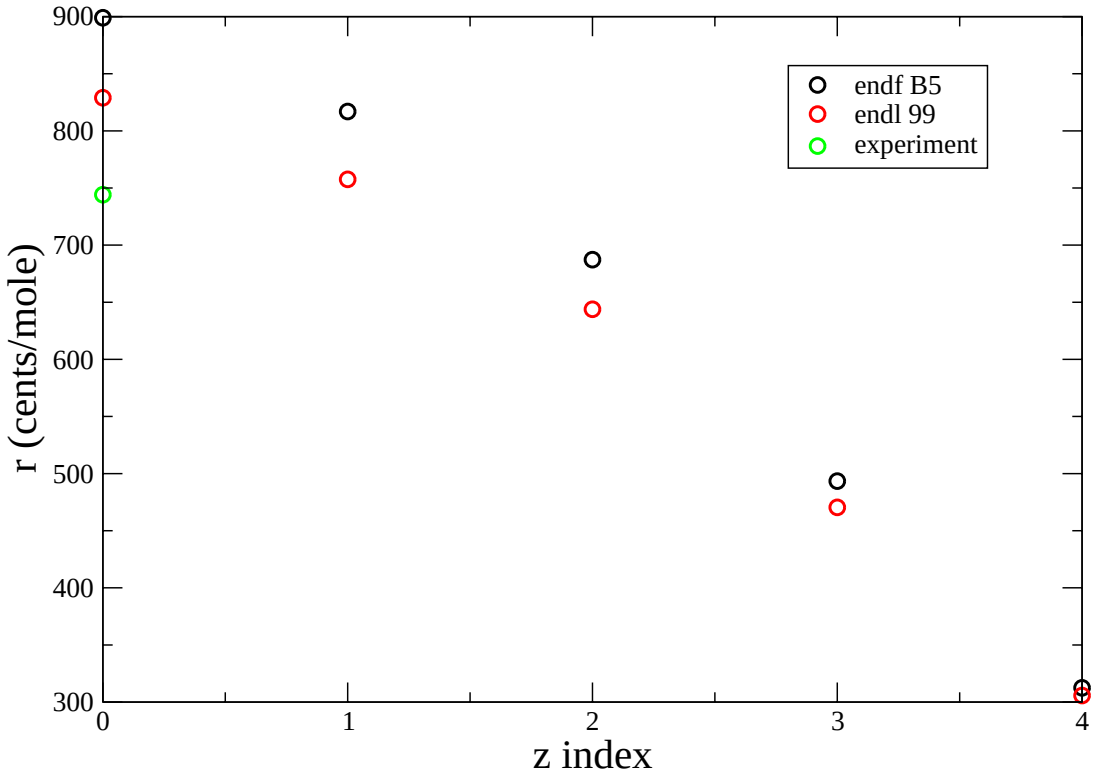

Fig. 62.— Replacement coefficients for ZA=93237 in the Jezebel assembly.

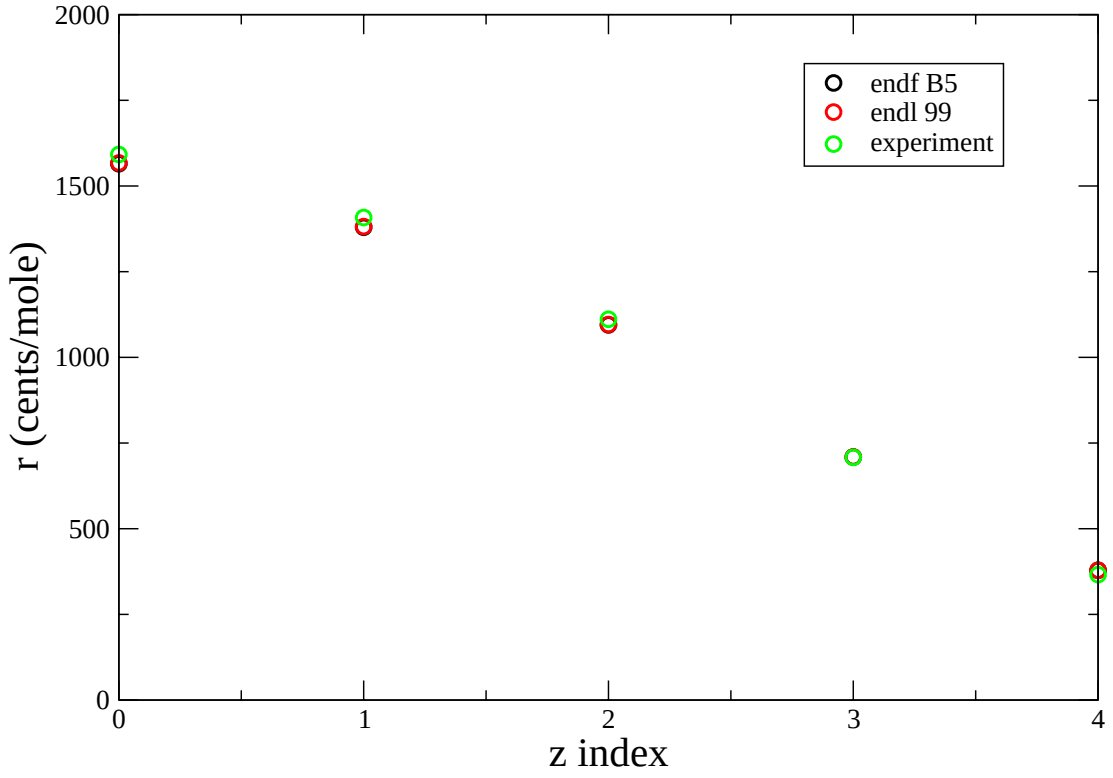

Fig. 63.— Replacement coefficients for ZA=94239 in the Jezebel assembly.

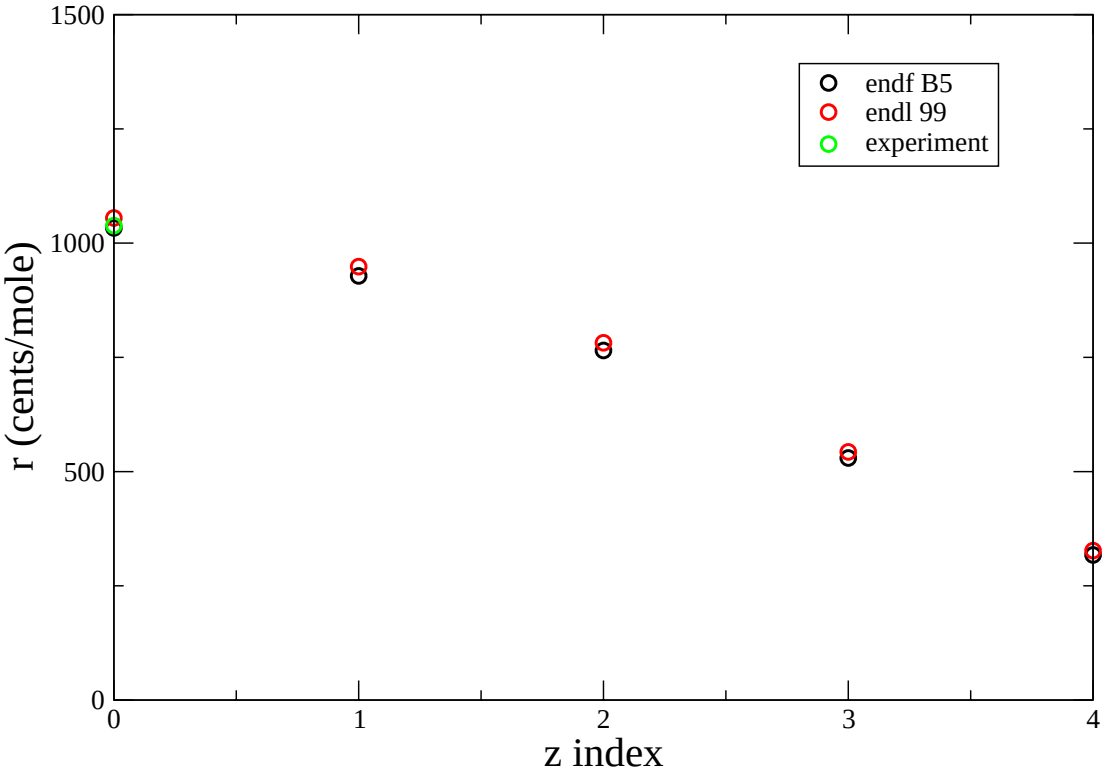

Fig. 64.— Replacement coefficients for ZA=94240 in the Jezebel assembly.